

REVIEW ARTICLE

[View Article Online](#)
[View Journal](#) | [View Issue](#)

Fluorescent monomers as building blocks for dye labeled polymers: synthesis and application in energy conversion, biolabeling and sensors

Alexander M. Breul,^{ab} Martin D. Hager^{*abc} and Ulrich S. Schubert^{*abc}

This review focuses on side-chain functionalized polymers derived from direct (co)polymerization of fluorescent dyes. This overview about polymerizable dyes includes 1,8-naphthalimides, fluoresceins, rhodamines, coumarins, azo-dyes, oxadiazoles, diverse aromatic dyes as well as selected other dyes that cannot be classified within these groups. The discussed dyes have been functionalized with a polymerizable unit in order to apply straight-forward polymerization procedures. Therefore, the center of attention is set to the optical properties of the polymerizable dyes and the applicable polymerization techniques. Furthermore, the various applications (*i.e.*, in biomedicine and pharmacy, as thermo-responsive materials and energy transfer materials, for dispersion of carbon nanotubes and others) of each polymer are discussed.

Received 26th November 2012

DOI: 10.1039/c3cs35478d

www.rsc.org/csr

^a Laboratory of Organic and Macromolecular Chemistry (IOMC), Friedrich Schiller University Jena, Humboldtstraße 10, 07743 Jena, Germany.

E-mail: ulrich.schubert@uni-jena.de, martin.hager@uni-jena.de

Fax: +49 (0)3641 9482 02; Tel: +49 (0)3641 9482 00

^b Jena Center for Soft Matter (JCSM), Friedrich Schiller Universität Jena, Philosophenweg 7, 07743 Jena, Germany

^c Dutch Polymer Institute (DPI), P.O. Box 902, 5600 AX Eindhoven, The Netherlands



Alexander M. Breul

Alexander M. Breul was born in Gera (Germany) in 1986. He studied chemistry at the Friedrich Schiller University Jena (Germany), where he graduated in 2010. Since 2010 to date, he has been a PhD student in the group of Prof. Ulrich S. Schubert at the Friedrich Schiller University Jena, where he has been working on the design of polymers with light-harvesting units.



Martin D. Hager

Martin D. Hager was born in Coburg (Germany) and studied chemistry at the Friedrich Schiller University Jena (Germany), where he graduated in organic and macromolecular chemistry in 2005. In 2007, he received his PhD in chemistry (Friedrich Schiller University Jena, Germany) for work on conjugated rod-coil polymers under the supervision of Prof. E. Klemm (scholarship of the Fonds der Chemischen Industrie). Subsequently, in 2007 he joined the group of Prof. U. S. Schubert (Eindhoven University of Technology, the Netherlands and then Friedrich Schiller University Jena, Germany). His research is focused on conjugated polymers for solar-cell applications and self-healing materials.

or synthetic polymers² to light harvesting arrays.¹⁵ Furthermore, organic dyes are applied in hair colorings, paper production, textile industry, leather tanning industry, food technology as well as in agricultural research,¹⁶ resulting in a worldwide production of approximately 70 000 tons per year.¹⁷

The incorporation of organic dyes into polymeric architectures attracted interest due to their potential application in organic electronic devices, in particular, in organic light emitting diodes (OLEDs),^{7,18,19} white polymer light emitting diodes (WPLEDs)^{7,20–22} as well as in sensor molecules in biochemical and environmental applications.^{23–25} Additionally, fluorescent systems are capable of mimicking photosynthetic proteins in plants by incorporating the chromophores into polymers as donor molecules for Förster resonant energy transfer (FRET) processes.^{26,27} In contrast to main-chain π -conjugated polymers, in side-chain pendant monomers, covalently attached to a polymeric backbone, the optoelectronic properties are mostly independent from the degree of polymerization and the number of repeating units, respectively. Furthermore, monomers that carry polymerizable functionalities, *e.g.*, double bonds in terms of (meth)acrylate-, vinyl- or styrene units, are capable to be directly polymerized either by a straight-forward free radical polymerization (FRP) technique or by one of the commonly applied controlled radical polymerization (CRP) techniques, in particular, by the reversible addition–fragmentation transfer (RAFT) polymerization,^{7,28} or the atom transfer radical polymerization (ATRP),^{29,30} or the nitroxide mediated polymerization (NMP).³¹ Additionally, the living anionic polymerization technique can also be applied for the synthesis of well-defined polymers.³²

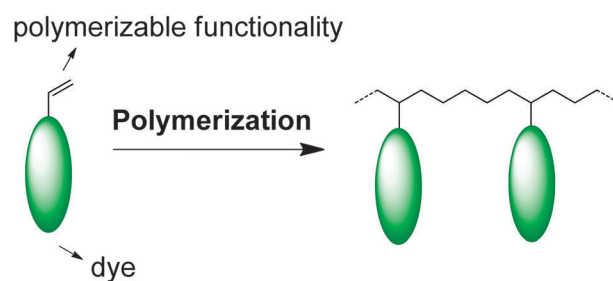


Ulrich S. Schubert

his habilitation in 1999 (with Prof. O. Nuyken). From 1999 to 2000, he held a temporary position as a professor at the Center for NanoScience (CeNS) at the LMU Munich (Germany). From 2000 to 2007, he was Full-Professor at the Eindhoven University of Technology, the Netherlands. Since 2007, he has been Full-Professor at the Friedrich Schiller University Jena, Germany. His awards include the Habilitandenpreis of the GDCh (Makromolekulare Chemie), the Heisenberg-Stipendium of the DFG, the Dozenten-Stipendium of the Fonds der Chemischen Industrie and the VICI award of the NWO.

In contrast to postpolymerization labeling procedures, the content of the dye in the polymer can be adjusted by the amount of dye-functionalized comonomers in the polymerization feed. However, the reactivity ratios of dye-functionalized monomers must be considered. Depending on the structure of the monomer, copolymerization of bulky moieties can be unfavorable. In addition, this procedure avoids additional polymer analogous reactions and, thus, it is more efficient. In the case of polymer-labeling at specific sites with exactly one dye, *e.g.*, chain-end-labeling or labeling of linkers in block copolymers, the modification by postpolymerization attachment of a fluorescent dye is still the method of choice.² The drawbacks of polymer analogous reactions are functionalization efficiencies below 100% as well as partially sophisticated purification techniques in order to separate the desired polymer from the corresponding reagents. Due to the coiling of polymers in solution, highly efficient reactions, in particular, click-reactions, are required for polymer modifications, which limits the number of possibilities for potential reactions.³³ In the case of unspecific polymer-labeling along the polymer chain, another tailor-made monomer that is bearing the corresponding anchoring group must be added to the polymerization feed.⁷ Moreover, a wide range of applications of polymerizable dyes is based on the donation of fluorescent nanoparticles to biological substrates, in particular, living cells. These particles are typically prepared by postpolymerization conjugations of dyes onto preformed particles. The advantage of directly polymerizing the dyes into the polymers as comonomer is the location of the dyes in the core and not only on the surface of the particle, resulting in an enhanced fluorescence of the particles, which are, in addition, not vulnerable to dye-leakage.^{34,35} Furthermore, this distribution within the whole particle avoids the blocking of functional groups on the surface of the nanoparticles, which are required for the interaction with specific substrates (*e.g.*, proteins or enzymes). By introducing targeting units (*e.g.*, peptides or sugar moieties), the binding efficiency can be enhanced and targeted delivery can be attained.

This review article covers the developments during the past three years that have been made in the field of fluorescent polymers derived from monomeric building blocks that carry polymerizable functionalities (the number of publications shows the viability of this research area). For this purpose, this



Scheme 1 Schematic representation of the monomeric building blocks and their corresponding (co)polymer structures reviewed in this contribution.

contribution was subdivided according to the class of fluorescent polymerizable dyes. Herein, the most important classes of dyes, which were incorporated into polymer backbones as side-chains by direct polymerization, are described, focusing on the optical properties and application of the luminescent polymers. Scheme 1 depicts the typical structure of (co)polymers bearing fluorescent chromophores as side-chains.

Application of fluorescing monomers

The majority of all examples given in this review exclusively deal with the labeling of polymer nanoparticles (NPs) for cell uptake studies. One possibility for the preparation of these particles is the miniemulsion polymerization.³⁶ For this purpose, a liquid two-phase system is typically sonicated *via* ultrasound to form an emulsion with well-defined compartments. The hydrophobic phase contains styrene and the fluorescent monomer, whereas functionalized acrylic acid (AA) or aminomethyl methacrylate monomers are applied in the hydrophilic phase. Furthermore, amino acids, DNA, antibodies or peptides, for instance, can be added to the stock solutions for specific functionalization of the resulting nanoparticles. After initiation and polymerization, the particle sizes are in the range of 50 to 200 nm. A second method for NP formation is the nanoprecipitation of polymers. In this case, a polymer solution is dropped into water or *vice versa*: water is dropped into a polymer solution.^{37,38} The nanoprecipitation method represents a versatile method because theoretically every hydrophobic polymer prepared by any polymerization technique can be precipitated. However, the stability of the particles is strongly influenced by the type and the chain-length of the polymer. The miscibility of the polymer solution in water must also be considered. For this purpose, an acetone–water system is typically applied. Depending on the concentration of the polymer solution, well-defined NPs in the range of 50 to 500 nm can be obtained. The concentration of the dye monomers in the polymers for the nanoprecipitation procedure can in theory be varied up to 100%. Practically, dye contents up to 10% are applied. In contrast, the amount of fluorescence dye in the miniemulsion polymerization is 1 to 2 mol%. As the third method, the dialysis procedure can be mentioned. In the following sections, it plays a minor role, but the principle is analogous to the precipitation.³⁹ As further NP preparation methods, emulsification–solvent evaporation, spray drying, salting out and milling can be listed.³⁹ The size and shape of the nanoparticles can be directly characterized by dynamic light-scattering (DLS) techniques, transmission electron microscopy (TEM) and secondary electron microscopy (SEM) as well. In selected cases, also analytical ultracentrifugation (AUC) can be applied as a characterization method. For cell imaging tests, living cells in a culture medium are incubated for a specific time with a labeled nanoparticle suspension. After some washing steps, these cells are investigated by confocal laser scanning microscopy. In the case of a successful uptake of the nanoparticles, the cells show the emission of the dye NP upon irradiation of the dye in the absorption maximum. It is also

possible to quantify the uptake by a fluorescent activated cell sorter (FACS). So far, only fluorescein and rhodamine dyes were utilized for applications with a biological background. In two examples, also coumarin and thiazole dyes were applied.^{35,40} Recently, a comprehensive study about the whole range of possible organic fluorophore platforms for fluorescence imaging was published.⁴¹ The authors provide a guide structured according to the emission of utilized dyes from far-red to near infrared fluorescence.

A wide range of applications focuses on electronical devices. Therein the active layer material generally consists either of homopolymers of the corresponding fluorescent dyes or of (block)copolymers which are bearing a second functional moiety (*e.g.*, electron- and hole-transporting monomers). Due to the fact that the efficiency intrinsically drops down if unfunctionalized monomers are incorporated into the polymer backbone, the degree of functionalization should be 100% in the ideal case. The direct polymerization of functional dyes covers this advantage in contrast to post-functionalization methods of polymer analogous reactions. Only in exceptional cases, homopolymers were copolymerized with nonfunctional monomers (*e.g.*, styrene) to tune the phase separation behavior which strongly influences the performance of organic electronic devices.⁴² In general, organic electronics are characterized by recording a current–voltage curve. The efficiency of an organic solar cell device is calculated by several values: the fill factor (FF) as the maximum rectangular area under curve, the short circuit current (I_{SC}) as the intersection with the y-axis, and the open circuit voltage (V_{OC}) as the intersection with the x-axis.⁴³ A variation of the graphical illustration of these characteristics is the plotting of the current density *versus* the voltage. So far, poly(3-hexyl thiophene) (P3HT) has been considered as the gold standard for organic solar cell devices because it combines a low bandgap and high quantum yield with easy processability and low production costs. Side chain dye-pendant macromolecules do not reach high efficiencies of up to 10% because the introduction of dyes with a maximum conjugation length in the side chain is a synthetic challenge.⁴⁴ For this purpose, usually polymerizable conjugated oligomers are applied for organic electronics. In particular, the conjugated system of fluorine chromophores as well as small heterocycles can be extended with a limited synthetic effort.

The following sections also contain information on copolymerized fluorescence dyes that were successfully applied as sensor materials. In this context, two basic concepts were observed. Firstly, polymeric sensors were synthesized where sensitive moieties were directly attached to the chromophore or the chromophore itself is directly changed by the analyte. Thus, the absorption and emission spectra are altered upon exposure of the sensor material to the analyte. For these systems, the sensitivity as well as the stimulus concentration range of the material strongly depends on the content of dye. In the second approach, two or more fluorescent dyes are copolymerized with functional monomers that interact with several stimuli (*e.g.*, pH-value or temperature). The most prominent candidate is the *N*-isopropylacrylamide (NIPAM) monomer that shows a lower

critical solution temperature (LCST) behavior. Polymers based on NIPAM monomers feature shrinkage and/or precipitation above the lower critical solution temperature in aqueous media. In block copolymer architectures where different dyes are incorporated in each block, this shrinkage leads to a decrease in the distance between two different chromophores. In case of an overlap between the emission of a donor dye and the absorption of a corresponding acceptor dye, a quenching of the donor emission in combination with the appearance of the acceptor emission occurs. If the distance between two different chromophores is below the Förster radius, an energy transfer takes place – the Förster resonant energy transfer (FRET). Hence, the emission of the polymer can be tuned by external stimuli. In general, the existence of a FRET process is proven by excited-state lifetime studies. For this purpose, the decay of the excited-state lifetime of the donor is recorded. A faster decay (*i.e.*, shorter lifetime) of the donor luminescence provides evidence for the presence of FRET. In general, a block copolymer architecture requires the application of a controlled and/or living polymerization technique. In order to prevent self-quenching of the dyes in one block, the content must be low enough on the one hand and high enough that every polymer chain is statistically functionalized with at least one dye moiety. As sensing moieties, a wide range of chromophores can be applied. In the case of color changes, a difference in the emission intensity or wavelength is required. For this purpose, mainly two different types of chromophores are applied because the introduction of functional groups leads only to a fine-tuning of the emission for the majority of the dyes. Hence, it is often desired that the emission changes are visible to the naked eye. The typical emission for sensing dyes has eye-catching colors (*i.e.*, blue, green, yellow, red, sometimes also orange or purple). Small differences in the emission wavelengths are more difficult to quantify (*e.g.*, changes from turquoise to green) and, thus, the detection limit is degraded. For the FRET based sensors, a large Stokes-shift is required to avoid the self-quenching of the dye emission.

A series of carbon modifications are nowadays in the focus of intense research.^{45,46} In particular, single- and multi-walled carbon nanotubes are insoluble in several organic solvents. Thence, an interaction between organic molecules attached to polymers leads to a functionalization of these modifications. As a consequence, the solubilizing properties of the polymers are combined with the carbon nanotube features and, thus, the nanotubes can be suspended in organic solvents. In these cases, dye contents in the range of approximately 0.5% to 100% are applied. To obtain a homogeneous solubilization and functionalization, typically well-defined polymers are utilized, prepared by controlled or living polymerization techniques. In this context, aromatic dyes are exclusively applied due to their good interaction with NTs.

The last field of application of polymers labeled with polymerizable fluorescence dyes is the study of polymer properties. In order not to influence the general properties of a polymer too much by incorporating additional functionalities, in particular, by fluorescence dyes, the content of dye monomer must

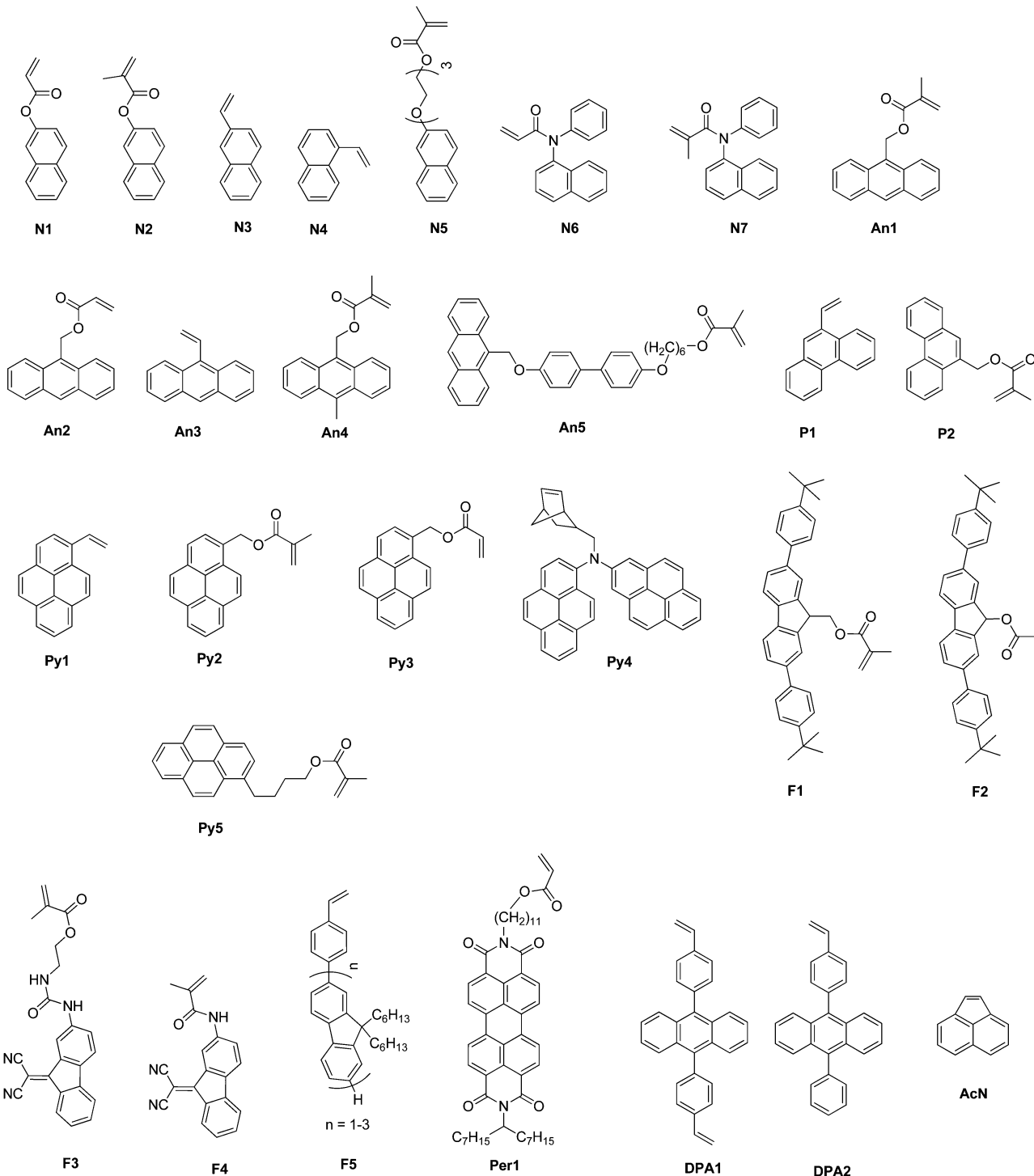
necessarily be kept as low as possible (*i.e.*, typically below 1 mol%). In general, the mechanical and thermal properties of polymers determine their application. For this reason, the experiments are a combination of standard experiments (*e.g.*, for film drying behavior or mechanical characteristics) with a fluorescence microscope which enables visualization of the observed process. The polymerizable dyes incorporated into these polymers require a high fluorescence intensity of the polymer. Furthermore, the dye itself should have a low influence on the overall properties of the observed polymer. Basically, commercially available polymerizable dyes fulfill these criteria.

All further tailor-made applications will be described in the following sections. According to their unique purpose, all polymers reveal an optimized content of dye. In all other cases, the characterization of these polymers was adjusted to their specialized field of interest.

Polymerizable aromatic dyes

This section contains information on side-chain pendant polymerizable dyes, *i.e.* polycyclic aromatic hydrocarbons in polymeric architectures (for the exact structures, see Scheme 2). The simplest alignment of two fused benzene rings is the naphthalene system. The most prominent candidates for polymerization are the 2-naphthalenes that can be directly functionalized with acrylate (**N1**), methacrylate (**N2**) as well as vinyl (**N3**) units. Naphthalene shows an absorption maximum at $\lambda_{\text{abs}} = 285$ nm and an emission maximum at 345 nm. Most of the naphthalene containing monomers are commercially available, in particular **N1** to **N3** and **N6** to **N7**. A large number of publications deal with naphthalene monomers for the labeling of polymers. In particular, **N1** was copolymerized with *N*-dodecylmethacrylamide.^{47,48} Additionally, **N3** was copolymerized with styrene⁴⁹ and maleic anhydride.⁵⁰ Furthermore, the copolymerization behavior of **N3** with ethylene,⁵¹ sodium 2-acrylamido-2-methylpropane sulphonate and acrylamide⁵² as well as sodium styrenesulfonate,^{53,54} and AA⁵⁵ was studied. In contrast, the aromatic anthracene moiety absorbs at 362 nm and emits at 407 nm. The synthesis of a series of polymerizable anthracene dyes has been described earlier.⁵⁶ Labeled **An1** containing copolymers could be obtained by copolymerization with styrene,^{57,58} methyl methacrylate (MMA),^{59–62} 2-(dimethylamino)ethyl methacrylate (DMAEMA),⁶³ azacrown ether methacrylate monomers,⁶⁴ *p*-tert-butoxy styrene (PTBS) and methacrylic acid (MAA),⁶⁵ as well as *N*-(4-cyanophenyl) maleimide (CyOPMI), 4-hydroxybutyl vinyl ether (HBuVE) and MMA.⁶⁶ **An3** could be polymerized with *N*-vinyl-2-pyrrolidone (VP),⁶⁷ as well as with vinyl terminated poly(siloxanes).⁶⁸ Besides their good labeling properties, anthracene containing monomers are also capable of undergoing Diels–Alder reactions, *e.g.*, in PMMA copolymers,⁶⁹ and photodimerization.^{59–71} Moreover, polymerizable pyrenes were used to label polystyrenes,^{72–77} AA in ionic liquids,⁷⁸ and MMA.^{49,76,79}

Due to the absence of any heteroatoms in the chromophore moieties, all monomers are suitable for advanced polymerization techniques, *i.e.* RAFT, ATRP, NMP, ROMP and living



Scheme 2 Schematic representation of the chemical structures of fluorescent aromatic chromophore bearing monomers.

anionic polymerization. Firstly, block copolymers from N2 and DMAEMA were obtained using ATRP.⁸⁰ Fluorescent Py2 bearing macroinitiators are also available for this kind of CRP technique.⁸¹ PPy2-*b*-PSt-*b*-PEO triblock copolymers could also be obtained using the ATRP technique.⁸² This triblock architecture enabled the encapsulation of the model drug Nile red by self-assembly (proven by TEM as well as AFM measurements)

and its release under UV-irradiation (proven by UV-vis absorption and emission spectroscopy). A schematic representation of this process is displayed in Fig. 1. For the RAFT polymerization as second prominent representative for CRP processes, a copolymerization with (acetoacetoxy)ethyl methacrylate (AEMA) was carried out using An1 as monomer for the second block.⁸³ Furthermore, diblock copolymer architectures of PPy2-*b*-PVP

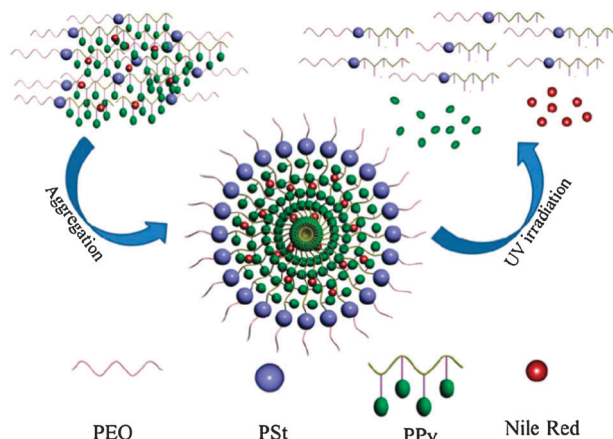


Fig. 1 Schematic representation of the encapsulation of Nile red within the hydrophobic core of the polymer aggregates of **PPy2**-*b*-**PSt**-*b*-**PEO** and its release upon disruption of the polymer aggregates by UV light.⁸² Figure copyright John Wiley and Sons and reproduced with permission.

are accessible.⁸⁴ CdSe/ZnS quantum dots (QDs) were coated with the diblock copolymer to prepare a color distinctive, ratiometric pH sensor. Due to the change in the PVP conformations dependent on the pH value, the color of the QDs in solution changed from blue to red. Schubert and coworkers reported the RAFT copolymerization of **Py2** with MMA and di(ethylene glycol) methyl ether methacrylate (DEGMA).^{85,86} The thermo-responsive behavior of the polymers was utilized for the application as temperature sensor. In addition, well-defined nanoparticles could be obtained from the PMMA-copolymers by applying fractionation by preparative analytical ultracentrifugation.⁸⁷ Ghiggino *et al.* provided evidence that diphenylanthracenes **DPA1** and **DPA2** are suitable monomers for the RAFT polymerization technique.⁸⁸ The authors formed an “oligomer” with one repeating unit by setting the monomer/CTA ratio to 1 in the polymerization feed (stoichiometric application of the RAFT agent), which determines the targeted degree of polymerization. In this manner, a “macro”-RAFT-agent could be obtained which is functionalized with exactly one fluorescent dye. As a consequence, the placement of the diphenylanthracene dye in the polymer chain is adjusted by the structure of the monomer: in the single functionalized **DAP1**, the dye is placed at the chain end; in contrast, the dye is placed in the middle of the chain in the case of the double functionalized **DPA2**. Both RAFT agents were applied for the polymerization of **AcN**. In principle, a sophisticated RAFT agent synthesis can be avoided because the RAFT polymerization procedure features a good tolerance towards many functional groups.²⁸ Moreover, fluorescent macroinitiators labeled with **Py2** for the nitroxide-mediated crosslinking polymerization process in aqueous miniemulsions were reported.⁸⁹ The norbornene-functionalized pyrene bearing two chromophores in the monomer unit (**Py4**) was synthesized and subsequently polymerized by ROPM.⁹⁰ Its synthesis by 5-(amino methyl)bicyclo[2.2.1]hept-2-ene (NBMA) and 1-bromopyrene as well as its subsequent polymerization is protected by the patent application.

The polymer featured good transmittance in combination with a high thermal stability.

Controlled radical polymerization techniques have also been applied for the production of organic photovoltaic devices. In this context, Thelakkat and coworkers designed block copolymers based on **Per1** where the poly(**Per1**)-block acted as the acceptor moiety of the active layer in organic bulk-heterojunction organic solar cells.^{42,91,92} A P3HT block had in this case the function of the donor material. **Per1** could be polymerized in a controlled manner by NMP. The material revealed a good phase separation behavior, resulting in a considerable performance of organic solar cell devices. A power conversion efficiency η of 0.2% could be observed.

During the last few years, several groups also published living anionic polymerization procedures using polymerizable aromatic dye molecules, in particular, **An3** by Natori and coworkers.^{93,94} By the application of an asymmetric anionic polymerization procedure, the polymerization of 2,7-bis(4-*tert*-butylphenyl)fluoren-9-yl methacrylate (**F1**) as well as the analogous acrylate (**F2**) was realized by Nakano *et al.*^{95,96} The authors were able to photoinduce racemization of this optically active polymer with helical conformation. Mezzenga *et al.* also polymerized styryl functionalized mono- and oligo-fluorenes (**F5**, $n = 1, 2$) using the living anionic polymerization procedure.⁹⁷ By copolymerization with VP, the authors obtained well-defined block copolymers, which resulted in a phase separation. Furthermore, the capability of the material to host COOH-modified single-walled carbon nanotubes (SWCNTs) in the PVP-block was described. Finally, star-shaped polymers, in particular, 3-, 4- as well as 8-arm star polymer architectures, could be obtained by anionic polymerization of **F5**.⁹⁸

Together with MAA and EGDMA, **An2** could be grafted from a modified glass surface.⁹⁹ For this purpose, borosilicate glass slides were modified with *N,N*-diethylaminodithiocarbamoyl-propyl(trimethoxy)silane followed by subsequent polymerization using the iniferter polymerization technique. It was found that the *N,N*-tetraethyl thiuram disulphide chain terminator enhanced the control over the polymerization. In this manner, well-defined polymer-films could be obtained. Moreover, further examples for fluorescent polymer composite materials can be found in the literature: Fe₃O₄ composite particles were prepared by the groups of Kim and Cheong.¹⁰⁰ This material combines the magnetic properties of the iron oxide particles with the fluorescent properties of the poly(styrene-*co*-MAA-*co*-**N2**). Moreover, the immobilization of naphthyl labeled colloids on Au-surfaces could be realized *via* supramolecular “handcuffs” (*i.e.* cucurbit[8]uril CB[8]).¹⁰¹ The CB[8] was able to incorporate one viologen moiety that was immobilized on the gold surface as well as one naphthalene moiety on the surface of the nanoparticles.

Another method used to produce monodisperse nanoparticles is the copolymerization of styrene in the presence of a polymerizable surfactant.¹⁰² In this case, **Py2** was added for labeling. It could be shown that highly monodisperse particles could be obtained (see Fig. 2 for a SEM image of the particles).

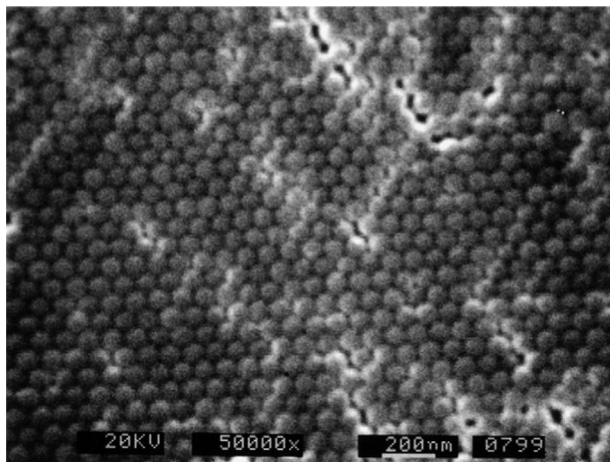


Fig. 2 SEM image of the fluorescent PS-co-PPy2 particles surrounded by a surfactant.¹⁰² Figure copyright Elsevier and reproduced with permission.

In general, aromatic dyes can also be applied for the separation of SWCNTs due to their strong interaction. Voit *et al.* copolymerized **Py3** with styrene for the dispersion of SWCNTs by adsorption of the copolymer on the surface of the nanotubes.^{45,46} These π - π stacking interactions of pyrene with SWCNTs were also used to functionalize nanotubes with azobenzene moieties (**Azo45** and **Azo46**, see the corresponding section below for the structures of the monomers)¹⁰³ as well as silica oxide networks with PEG coronas.¹⁰⁴ The dispersion process of SWCNTs is shown in Fig. 3. In the case of the P(Py2-co-Azo45) copolymer composites, the material revealed photoinduced birefringence. Moreover, Chan-Park *et al.* used **An1** for the separation of single walled carbon nanotubes.^{105,106} In this context, also **N2** was applied. Furthermore, copolymers consisting of PS and PEO macromonomers as well as **Py2** were utilized for the dispersion of multi-walled carbon nanotubes (MWCNTs) in organic solvents.¹⁰⁷ The role of the π - π interactions was also investigated by the group of Bucknall who focused their attention on poly(9-vinylphenanthrene)s (poly**P1**) with C₆₀ fullerenes.¹⁰⁸ The results were compared to the PS and poly**N3** as homologous series. It could be shown that the solubility of the fullerenes increases nonlinearly with increasing aromaticity. In this case, the experimental wide-angle X-ray scattering measurements correlated with DFT calculations.

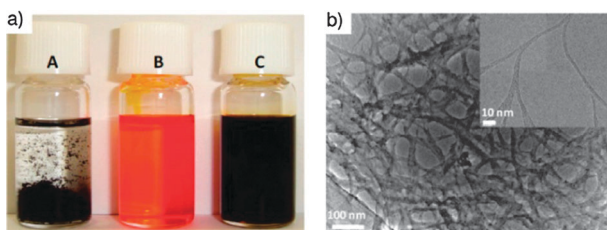


Fig. 3 (a) Dispersion of SWCNTs in THF (A), solution of polymer P(Py2-co-Azo45) in THF (B), and solution of polymer P(Py2-co-Azo45)/SWNT nanocomposite in THF (C). (b) TEM image of polymer P(Py2-co-Azo45)/SWNT nanocomposite with a zoomed image in the inset. Reprinted with permission from ref. 103. Copyright 2011 American Chemical Society.

Polymerizable aromatic dyes have also been studied for an application as sensor material. The group of García recently described a cyanide sensor with an extremely low detection threshold for aqueous media based on the fluorescence of copolymers bearing **F3** and **F4** in the backbone.¹⁰⁹ For this purpose, the monomers were copolymerized with ethoxy methacrylate, 2-(2-aminoethoxyethanol) methacrylamide and ethylene glycol dimethacrylate by FRP. Fluorescent polymers can also be applied as thermoresponsive materials. In this context, **F5** ($n = 1$) was copolymerized with DMAEMA and stearyl acrylate for the fabrication of thermoresponsive luminescent electrospun fibers by the group of Chen.¹¹⁰ In addition, the introduction of flexible spacers between the polymerizable methacrylate and the naphthalene unit (**N5**) enables the application of side-chain pendant naphthalenes in polymeric architectures for the reversible attachment of carbohydrates onto the copolymers by supramolecular self-assembly with cucurbit[8]uril.¹¹¹ To ensure a better visualization, poly(**N5**) was labelled with a polymerizable rhodamine dye (**Rh8**, Scheme 7 in the rhodamine section). **An3** was used for the production of stimuli-responsive Janus particles.¹¹² Amphiphilic particles were obtained by photoinitiation and several coupling steps. Fluorescence microscopy, scanning electron microscopy, and transmission electron microscopy measurements confirmed the asymmetrical morphology of the resultant particles.

Further applications of polymers composed of polymerizable aromatics are in organic electronic devices. Hirao and coworkers reported the fabrication of non-volatile memory devices based on the homopolymers of **F5** ($n = 1$ to 3).^{113–116} In particular, polymerizable naphthalenes were successfully applied in gate electrets (*i.e.*, chargeable thin polymer gate dielectrics) on non-volatile organic field-effect transistor memories.¹¹⁷ It could be demonstrated that the electron storing efficiency increases in a homologous polymer series from poly(vinyl alcohol) to poly(**N3**) (see Fig. 4 for the full series as well as the setting of the device).

The pyrene monomer **Py2** was applied as additive in a poly(styrene-*co*-acrylic acid-*co*-1-pyrenylmethyl methacrylate) copolymer in order to enhance the contrast in fluorescence microscopy measurements in thin film blends with poly[2-methoxy-5(2'-ethylhexyloxy)-*p*-phenylenevinylene]s (MEH-PPVs).¹¹⁸ In addition, a large number of patents was disclosed where polymers based on polymerizable anthracenes are applied as antireflective coatings,^{119,120} liquid crystalline polymer fibers for display application^{71,121} as well as photoresists.¹²² In this context, only some selected examples are cited.

Copolymerized naphthalenes were investigated in terms of their nonradiative energy transfer towards 1,4-bis(5-phenyl oxazolyl-2)benzene.¹²³ For this purpose, scintillation composites composed of **N2**, MMA and 1,4-bis(5-phenyl oxazolyl-2)-benzene were compared to a solid solution of naphthalene and 1,4-bis(5-phenyl oxazolyl-2)benzene in PMMA. It could be demonstrated that the emission intensity of the 1,4-bis(5-phenyl oxazolyl-2)benzene acceptor molecule increases by a factor of two when the naphthalene is covalently attached to the polymeric backbone.

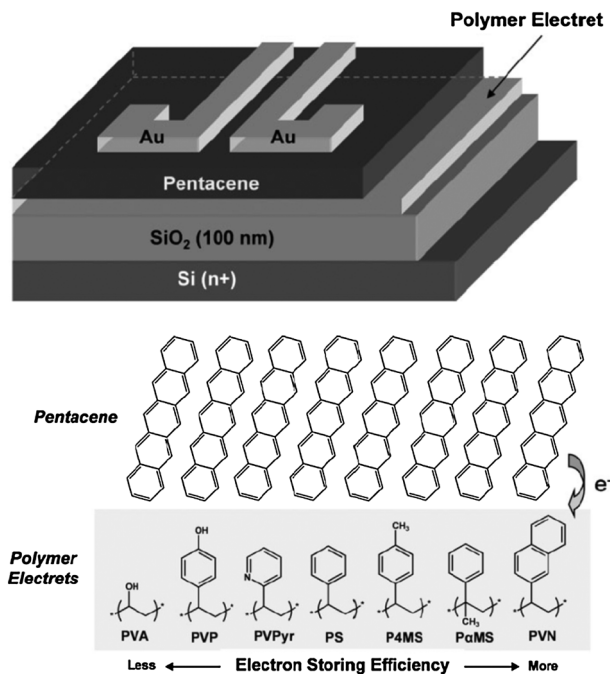


Fig. 4 Schematic representation of the device setting as well as the electron-storage efficiency of electret materials estimated from the polymer electrets memory characteristics.¹¹⁷ PVN≡poly(N3). Figure copyright John Wiley and Sons and reproduced with permission.

For the investigation of fundamental processes concerning polymer chemistry, several studies were performed. In order to investigate certain dynamic processes in polymers or properties of polymers, a wide range of polymer classes were labeled with a small amount of dye for the visualization of the respective process. Swanson could gain detailed insight into the conformational behavior of poly(methacrylic acid) (PMAA) at different pH-values and the transition thereof by copolymerizing MAA with **An1**.¹²⁴ Phenanthrene containing butyl acrylate–methyl methacrylate copolymers were used to determine the drying behavior of wet latex films *via* FRET.^{125,126} Winnik *et al.* studied several additional effects on the polymer diffusion of **P2** or **An4** labeled poly(butyl methacrylate),¹²⁷ and P(MMA-*co*-BA) latex films.^{102,128–133} Furthermore, **Py2** was added to a poly(dodecylmethacrylate) polymer for the real time monitoring of dynamic processes occurring during film formation of surfactant-templated mesostructured sol–gel films formed by evaporation induced self-assembly.¹³⁴ In order to determine the structure–property relationship for acrylic dye monomers (*i.e.* naphthalenes amongst others), two artificial neural network models have been developed for predicting reactivity parameters ($\ln Q$ and e values) by performing density functional theory (DFT) calculations at the B3LYP/6-31G(d,p) level.¹³⁵ Dye labeled polymers were applied for the T_g prediction of polymers by calculation.¹³⁶ Homopolymers based on **N3** and **N4** were utilized, amongst several other polymers, for the quantitative structure–property relationship correlation of the dielectric constant (ϵ) for polymers.¹³⁷ **An1** was copolymerized with *N*-neopentyl methacrylamide in a free radical polymerization

procedure in order to produce structured polymer Langmuir–Blodgett films.¹³⁸ **Py2** as well as **Py5** were also used in labeled PS films for investigations on the influence of nanoscale confinement on the glass transition temperature.¹³⁹ Moreover, the π – π stacking behavior of copolymers composed of pentafluorostyrene (PFS) and **N3** or **N4**, respectively, was examined by the group of Pugh.¹⁴⁰

So far, polymers based on polymerizable naphthalenes were applied in mixed ligand monolith capillary column material.¹⁴¹ The composition (including octadecyl acrylate (ODA), **N2** and trimethylolpropane trimethacrylate (TRIM) crosslinker) of the column material was altered. The separating capacity of a series of low molar mass organic molecules of this reversed-phase column material dependent on the composition is depicted in the corresponding chromatograms in Fig. 5.

Polymers derived from **N6** as well as **N7** were applied for load bearing hydrogel implants.¹⁴² The invention features dual network hydrogels that possess the structural, mechanical and biological properties required of load-bearing three-dimensional support structures.

Azo-dyes

The striking property of azo-dyes is the reversible photoinduced *cis*–*trans* isomerization and, thus, this class of dyes is mainly applied in switchable electronic devices or sensors. Nowadays, the **Azo1** (derived from the standard dye disperse orange 3) as azobenzene moiety containing monomer is commercially available (the schematic representation of the chemical structures of all azo-dye containing monomers are depicted in Scheme 3). Its synthesis under mild conditions as well as its copolymerization with BA, EtA and MMA was described by Qui and coworkers.¹⁴³ The polymers revealed a good stability and prevented an undesired phase separation behavior and chromophore precipitation. Furthermore, Nicolescu and coworkers provided a detailed synthesis and characterization of a series of azobenzene functionalized methacrylates (**Azo2** to **Azo6**).^{144,145} The monomers were copolymerized with MMA by FRP using AIBN as initiator in dioxane and their reactivity ratios ($Q\text{-}e$ values) were determined. The authors also applied detailed characterization methods including ¹H NMR, UV-vis, FTIR, SEC and DSC-TGA measurements.

Kannan *et al.* prepared a series of polymerizable azonaphthol dyes, which were functionalized with a variety of electron withdrawing as well as electron releasing groups (**Azo7** to **Azo15**).¹⁴⁶ The polymerization was achieved by a free radical polymerization procedure in THF using AIBN as initiator at 60 °C. Holographic grating formation studies were performed, whereas the diffraction grating efficiency was dependent on the time of exposure and intensity ratio of the incident laser beam. The grating efficiency of the polymers bearing the electron withdrawing substituents increased in comparison to the others. In addition, the authors prepared homopolymers from **Azo16** and **Azo17** as well as copolymers derived from one of these two monomers and a fulgimide functionalized monomer.¹⁴⁷ The FRP technique was applied using AIBN as initiator in THF at 60 °C. The copolymers

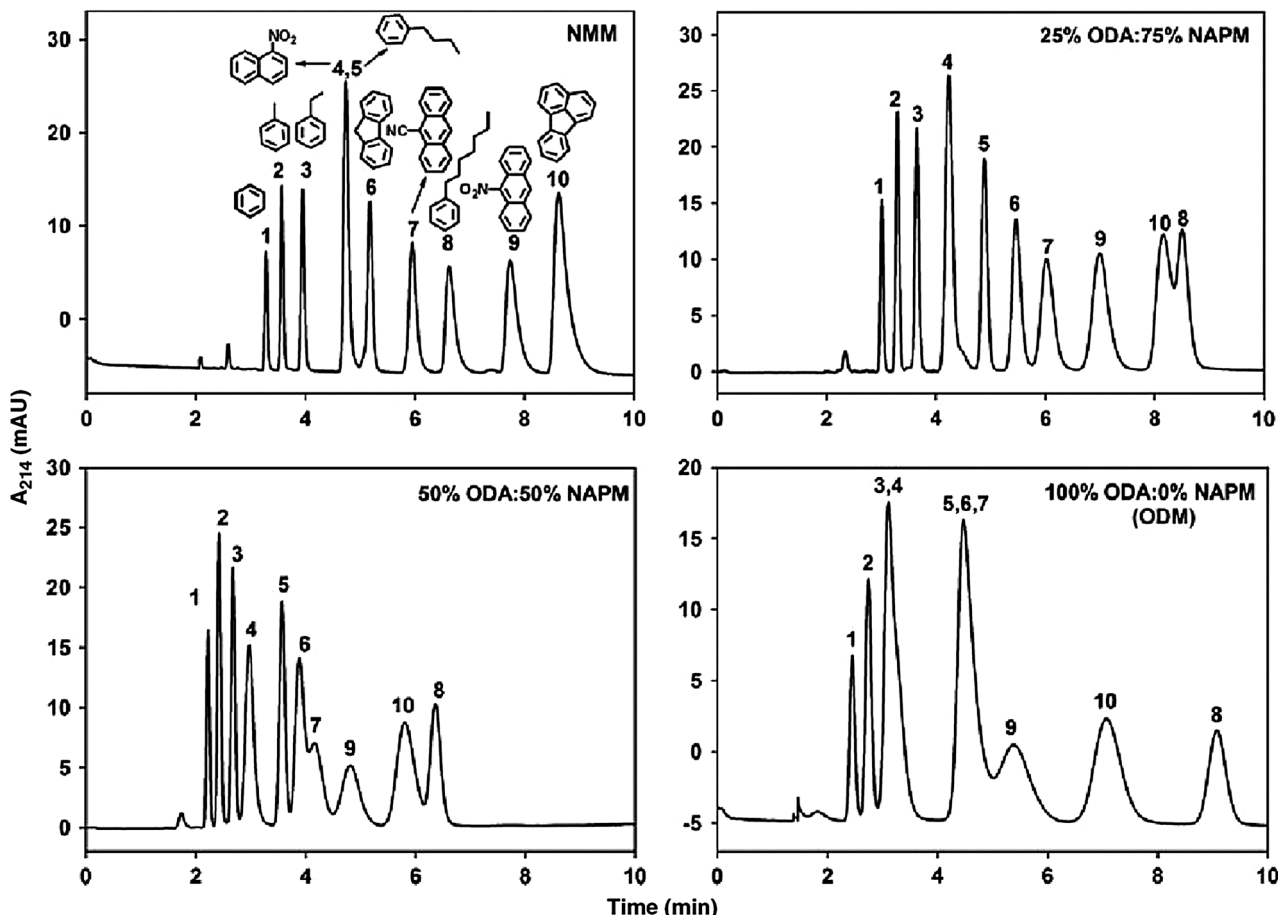


Fig. 5 Electrochromatograms showing the separation of a series of small organic compounds on monolithic columns with different mole fractions of ODA/N₂. NMM = 100% ODA.¹⁴¹ Figure copyright John Wiley and Sons and reproduced with permission.

revealed dual-mode optical switching properties due to the reversible *cis-trans* isomerization of the azobenzenes and the irreversible *cis-trans* isomerization of the fulgimide moiety (for the structure, see the **Fu** dye in the “Others” section, Scheme 14).

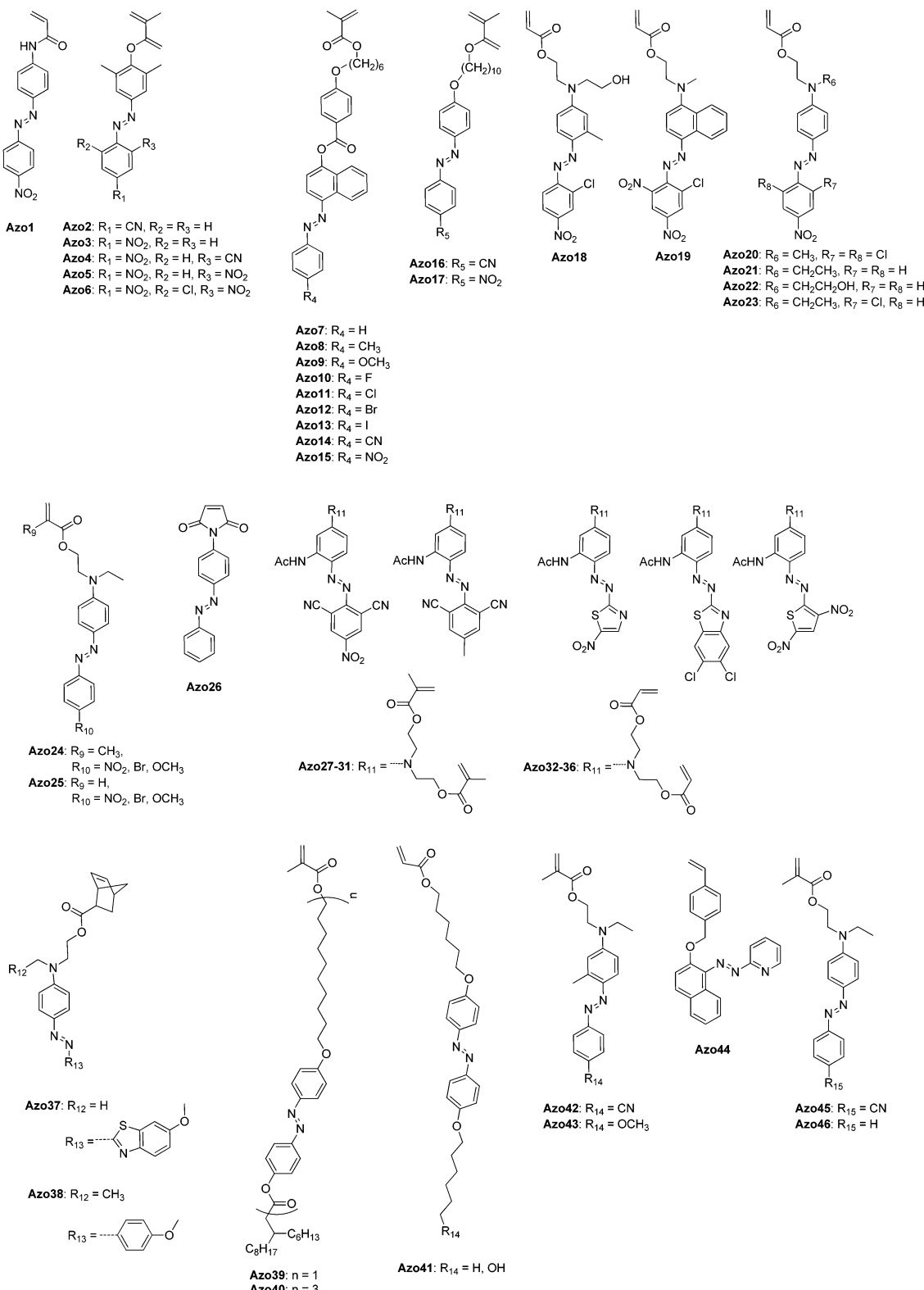
Colored pigments are usually applied in electronic inks. As a substituent thereof, Feng and coworkers cross-linked **Azo18** to **Azo23** as well as **Azo1** with divinylbenzene (DVB) and styrene.¹⁴⁸ These electrophoresis particles were applied for electronic inks. The particles revealed diameters between 200 and 300 nm in combination with a uniform spherical shape. This electrophoresis particle producing process overcomes the problem of the uneven shape of the organic dye particle's defects and the poor movement effect in disperse liquids under the influence of an electric field.

A more sophisticated characterization of the optical properties of azo-dye containing polymers was reported by Lu *et al.* The authors investigated the third-order nonlinear optical properties of the polymers based on **Azo24** and **Azo25**.¹⁴⁹ The ATRP technique was applied for the homopolymerization as well as for the copolymerization with MMA using ethyl 2-bromo isobutyrate, CuBr and PMDETA in cyclohexanone solution. All polymers revealed narrow PDI values. The influences

of the different substituents on the optical properties and the kinetics of the polymerization reaction were discussed. The materials revealed a high $\chi^{(3)}$ of about 10^{-11} esu and a rapid response time in the femto-second magnitude.

As example for an electronic device, Xu and coworkers produced memory devices using copolymers containing a maleimide functionalized azo-dye **Azo26** as comonomer in the active layer.¹⁵⁰ For this purpose, the azobenzene monomer was copolymerized with styrene as well as a carbazole functionalized styrene derivative in a FRP procedure. The introduction of the carbazole moieties reduced the voltage difference from the OFF to the ON state in the devices. The current-voltage (*I-V*) curves of the two copolymers are depicted in Fig. 6.

A series of azo-dye derivatives (blue, magenta, violet and red color depending on the substituent), which consist of two cross-linkable acrylate or methacrylate groups (**Azo27** to **Azo36**) in order to improve their thermal as well as their chemical resistance, have been synthesized by the group of Jaung.¹⁵¹ The materials were applied as color filters based on pigments instead of the established dispersion process. Moreover, surface morphology studies showed the capability of the dyes to act as photoresists.

**Scheme 3** Schematic representation of monomers bearing pendant azobenzene moieties.

In contrast to the electronic device applications, polymers composed of polymerizable azo-dyes can also be applied as sensor materials. The group of Abd-El-Aziz functionalized an

aryl azo-dye as well as a hetaryl azo-dye (**Azo37** and **Azo38**) with a norbornene moiety, which is suitable for ring opening metathesis polymerization using a 2nd generation Grubbs

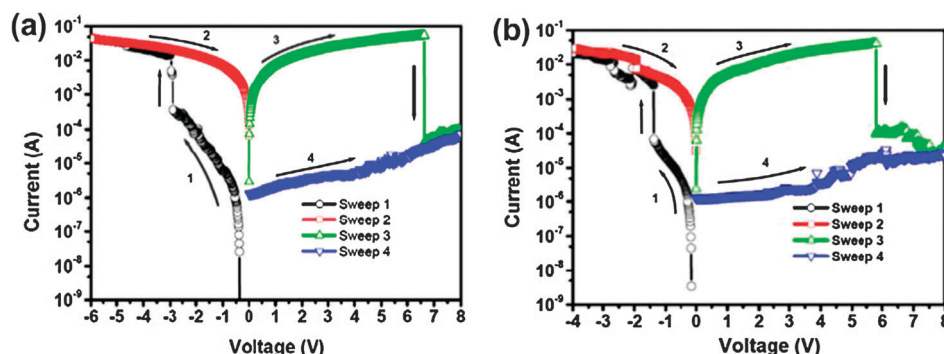


Fig. 6 Current–voltage (I – V) curve of the memory device based on PS-co-PAzo26 (a) and PStCz-co-PAzo26 (b) using a Hg top electrode.¹⁵⁰ Figure copyright Elsevier and reproduced with permission.

catalyst.¹⁵² Fig. 7 shows the absorption spectra of the *trans*–*cis* photoisomerization as well as the thermal *cis*–*trans* isomerization of selected copolymers. The synthesized homo- and copolymer films were tested as reusable acid sensors. The material also

changed the color upon variation of the pH value. Furthermore, the authors described methacrylates bearing an azo-dye-coumarin combination as dye.¹⁵³ For details, see the coumarin section (**Cou31**, **Cou32**, **Cou34**, **Cou36** to **Cou38**).

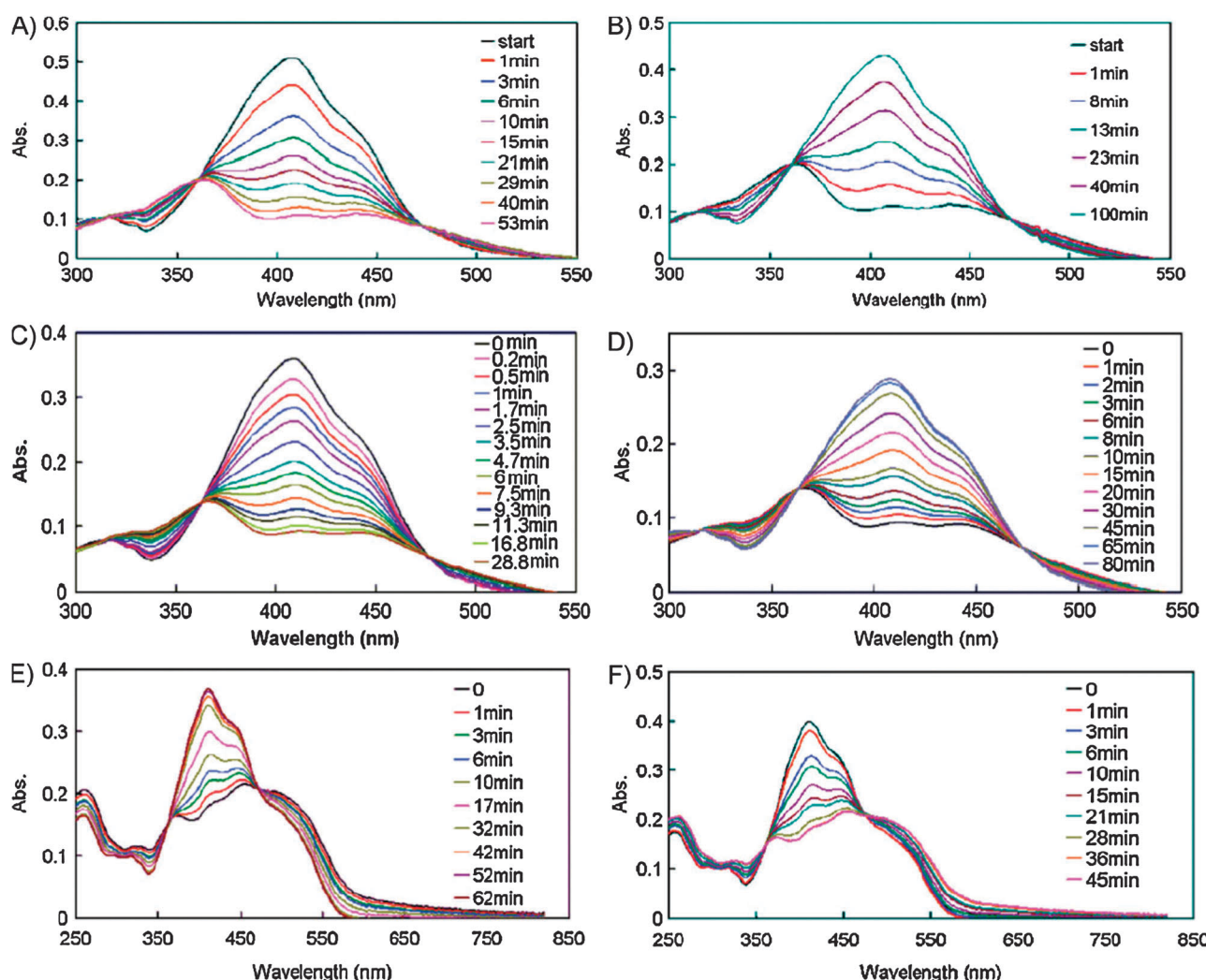


Fig. 7 UV-vis absorption spectra of selected copolymers containing Azo37 or Azo38 of the *trans*–*cis* photoisomerization (left column, (A), (C) and (E)) as well as the reversible thermal *cis*–*trans* isomerization (right column, (B), (D) and (F)).¹⁵² Figure copyright John Wiley and Sons and reproduced with permission.

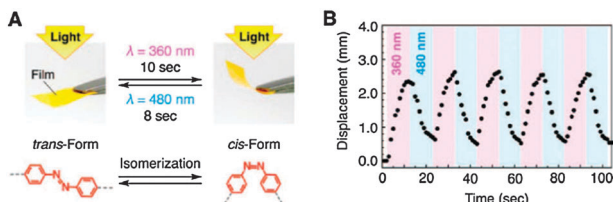


Fig. 8 Photomechanical responses of hot-pressed films of poly(Azo40) prepared with parallel arranged Teflon sheets. (A) Photographs of a hot-pressed film (5 mm by 6 mm by 10 mm) before (left) and after (right) exposure to UV light ($\lambda = 360 \pm 2$ nm). The bent film recovered the initial flat shape upon exposure to visible light ($\lambda = 480 \pm 2$ nm). (B) Time-dependent change in displacement of the free edge of a hot-pressed film prepared with parallel-arranged Teflon sheets upon alternating irradiation with UV and visible lights.¹⁵⁴ Figure copyright AAAS and reproduced with permission.

Aida and co-workers published the synthesis of molecular bottlebrushes using **Azo39** as well as **Azo40** as monomers.¹⁵⁴ In this context, a FRP procedure using AIBN as initiator in benzene was applied. The authors could fabricate a free-standing film with a specific alignment (*i.e.*, vertical alignment of the backbone relative to the plane and horizontally aligned side-chains) of the macromolecules. For this purpose, a hot-pressing method between Teflon sheets was utilized. The material featured a reversible bending behavior on a macroscopic scale under UV- and visible light irradiation due to the *cis*-*trans* isomerization of the mesogenic side-chains. Fig. 8 shows the displacement of the polymer film. A similar effect could be demonstrated by Ikeda *et al.* using **Azo41** in liquid-crystalline polymer fibers.¹⁵⁵

Furthermore, a dual-responsive polymer was obtained by copolymerization of **Azo24** ($R_{10} = NO_2$) with DEGMA.¹⁵⁶ The group of Schubert applied the RAFT polymerization technique using AIBN as initiator and CBDB as chain-transfer agent in toluene at 70 °C. The chromophore of disperse red 1 combined with the LSCT behavior of the DEGMA comonomer leads to a color change upon the variation of the pH value and the temperature. Images of the color changes are depicted in Fig. 9. Furthermore, the authors also copolymerized the azo-dye with MMA in the same manner for the investigation of the UCST behavior of PMMA.⁸⁶ However, the UCST sensing regime of the PMMA is much broader than the one of the analogous LCST polymer.



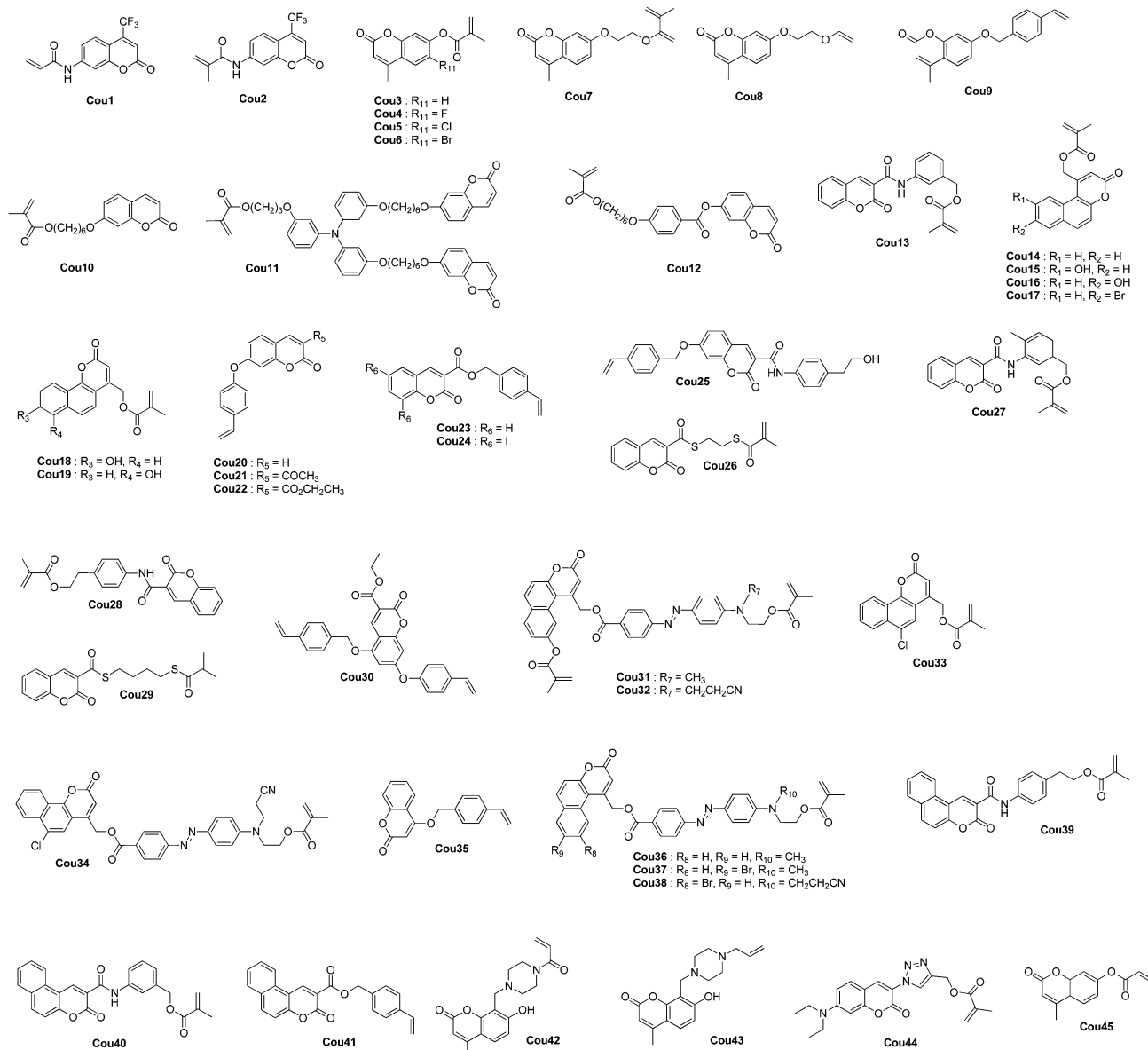
Fig. 9 Photograph images of the observed color shifts above and below the LCST temperature of copolymer P(DEGMA-co-**Azo24**) in aqueous solution at pH 7 (left) and pH 1 (right).¹⁵⁶ Figure copyright John Wiley and Sons and reproduced with permission.

Zhu *et al.* polymerized **Azo42** and **Azo43** in a controlled manner using the RAFT polymerization procedure.¹⁵⁷ For this purpose, CPDB was utilized as chain-transfer agent and AIBN as initiator in anisole as solvent at 80 °C. Furthermore, the authors applied these homopolymers as macro chain-chain transfer agent for the preparation of PS block copolymers. Controlled radical polymerization behavior was proven by a kinetic study. The photoinduced *trans*-*cis*-*trans* isomerization rate of the polymers was determined in chloroform solution. The kinetics of this isomerization displayed a dependence on the different CN and OCH₃ substituents. The CN substituted **Azo42** revealed a much faster isomerisation rate due to the donor-acceptor effect of the substituted azobenzene. Moreover, photoinduced birefringence and surface relief grating of the homopolymers were investigated in thin films. In addition, the group synthesized a PS-copolymer containing **Azo44** as comonomer using the RAFT polymerization technique.¹⁵⁸ In contrast to **Azo42** and **Azo43**, respectively, DMF was used as solvent and 2-cyanoprop-2-yl-1-dithionaphthalate (CPDN) as RAFT agent. In this case, the chain was also extended by a further PS block under application of the macro-RAFT agent approach. The polymer was capable of forming complexes with metal ions, *i.e.* Cu(II) and Eu(III), and is therefore suitable for application as a metal ion sensor.

Coumarins

It has long been known that the absorption and the emission behavior of coumarins can be tuned depending on their functionalization. Nowadays, only the acrylamides and the methacrylamides of CF₃-functionalized coumarin dyes **Cou1** and **Cou2** (Scheme 4) are commercially available (derivatives of Coumarin 120). A copolymer of **Cou1** and MMA was successfully applied in an OLED by Haishi *et al.*^{159–161} So far, this was the only example of application in organic electronic devices.

The group of Qiao prepared a PMMA-*b*-P(**Cou2**) block copolymer using ATRP as the controlled polymerization technique.¹⁶² The general tendency of the coumarin dye to dimerize under certain UV-irradiation wavelengths was utilized to form star-shaped polymers bearing fluorescent cores. Furthermore, Hampp and coworkers studied the copolymers containing **Cou3** to **Cou6** for application as intraocular lenses.¹⁶³ The variation of three halide substituents, in particular F, Cl and Br, caused increased dimerization rates and decreased the energy dose required for photochemical dimerization of the coumarin side groups. Furthermore, these materials enabled the tuning of the focal length of an already implanted intraocular lens by 2 diopters. In addition, Wang *et al.* demonstrated a reduced decoloration of a copolymer bearing naphthopyran and **Cou7** moieties in the side-chains due to the preferred dimerization of the coumarin in comparison to the photo-induced ring-opening of the naphthopyran.¹⁶⁴ The copolymers were obtained by ATRP using CuBr complexed with PMDETA as catalyst and ethyl-bromo-isobutyrate as initiator. In contrast, a living cationic polymerization of **Cou8** was reported by Minoda and coworkers.¹⁶⁵ For this purpose, SnCl₄ and a tertiary ammonium salt were applied for the polymerization procedure in order to obtain homopolymers as well as



Scheme 4 Schematic representation of the monomers functionalized with coumarin dyes.

amphiphilic diblock copolymers. The homopolymers revealed reversible photoinduced crosslinking features due to the dimerization of the coumarin moiety.

Finally, Liu *et al.* synthesized an amphiphilic copolymer by FRP using maleic anhydride, styrene and **Cou9** as monomers.¹⁶⁶ The polymer revealed a self-assembly to colloids in a selective solvent mixture, *i.e.* DMF–H₂O. Additionally, the emulsification and encapsulation of these colloid particles were investigated. It could be demonstrated that UV cross-linked particles (by coumarin-dimerization) revealed enhanced emulsification and encapsulation of oil-soluble dyes.

Coumarin containing polymer films based on **Cou10** to **Cou12** were investigated in terms of effects of dilution, polarization ratio, and energy transfer on the photoalignment of the nematic liquid crystalline material E-7 (a commercially

available LC mixture consisting of several cyanobiphenyls with long aliphatic tails used for the manufacturing of LC displays).¹⁶⁷ Chen and coworkers obtained the polymers utilizing the corresponding monomers by FRP using AIBN as initiator. Adverse effects on a nematic cell's number density of disclinations and its orientational order parameter in the parallel but not the perpendicular regime were observed by dilution of coumarin by inert moieties. In addition, the extent of coumarin dimerization at crossover, X_c , was lowered both by dilution of coumarin and a decreasing polarization ratio.

Abd-El-Aziz and coworkers extensively studied the field of polymerizable coumarin dyes concerning the thermal properties of the resulting polymers, in particular T_g as well as T_d values.¹⁵³ For this purpose, the authors provided a detailed synthetic description of a series of the monomers **Cou13** to

Cou41 and their corresponding homopolymers obtained by FRP using AIBN as initiator. In this context, the type of polymerizable unit – *e.g.*, methacrylate, styrene and methacrylamide – and the influence – *e.g.*, halides, –OH and azo-mieties – of a wide range of substituents were discussed in detail. All polymers were highly insoluble or poorly soluble in common organic solvents and displayed glass-transition temperatures between 70 and 130 °C. These polymers also revealed a high thermal stability. For selected samples, fluorescence quantum yields of $\Phi_F = 0.1$ were determined.

Related to sensor applications, polymerizable coumarin dyes were also discussed in the literature: Su and coworkers prepared a water-soluble copolymer based on VP or acrylamide as well as **Cou42** and **Cou43**, respectively.^{168–170} These materials were applied as chemosensors for protons and Ni²⁺ ions. In this case, the authors took advantage of the ability of the piperazine moiety to quaternize under protonation as well as its ability to act as chelating ligand for metal ions.

In addition, Zhu and coworkers provided a versatile approach for the functionalization of dyes by click-chemistry.¹⁷¹ For this purpose, an azide-substituted coumarin dye was converted with propargyl methacrylate in order to form the clicked coumarin monomer **Cou44**. A RAFT polymerization procedure including a kinetic study finally proved the suitability of the monomer for this type of controlled radical polymerization procedures. In addition, the resulting polymer was capable of forming Eu(III) ion complexes.

With respect to biological applications, **Cou2** labeled polymer nanoparticles were injected into a living pig by Grinstaff and coworkers.⁴⁰ The migration of the particles over 20 cm to the sentinel lymph node could be monitored.

Patel *et al.* tested the antimicrobial properties of **Cou45** based homo- and copolymers with vinyl acetate (VAc) against selected microorganisms, *i.e.* bacteria, fungi and yeast.¹⁷² Fig. 10 shows a reduced growth of these microorganisms dependent on the **Cou45**-content in the obtained (co)polymer films. **Cou45** homopolymers revealed the best antimicrobial performance, which can be tuned by the subsequent addition of VAc as comonomer. Furthermore, the authors provided reactivity ratios for the copolymerization behavior of the fluorescent dye according to three linearization methods.

Fluorescein

Fluorescein is a very common dye that is used for labeling purposes. Actually, it belongs to the class of xanthene dyes, but the large amount of publications based on polymerizable fluorescein containing polymers made it necessary to dedicate fluorescein an own section. The chromophore reveals a typical UV-vis absorption band at approximately 490 nm as well as an intensive green fluorescence ($\lambda_{em} = 520$ nm). Generally, fluorescein isothiocyanate (FITC) is applied to label antibodies, enzymes, proteins or polymers in order to visualize the cellular uptake of the labeled substances. Scheme 5 shows the structures of seven different polymerizable fluorescein containing monomers **Fl1–Fl7**, whereas **Fl1** and **Fl2** are commercially available from Sigma-Aldrich.

With respect to future biological applications of the labeled polymers, **Fl1** or **Fl2** were copolymerized with a wide range of different monomers, including NIPAM and *N*-acryloxsuccinimide (NAOS),¹⁷³ HEMA,¹⁷⁴ NIPAM, AA, *N*-*tert* butyl acrylamide (TBAM) and *N,N'*-methylenebisacrylamide (BIS),¹⁷⁵ styrene,^{176,177}

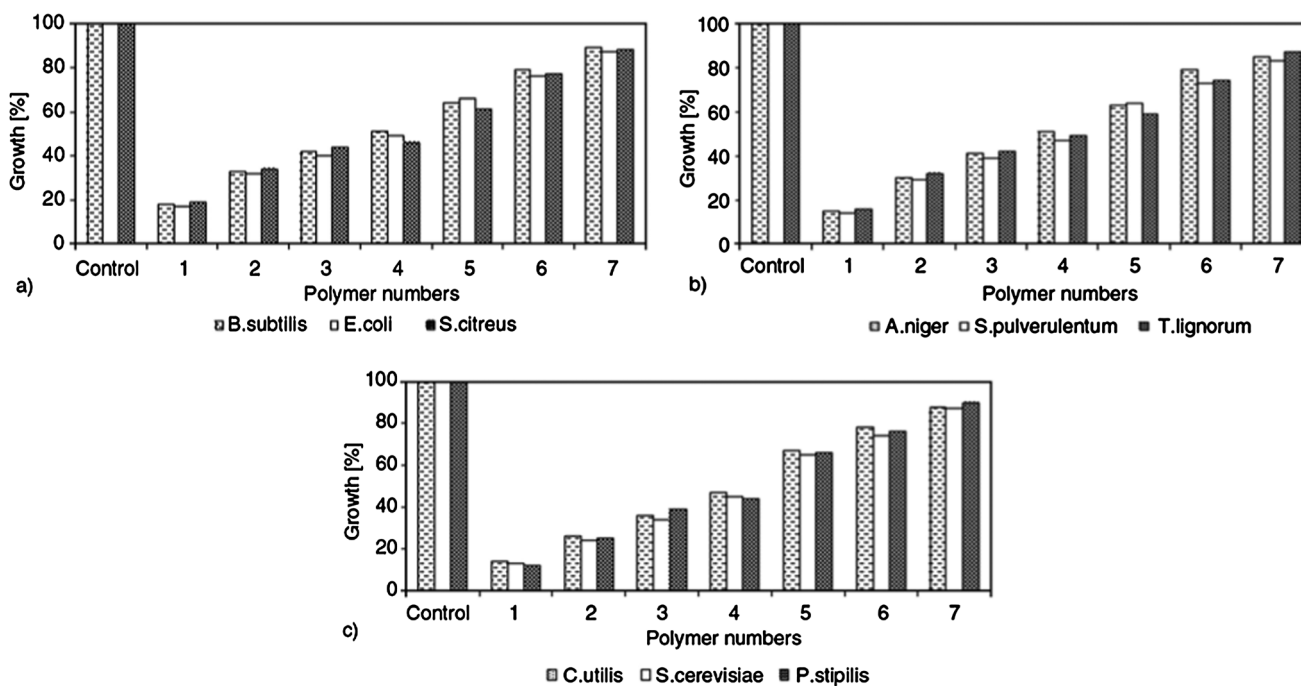
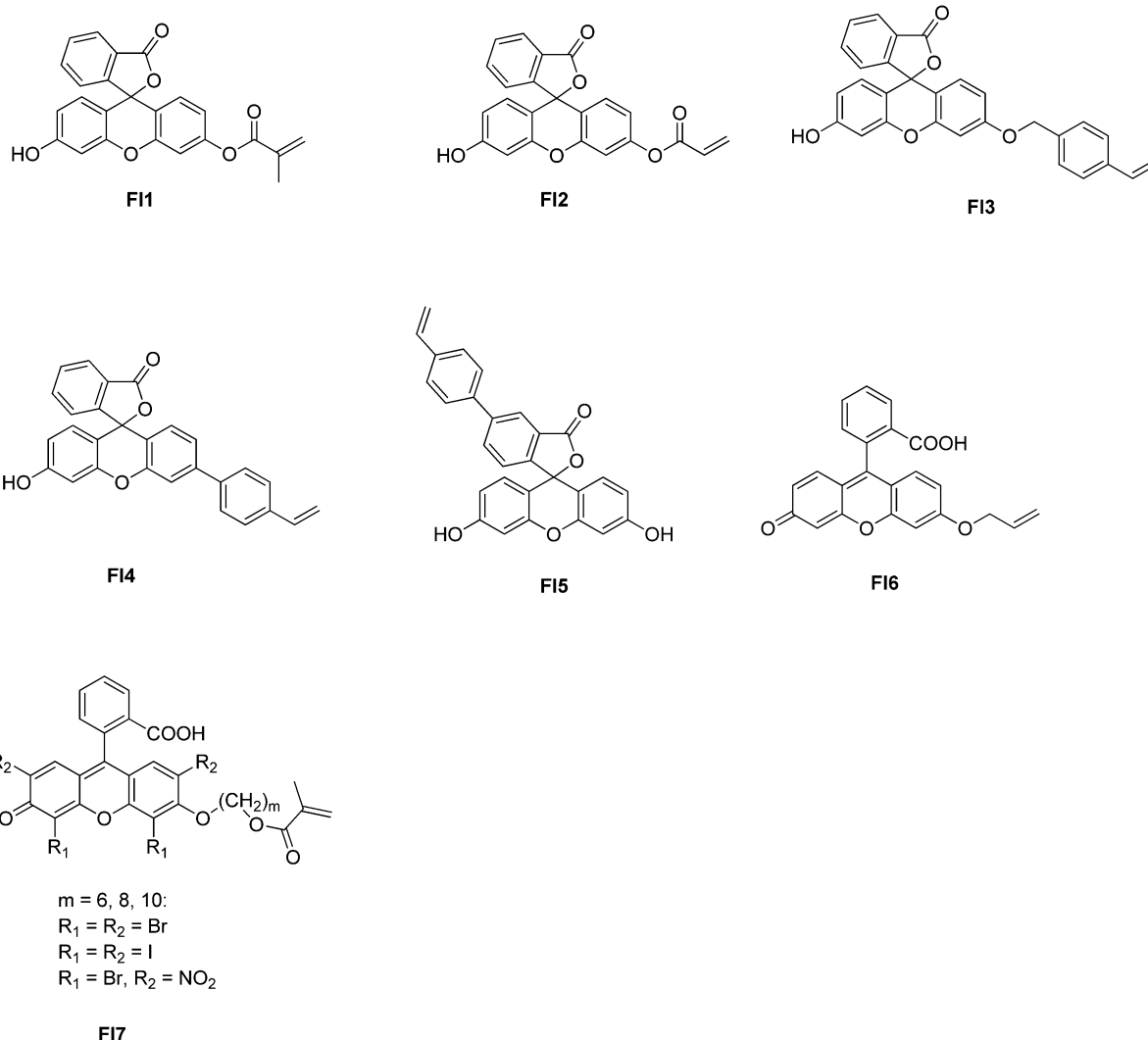


Fig. 10 Effect of P(Cou45-co-VAc) on the growth of (a) bacteria, (b) fungi and (c) yeast. The increasing polymer numbers indicate the increasing VAc-content (decreasing Cou45-content) of the samples.¹⁷² Figure copyright Xpress polymer Letters and reproduced with permission.



Scheme 5 Schematic representation of the polymerizable dyes containing fluorescein as chromophore.

N-(3-aminopropyl) methacrylamide, poly(ethylene glycol) methacrylate (PEGMA) and BIS,^{178–180} 2-hydroxyethyl acrylate and PEG₅₇₅ diacrylate,¹⁸¹ as well as DVB,¹⁸² as label for fluorescence microscopy imaging. Additionally, Hwang could show that fluorescent, polyacrylic acid coated magnetic nanodiamonds could be ingested into HeLa cells.¹⁸³ Fl1 was used as dye-comonomer in these experiments.

The group of Guy performed particle penetration tests on porcine skin using PS, PMMA and poly(styrene-*co*-HEMA) polymer particles.^{184,185} Fl1 was added in small amounts during the polymer synthesis in order to label the particles which were able to deliver Nile red (NR) as model substance into the skin. In the case of PS-*co*-PHEMA polymer particles, the loading of the model drug was dependent on the hydrophobicity of the polymer that could be tuned *via* the styrene/HEMA ratio. It could be demonstrated that the NR was released and penetrated into deeper skin layers while the particles remained in the superficial stratum corneum layer. Fig. 11 shows the laser scanning confocal microscopy images of the skin surface

indicating the uptake of the labeled nanoparticles as well as the release of NR.

Furthermore, Fl1 was copolymerized with MAA using a free radical polymerization procedure by Stöver and coworkers in order to label cross-linked Ca-polyurea microcapsules and alginate beads, which could be further used to follow the encapsulation process in mouse cells.^{186,187}

The polymerizable methacrylate was also incorporated into cross-linked poly(*N*-vinylimidazole) hydrogels by Piérola and Pacios to investigate the swelling behavior of these hydrogels, in particular, the morphology and the cross-linking density in different media.¹⁸⁸

DeSimone and coworkers fabricated nanoparticles based on polymers bearing fluorescein pendant side chains.^{189–191} The PRINT method (Particle Replication In Non-wetting Templates) allows the production of monodisperse, shape-specific particles, in particular disk, rod, fenestrated hexagon (hexnut), and boomerang shapes, from an extensive array of organic precursors (for dimensions of different nanoparticle shapes, see Fig. 12).

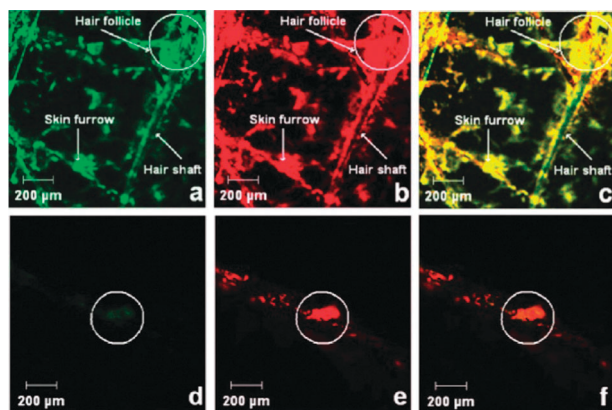


Fig. 11 Laser scanning confocal microscopy images of the skin surface after incubation with NR loaded **F11** labeled PS nanoparticles. Panels a and b show fluorescence emission from the skin surface from the NP (panel a) and NR (panel b), respectively. Panel c shows the overlay of panels a and b and the colocalization of NP and “active” at the skin surface. Panels d and e illustrate cross-sectional images, respectively, highlighting fluorescence from the NP and from NR. A distinctly labeled, short, trimmed hair is visible. Panel f is the overlay of panels d and e and suggests some permeation of released NR to the deeper skin layers. Reprinted with permission from ref. 184. Copyright 2009 American Chemical Society.

Particle	Primary Axis (μm)	Secondary Axis (μm)	Tertiary Axis (μm)	Surface Area (μm ²)	Volume (μm ³)	SA:Vol	Aggregation Threshold (minutes)
Hexnut	2.9	2.5	1	21	4.6	4.56	44.5
Rod	5	1.6	1.6	37.1	12.8	2.89	39
Disc	6.1	1	-	82.7	26.5	3.12	-
Boomerang	-	1	-	146	53.7	2.71	9

Fig. 12 Table of dimensions of the different shapes of nanoparticles produced by the PRINT method. Reprinted with permission from ref. 191. Copyright 2008 American Chemical Society.

Furthermore, it is possible to control the size of the nanoparticles using this technique as representative of the “top-down” strategy. As a consequence, sufficiently small particles ($d = 200$ nm) can be taken up by cells. An additional feature of these particles is the specific alignment of the polymer chains in each type of shape. One utilized polymer is composed of poly(ethylene glycol) monomethylether methacrylate, trimethylolpropane ethoxylate triacrylate as cross-linker, 2-aminoethyl methacrylate hydrochloride and **F12**. The group determined the cellular internalization of cylindrical particles as well as the cytotoxicity on HeLa, NIH 3T3, OVCAR-3, MCF-7, and RAW 264.7 cells. No significant cytotoxicity was observed for the taken up particles. Furthermore, the authors succeeded to postfunctionalize the PRINT particles with human/bovine

transferrin through lysine-maleimide reactions, resulting in a highly specific transferrin-mediated uptake by all human tumor cell lines tested. Besides the PRINT process fabricated particles, DeSimone *et al.* could synthesize fluorescein labeled di- and triblock copolymers.¹⁹² The hydrophobic blocks contained basically trimethylolpropane ethoxylate triacrylate (TETA) and **F12**, whereas the hydrophilic part was composed of mono-hydroxytetraethyleneglycol methacrylate (HP₄MA), poly(ethylene glycol) diacrylate (PEG₇₀₀DA) and a rhodamine B carrying red fluorescent monomer (**Rh1**, Scheme 7, rhodamine section). The self-assembly into ribbons and bilayers could be visualized *via* fluorescence microscopy.

For additional biological studies, Bradley *et al.* performed systematic copolymerizations of alternatives to the commercial available polymerizable fluoresceins based on styryl functionalities as polymerizable unit.³⁴ For this purpose, the polymerizable unit was introduced on three different positions: analogous to the commercially available acrylate and methacrylate, *O*-styryl fluorescein **F13** could be obtained in good yields, while the xanthine-styryl fluorescein **F14** and phthalic-styryl fluorescein **F15** were synthesized in moderate yields by various cross-coupling reactions. The fluorescence intensity of the fluorescein incorporated polymer nanoparticles was compared to commonly used 5(6)-carboxyfluorescein surface-labeled polymer nanoparticles as reference. With exception of nanoparticles based on **F14**, the particles revealed an insignificant loss of fluorescence intensity in comparison to the reference samples. As expected, the fluorescence of **F14** is significantly lowered by the interference with the conjugated system by suppressing the fluorescent anionic quinone form. Finally, the polymer nanoparticles were investigated in terms of cellular uptake using human embryonic kidney cells (HEK293T) as well as human cervical cancer cells (HeLa). In conclusion, the attachment of the polymerizable functionality to the chromophore affects the fluorescence intensity but not the absorption and emission maxima.

Stenzel *et al.* functionalized honey comb structured films with RAFT agents and subsequently polymerized **F12** on the surface.¹⁹³ After a washing step, the structure of the porous film could be visualized *via* fluorescence microscopy. Furthermore, the group of Stenzel successfully bound biodegradable glycoparticles bearing glucose units to plant lectin (Concanavalin A, *Canavalia ensiformis*) and bacteria lectin (fimH, from *Escherichia coli*).¹⁹⁴ The particles were prepared by a controlled RAFT polymerization using styrene, 2-(methacrylamido)glucopyranose and a disulfide diacrylate cross-linker. **F12** was added during the cross-linking step.

In the context of sensing applications, Ionov coated red fluorescent microtubules with a brush-like PNIPAM and **F12** containing polymer.¹⁹⁵ The brushes were synthesized using the ATRP technique. The authors showed a stimuli-responsive behavior under the influence of the temperature, whereas the coating could swell at temperatures below 35 °C. The swollen microtubules revealed an overlapping emission of the red core and the green fluorescein, while the collapsed species was only red emissive. The fluorescence images of the

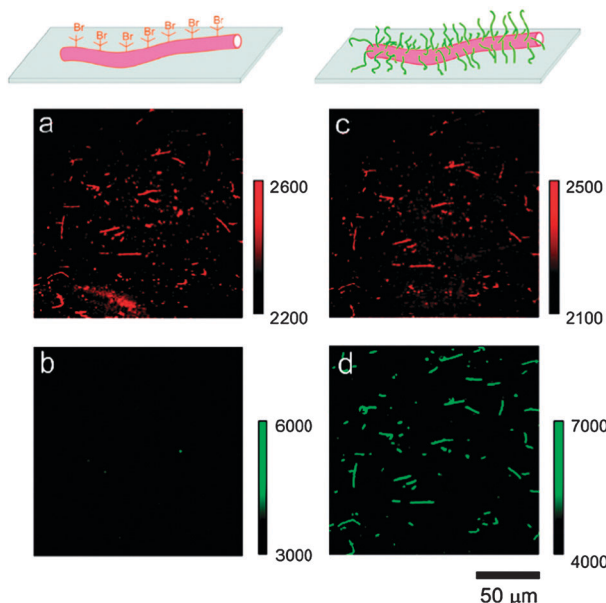


Fig. 13 Epi-fluorescent images of surface-adsorbed microtubules after immobilization of initiator (a: microtubule signal, b: polymer signal) and after grafting of poly(*N*-isopropylacrylamide-*co*-fluorescein *O*-acrylate) (c: microtubule signal, d: polymer signal).¹⁹⁵ Figure copyright Royal Society of Chemistry and reproduced with permission.

unfunctionalized as well as the functionalized microtubules are depicted in Fig. 13.

Matyjaszewski *et al.* prepared fluorescent comb-copolymers *via* a “grafting-from” reaction from a multifunctional methacrylate backbone polymer which contains ATRP initiator functionalities as side chains.¹⁹⁶ On this macroinitiator, the arms were grown in a controlled fashion using butyl acrylate (BA) and **Fl2** as monomers. The comb-polymer revealed a pH-dependent fluorescence response.

Further sensor materials were prepared by Syntska and coworkers. The authors coated wax particles with different specifically labeled polymers on each hemisphere, so-called Janus particles.¹⁹⁷ For that purpose, the particles were immobilized on relatively large silica particles in order to block one hemisphere from functionalization. A NIPAM-**Fl2** monomer mixture could be grafted from the free surface of the particles using the ATRP procedure. The one-side coated wax particles were removed from the silica particles and subsequently functionalized *via* grafting onto of red fluorescent rhodamine B (**Rh9**, see Scheme 7 for the exact structure in the rhodamine section) labeled PAAs and PVPs. The complete procedure is illustrated in Scheme 6. A stimuli-responsive aggregation-disaggregation behavior upon pH changes could be observed for selected particles.

Additionally, Lai and coworkers published a detailed synthesis and characterization of an allyl-functionalized fluorescein dye (**Fl6**) and its subsequent polymerization with acrylamide by FRP.¹⁹⁸ The material revealed a pH and temperature dependent behavior in solution. Although the monomer **Fl2** was already commercially available, the authors published the synthesis as

well as an analogous copolymer based on poly(acrylamide), again featuring the same behavior.¹⁹⁹

For the improvement of the mechanical properties of PMMA, Liu and Chan-Park coated disperse SWCNTs in dimethylformamide with poly[methyl methacrylate-*co*-(fluorescein *O*-acrylate)] as a surfactant, and subsequently fabricated the resultant poly(methyl methacrylate) (PMMA)-based nanocomposites *via* solution casting.²⁰⁰ This material revealed improved tensile properties *versus* pure PMMA, showing 56 and 30% enhancements of the tensile modulus and tensile stress, respectively.

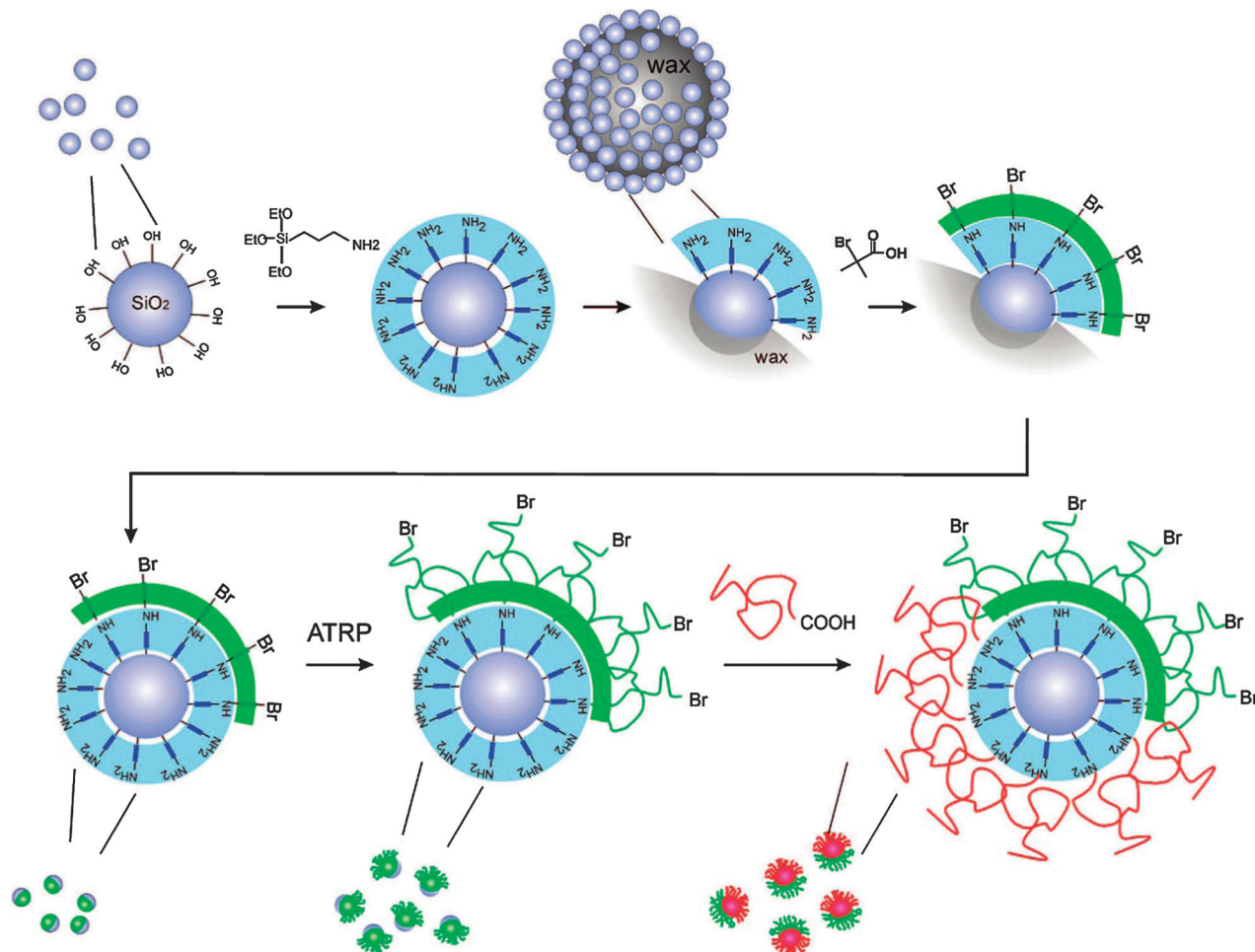
Amongst others, a **Fl2** containing polymer was further used for the separation of SWCNTs in terms of their metallicity and diameter by Chan-Park *et al.*¹⁰⁶ A poly(methyl-methacrylate-*co*-fluorescein-*O*-acrylate) polymer could enrich the semi-conducting fraction of SWCNTs in solution and, thereby, significantly enhance the performance of field effect transistors (FETs).

The group of Kannan provided the synthesis and subsequent free radical polymerization of **Fl7** for holographic grating studies.²⁰¹ The variation of the spacer-length showed an improved film formation for longer spacing units ($m = 10$) in comparison to shorter ones ($m = 6$). In contrast, the thermal stability decreases with increasing spacer length. Furthermore, the influence of the different substituents (*i.e.*, Br, I and NO₂) on the lifetime decay and diffraction efficiency was investigated. It could be shown that the different substituents affect the kinetics of the bleaching behavior of the polymers.

Rhodamines

Besides the green emitting fluorescein containing acrylates and methacrylates, the rhodamine functionalized monomers are the second largest group of polymerizable dyes. Similar to fluorescein, the rhodamines also represent a sub-group of xanthene dyes. Their intense red fluorescence ($\lambda_{\text{abs}} = 548 \text{ nm}$, $\lambda_{\text{em}} = 570 \text{ nm}$) cause a good contrast to the green fluorescence of fluorescein in confocal microscopy images. So far, the rhodamine B (bearing two diethyl amino substituents) is the most important representative which has been functionalized with polymerizable units. Scheme 7 depicts the structures of monomers (**Rh1** to **Rh9**) that have already been copolymerized. Furthermore, **Rh1** and **Rh2** are commercially available under the synonym “PolyFluor 570” from Polyscience. Carter *et al.* functionalized Lissamine rhodamine B with several polymerizable units, in particular, a methacryl functionality (**Rh3**) as well as a methacrylamide and an allyl unit.²⁰² Amongst these three monomers, only **Rh3** underwent free radical polymerization using DMF as solvent and AIBN as initiator. The synthesis of the monomer and the homopolymer is described in detail in this reference.

Barthélémy and coworkers prepared a PMMA based copolymer where cholesterol moieties and **Rh1** were introduced as comonomers.²⁰³ Having this terpolymer in hand, the authors performed *in vivo* cell uptake studies of this microsphere-forming material in mesostoma flatworms. Selected fluorescence microscopy images of labeled cells of the organism are depicted in Fig. 14.



Scheme 6 Schematic representation of the bicomponent Janus particles by “grafting from” and “grafting to” approaches. Reprinted with permission from ref. 197. Copyright 2008 American Chemical Society.

Further biological studies by Vauthier *et al.* included the synthesis of **Rh1** labeled core–shell nanoparticles composed of chitosan and an isobutylcyanoacrylate (IBCA)–isohexylcyanoacrylate (IHCA) mixture.²⁰⁴ Using these particles, the authors succeeded in delivering siRNA to tumor bearing mice.

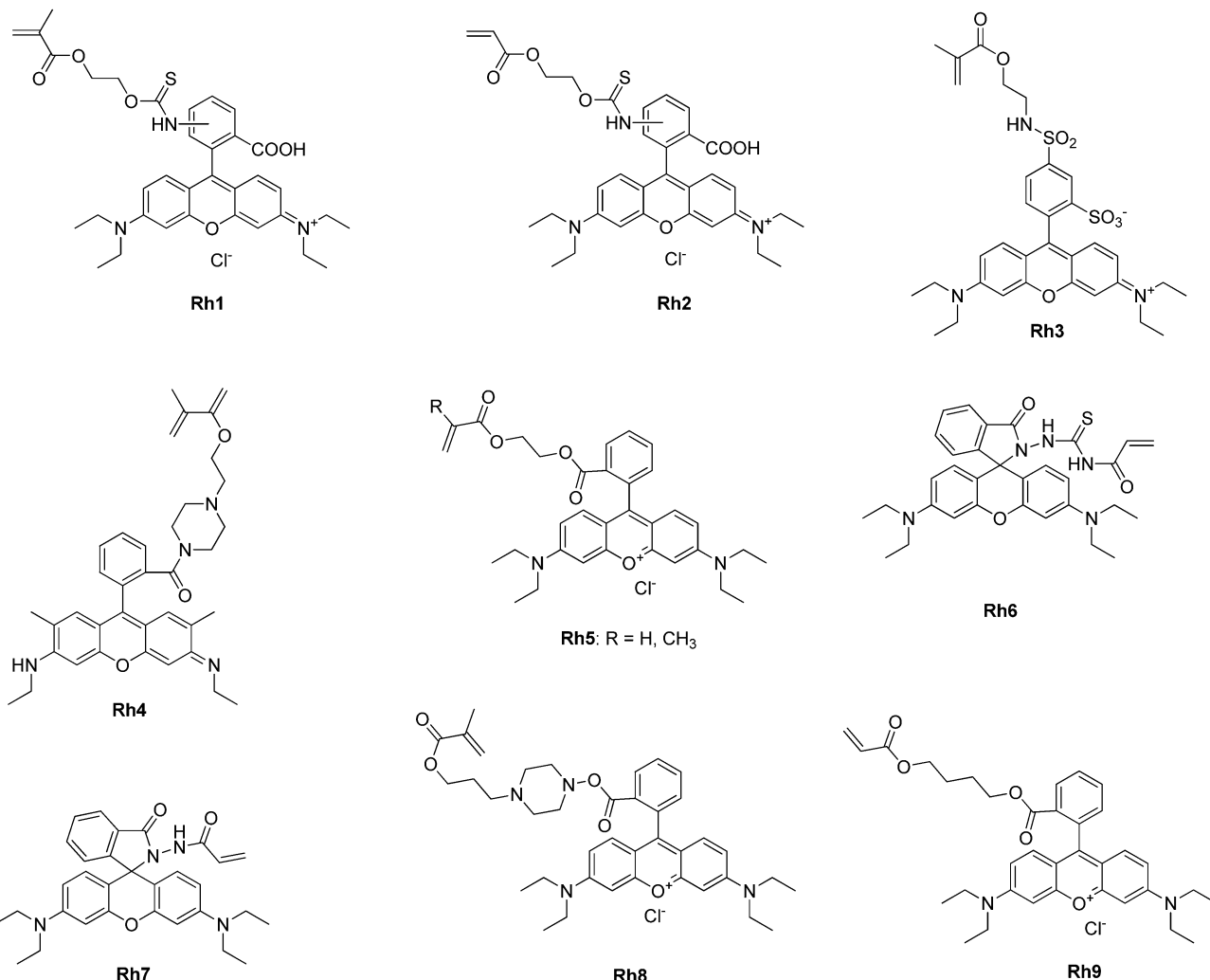
The group of Ishihara synthesized a copolymer consisting of **Rh1**, BMA and 2-methacryloyloxyethyl phosphorylcholine (MPC).²⁰⁵ The material is able to cell-penetrate non-endocytically or to fuse with plasma membranes without overt membrane disruption. With the help of this amphiphilic phospholipid polymer, the mechanism of direct cell-penetration was discovered.

Opaque microparticles on the basis of PEG₇₀₀ diacrylate and **Rh1** made *via* stop-flow lithography were reported by Doyle and coworkers.²⁰⁶ During this semicontinuous method for the fabrication of hydrogel particles, two anisotropies, in particular magnetic and geometric anisotropy, could also be introduced into the material. Furthermore, genotyping by alkaline dehybridization was reported using that material as substrates.²⁰⁷ The authors were able to discriminate single-nucleotide polymorphisms by the pH-value as an alternative to the

temperature-driven non-enzymatic discrimination. A schematic representation of the working principle of the stepwise cleavage of DNA under basic conditions is depicted in Scheme 8.

The only modification on the xanthene moiety of the rhodamine chromophore (**Rh4**) was described by Armes and coworkers.²⁰⁸ In this case, the rhodamine 6G was equipped with a polymerizable unit as well as an ATRP initiator functionality. The monomer was copolymerized with a biomimetic comonomer, the 2-(methacryloyloxy)ethyl phosphorylcholine (MPC) and 2-(diisopropylamino)ethyl methacrylate (DPMA) as block copolymer, using the ATRP technique. In contrast to the commonly applied rhodamine B monomers, **Rh4** is highly fluorescent at physiological pH-values.

Besides biological applications, the formation of three-dimensional hydrogel multilayers using the enzyme-mediated redox chain initiation method has been described by Bowman *et al.* using **Rh2** as well as a 2-hydroxyethyl acrylate (HEA)/PEG₅₇₅ diacrylate monomer mixture for the polymerization.¹⁸¹ One of the three layers was rhodamine labeled, while another was colored with fluorescein (**Fl2**, see fluorescein section, Scheme 5).



Scheme 7 Schematic representation of the polymerizable dyes containing rhodamines as chromophores.

Copolymers, in particular stimuli-responsive nanoparticles and microgels, composed of **Rh1** or **Rh2** as well as NIPAM, have been intensively studied in terms of temperature sensitive swelling/deswelling behavior,^{209–213} repeated transport of specifically assembled patterns by a reversible buckling process,²¹⁴ multi-agent delivery in core-stealth nanofibers,²¹⁵ thermo-responsive behavior of layer-by-layer coated nanogels,²¹⁶ and nanoparticle distribution in cells depending on the type of dye-attachment (*e.g.*, labile or covalent).²¹⁷

A FRET process was observed in polymeric ionic liquid polymers containing **Rh5** ($R = \text{CH}_3$) as comonomer.²¹⁸ For this purpose, **Rh5** was esterified using rhodamine B and 2-hydroxyethyl methacrylate, as reagents. A subsequent free radical polymerization using AIBN as initiator and two polymerizable ionic liquids yielded the final polymer.

Rhodamine containing copolymers were also investigated in terms of sensor materials. Liu and coworkers investigations focused on poly(ethylene oxide)-*b*-poly(*N*-isopropylacrylamide-*co*-**Rh6**) block copolymers, which revealed fluorescence after opening the nonfluorescent spirolactam form to an open amide

structure.²¹⁹ For this purpose, a thiourea functionality was introduced as spacer between the polymerizable group and the chromophore, which enables the switching on of the fluorescence either by Hg^{2+} ions or pH-values below 6. In addition, the fluorescence can be further enhanced by thermal induced micelle-formation (heating above 34 or 36 °C depending on the composition of the blocks), bearing the labeled NIPAM-block in the core. The polymers were obtained by using a PEO-RAFT agent as a macro-chain-transfer agent for the RAFT polymerization of NIPAM and **Rh6**. Upon substitution of the PEO block by a PS that was labeled with a second polymerizable dye [*i.e.*, 4-(2-acryloyloxyethylamino)-7-nitro-2,1,3-benzoxadiazole (**Oxa11**, see Scheme 14 in the oxadiazole section)], a FRET process was induced by the Hg^{2+} ions which could be enhanced by collapsing the poly(NIPAM)-block upon heating.²²⁰ Furthermore, a P(NIPAM-*co*-FITC)-*b*-P(PEGMA-*co*-**Rh7**) was prepared.²²¹ In contrast, **Rh7** does not reveal the Hg^{2+} sensitive thiourea functionality but still shows a pH-responsive behavior. At pH < 6, the polymers exhibit a green fluorescence, whereas the red emitting species is formed at higher pH-values.

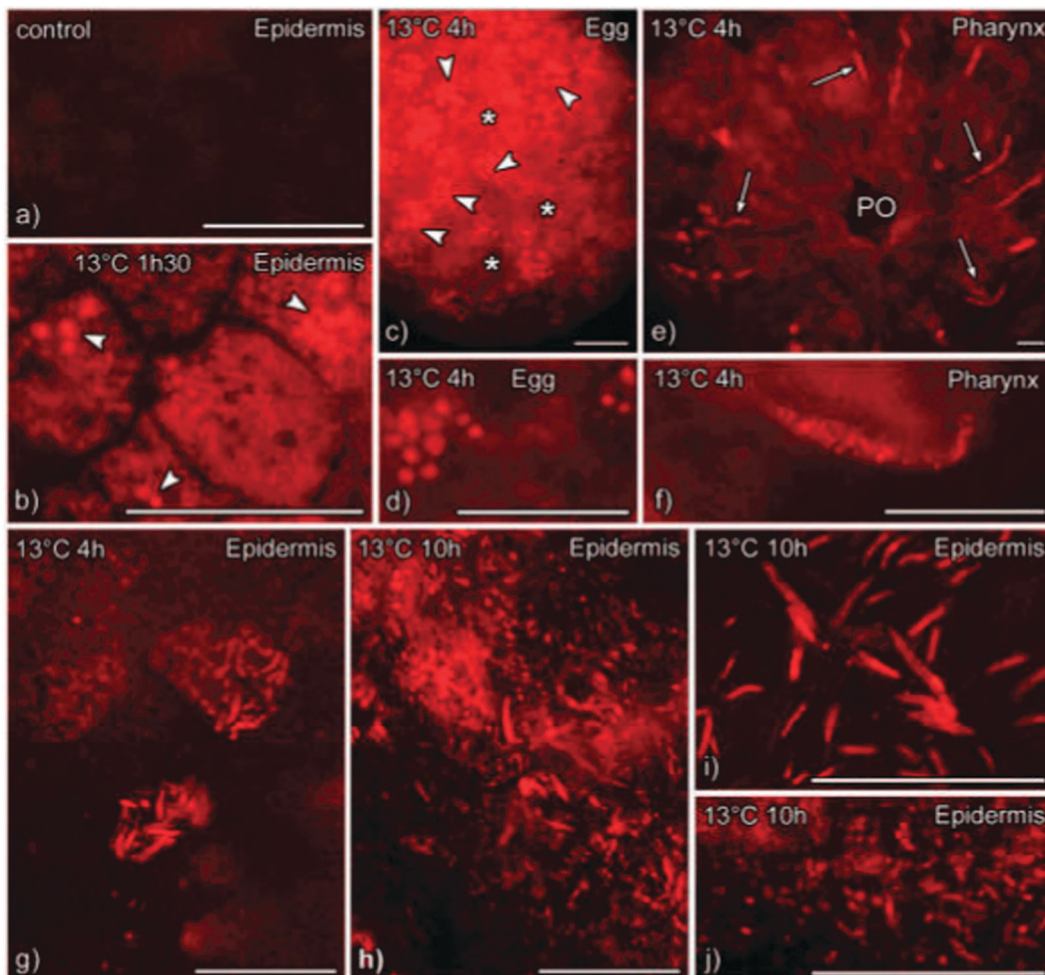


Fig. 14 Fluorescence microscopy images showing the *in vivo* uptake of rhodamine B-labeled amphiphilic copolymers ($5 \mu\text{g mL}^{-1}$) into certain cells in selected areas by *Mesostoma* flatworms at 13°C . Bars = $50 \mu\text{m}$. Reprinted with permission from ref. 203. Copyright 2008 American Chemical Society.

The collapsing of the NIPAM-block and simultaneous micelle-formation induces a FRET process upon heating the polymer. For further approaches, a P(St-*co*-Oxa11-*co*-Sp2)-*b*-P(NIPAM-*co*-Rh7) was synthesized.²²² Sp2 is a UV- and visible light switchable fluorescent spiropyran methacrylate monomer used to introduce an additional responsiveness depending on the type of irradiation (for exact structure, see Scheme 14 in the “others” section). In this way, another multi-responsive polymer was obtained. Scheme 9 shows the working principle of this polymeric-micelle-based reversible three-state switchable multicolor luminescent system. These states (*i.e.*, red emissive particle shell, orange emissive particle shell and green emissive particle shell) can be reached *via* pH-variation, selective irradiation, temperature variation as well as one combination of all parameters.

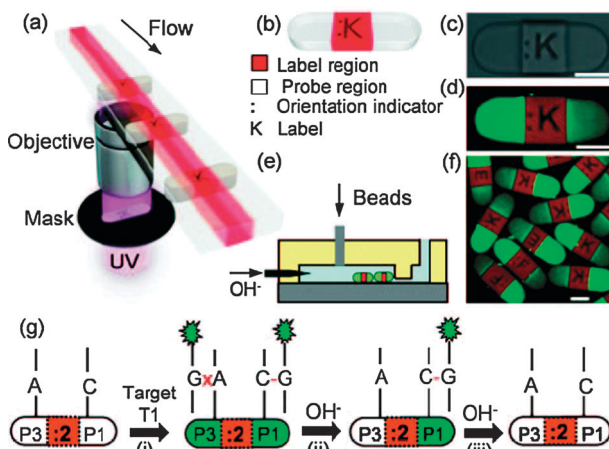
1,8-Naphthalimides

1,8-Naphthalimide functionalized monomers are synthetically accessible in moderate to very good yields by introducing substituents in the 4-position as well as on the nitrogen of the imide-functionality. The modification of the optical

properties or the introduction of additional tailor-made units is most frequently realized by amination of the 4-position on the aromatic system. In contrast, a functionalized imide-functionality can be obtained by imidation of the naphthalic anhydride using the corresponding amine. In every case, the introduction of the polymerizable unit, in particular allyl, acrylate- and methacrylate functionalities, does not significantly influence the optical properties of the chromophore. The structures of the polymerizable naphthalimides are depicted in Scheme 10. The typical synthetic routes and detailed characterization of 1,8-naphthalimides (**Nap1** and **Nap2**) that were copolymerized with MMA were reported by Khosravi *et al.*²²³

The groups of Yi and Zeng prepared photo-switchable nanoparticles by miniemulsion polymerization bearing **Nap3** as well as spiropyran-linked methacrylate moieties.²²⁴ The open or closed form of the spiropyran functionality enables or disables a FRET process upon UV or visible light irradiation, respectively, and, thus, the emission color of the nanoparticles can be switched from cyan to red.

Konstantinova *et al.* synthesized 1,8-naphthalimides bearing a polymerizable allyl functionality at the nitrogen atom of the

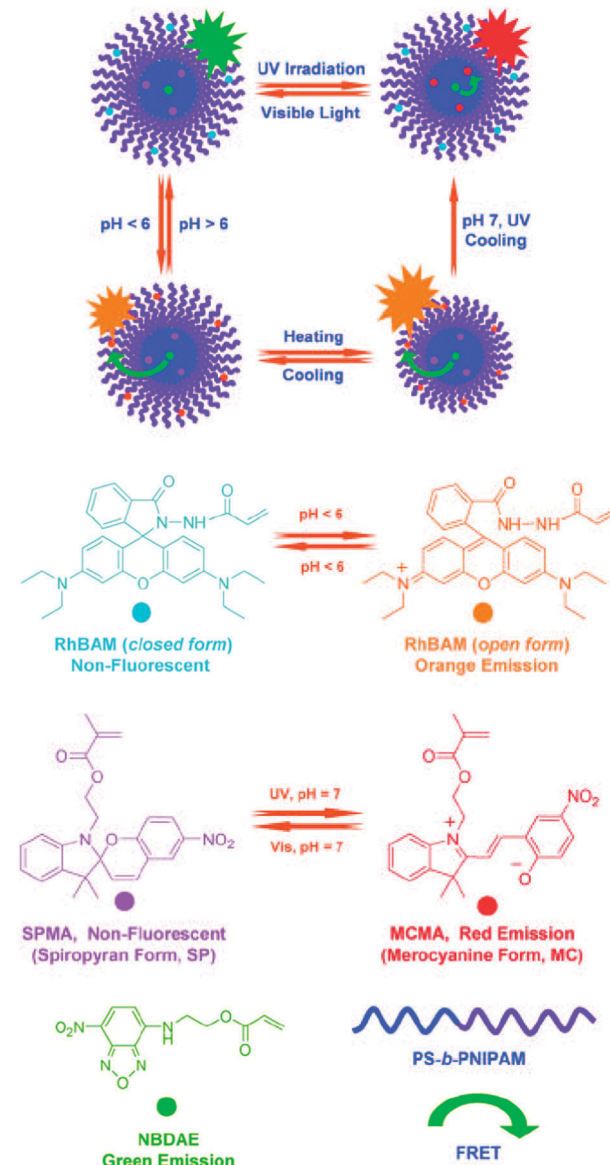


Scheme 8 (a) Illustration of the stop-flow lithography. (b, c) Multifunctional encoded hydrogel particles that contain DNA probes on either side and a fluorescent dye (**Rh1**) in the center. (d) Fluorescence microscopy image of the hydrogel particle after hybridization with fluorescently labeled (green) target DNA. (e) Scheme of the immobilization of the particles by a barrier in a microfluidic channel to form a multiplexed particle assay. (f) Fluorescence microscopy image of the multiplexed immobilized particle assay. (g) Schematic representation of a genotyping method using these particles in an alkaline dehybridization protocol. Scale bars = 100 nm.²⁰⁷ Figure copyright John Wiley and Sons and reproduced with permission.

imide-unit (**Nap4** to **Nap6**) and, subsequently, copolymerized these monomers with MMA using a free radical polymerization (0.1 wt% dye).²²⁵ Due to their intense yellow-orange color and bright yellow fluorescence, these three polymers were applied as coloring agents of polyamides fabrics. In addition, **Nap14** and **Nap15** were also copolymerized with MMA and proved to be good whitening materials for 100% cotton fabrics due to their bright white color and intense bluish fluorescence. For all copolymers, an enhancement of the photo-stability after the polymerization was observed.

Grabchev and coworkers investigated the photophysical properties of styrene-based copolymers bearing 1,8-naphthalimides as side-chains, which are substituted with a chelating ligand at the 4-position (**Nap7**).²²⁶ The polymer acts as sensor for several metal ions, in particular, Zn^{2+} , Fe^{3+} , Co^{2+} , Pb^{2+} , Cu^{2+} , Ni^{2+} , and Mn^{2+} , in acetonitrile. The mechanism of the fluorescence enhancement (FE) of the monomer as well as its dependency on the metal cation is depicted in Scheme 11. In contrast to the other metal ions, an additional response only for Fe^{3+} ions could be observed in aqueous solutions. After complexation of the metal ions, the material revealed an increase of the fluorescence and, in the case of Fe^{3+} ions, also a shift of the maximum emission wavelength. Grabchev *et al.* also suggested an application as an ON-OFF probe due to a considerable increase of the fluorescence intensity under acidic pH-values and the presence of protons, respectively.

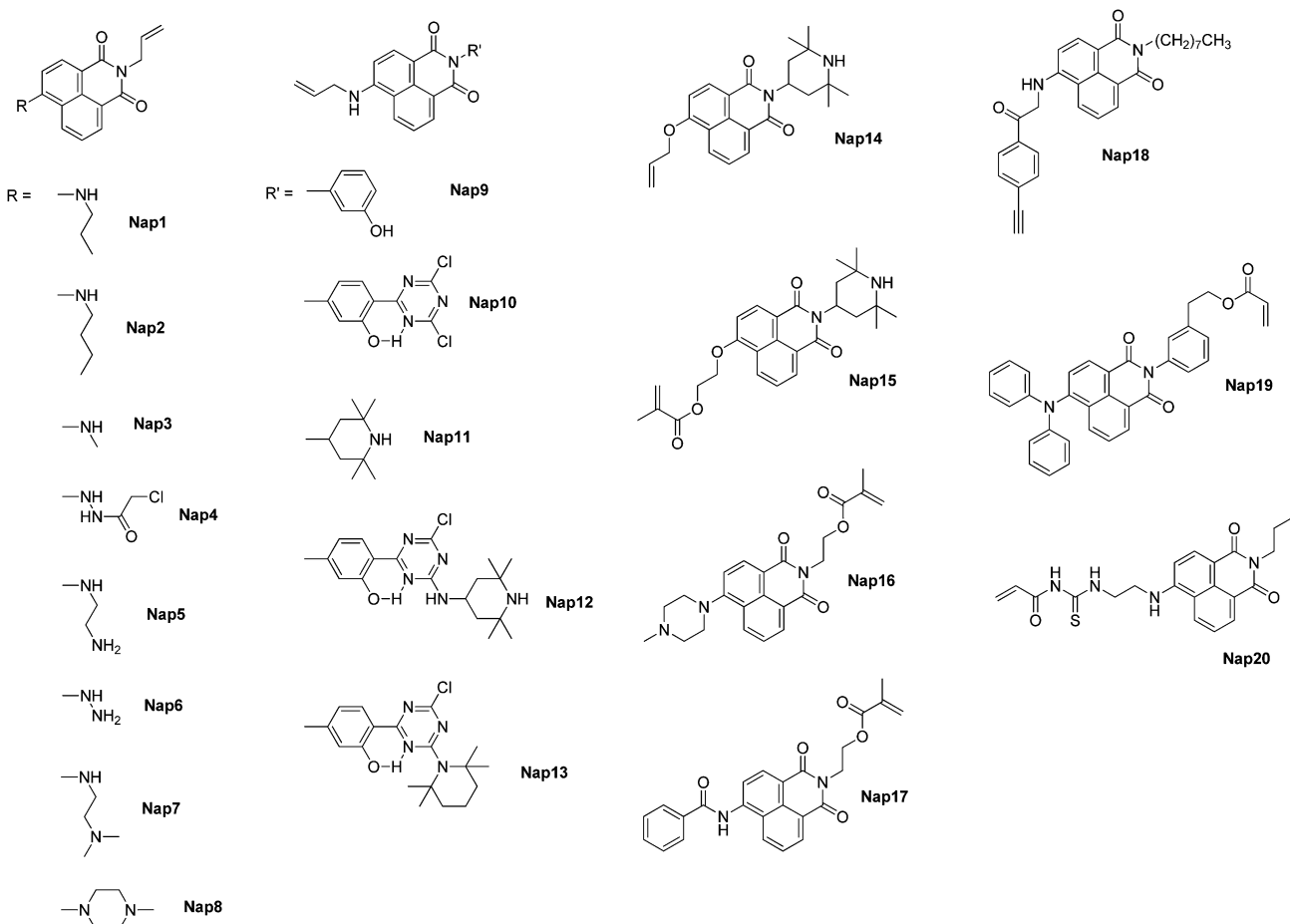
An optical fiber, coated with a polymer that was obtained by auto-polymerization at elevated temperatures of *N*-allyl-4-(4'-methyl-piperazinyl)-1,8-naphthalimide (**Nap8**), was utilized for intra-arterial blood pH monitoring in rabbits.²²⁷ Bai and coworkers developed a pH-sensor device for *in vivo* and *in vitro*



Scheme 9 Schematic representation of a polymeric-micelle-based reversible three state switchable multicolor luminescent system from amphiphilic and thermoresponsive diblock copolymer P(St-co-Oxa11-co-Sp2)-b-P(NIPAM-co-Rh6). RhBAM \equiv Rh6, SPMA \equiv Sp2.²²² Figure copyright John Wiley and Sons and reproduced with permission.

application that can potentially be used to monitor acidosis and alkalosis in human patients.

Bojinov *et al.* successfully incorporated 1,8-naphthalimides **Nap9** to **Nap13** as comonomer into polyacrylonitriles.^{228,229} The resulting polymers were investigated in terms of their photo-stability. In this context, the 1,8-naphthalimides serve as UV absorber or hindered amine light stabilizer (HALS) in order to protect the materials from photo-degradation. The design of the yellow-green emitting monomers combined the UV-absorbing characteristics of the 2-(2-hydroxyphenyl)-1,3,5-triazine moiety with the radical scavenging property of the 2,2,6,6-tetramethylpiperidine unit. In order to determine the photo-stability, the compounds were irradiated for 10 h and the



Scheme 10 Schematic representation of the polymerizable dyes containing 1,8-naphthalimides as chromophore.

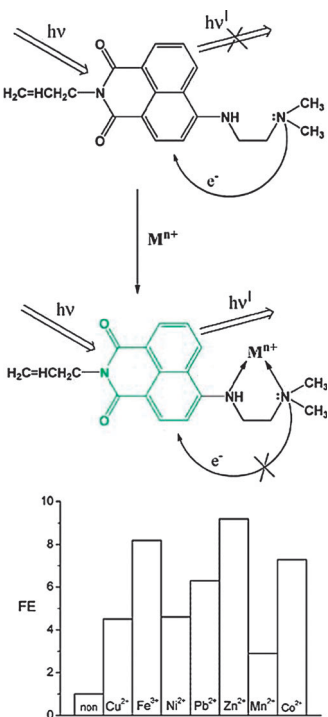
degradation was monitored colorimetrically. The compounds including the modified 1,8-naphthalimides revealed a significantly increased photo-stability after copolymerization with acrylonitrile (AN) using a free radical polymerization technique and 0.1 wt% of the dyes.

The group of Tian *et al.* used tertiary amine and methacrylate substituted 1,8-naphthalimides (**Nap16**) as “OFF-ON-OFF” switches for proton detection *via* fluorescence spectroscopy.²³⁰ In this case, a well-defined polymer could be obtained by polymerization of the dye using the RAFT polymerization technique. In the pH range between 11 and 3.5, the polymer acts as fluorescence enhancement sensor (OFF to ON). In contrast, the fluorescence intensity decreased at pH-values lower than 3.5 (ON to OFF). These effects were attributed to the different possibilities of the protons to quaternize the two different amines. Moreover, the authors modified the polymerizable 1,8-naphthalimide at the 4-position by introducing an amide functionality instead of the tertiary amines (**Nap17**).²³¹ In this context, the sensing application of the homopolymer could be extended from protons to fluorine ions. In this case a dependency of the response on the molar mass could be observed. Further investigations of Tian and coworkers concerning 1,8-naphthalimides included a polyacetylene based fluorine chemosensor.²³² For this purpose, the naphthalimide

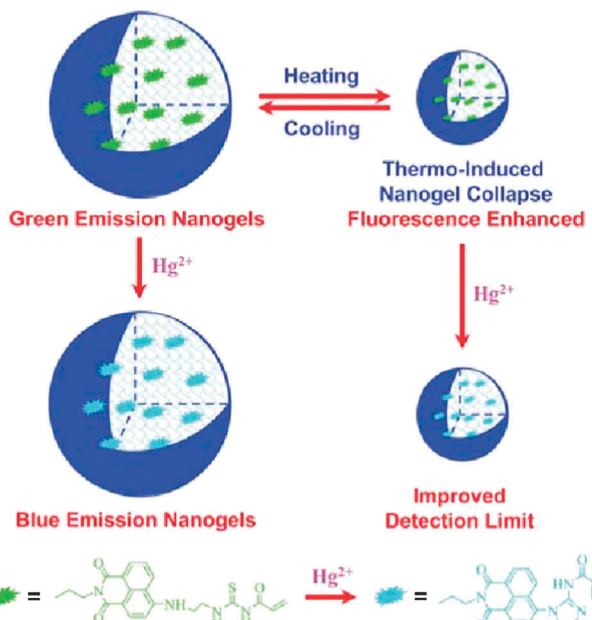
moiety was functionalized with an alkyne functionality (**Nap18**) that undergoes polymerization using an organorhodium complex as catalyst resulting in a conjugated polyacetylene backbone. In contrast to I⁻, Br⁻ and Cl⁻, a colorless-to-yellow color change as well as a blue-to-orange emission color change upon F⁻ concentrations between 10 and 100 μM could be observed by the naked eye.

A luminescence conversion light-emitting diode (LUCO LED) based on 1,8-naphthalimides bearing a diphenyl amino group on the 4-position was constructed by Lee *et al.*²³³ For this purpose, the dye (**Nap19**) was copolymerized with MMA in a free radical polymerization procedure (0.05 wt% dye). However, the UV-vis absorption as well as emission of the dye was redshifted after polymerization. The reasons for the behavior were not discussed in this contribution. Nevertheless, the device based on that material featured a good long-term stability for 288 h at 20 mA. The luminescent power *versus* time plot as well as the layout of the device is depicted in Fig. 15.

Lu and Liu synthesized NIPAM based nanogels containing side chain pendent 1,8-naphthalimide chromophores (**Nap20**).²³⁴ The near monodisperse dual responsive polymer particles were obtained by free radical emulsion polymerization. The particles collapse upon heating from 25 to 40 °C, which causes a change in the microenvironment of embedded



Scheme 11 Schematic representation of the mechanism of the FE by metal ion complexation (top) and its dependency on the metal ion (bottom).²²⁶ Figure copyright John Wiley and Sons and reproduced with permission.



Scheme 12 Schematic representation of the construction of thermoresponsive PNIPAM nanogel-based dual fluorescent sensors for temperature and Hg^{2+} ions with enhanced detection sensitivity.²³⁴ Figure copyright Royal Society of Chemistry and reproduced with permission.

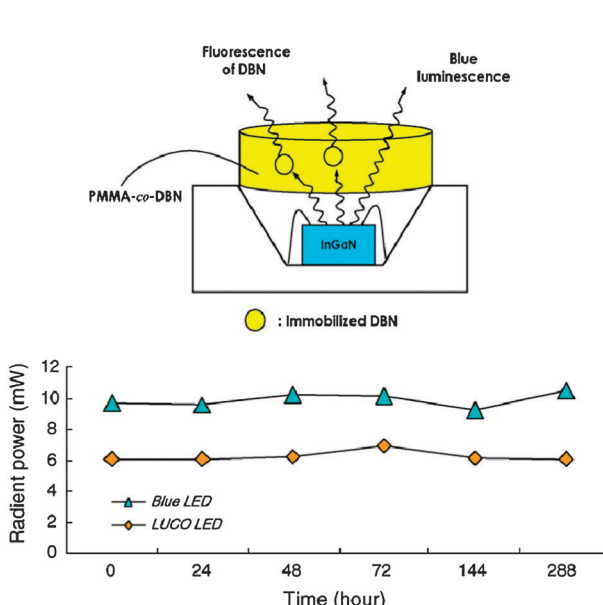


Fig. 15 Schematic representation of the architecture of LUCO LEDs and luminescent power versus continuous operating time at 20 mA (DBN \equiv Nap19).²³³ Figure copyright Elsevier and reproduced with permission.

dyes by shrinkage of the hydrodynamic volume and, thus, the fluorescence intensity increases by a factor of 3.4. Furthermore, the nanoparticles respond to Hg^{2+} ions. For this purpose, the fluorescence of the nanogels was studied at 25 and 40 °C in the presence of mercury ions. A 57 fold enhancement of the fluorescence intensity could be observed at 40 °C,

whereas the intensity increased by a factor of 10 at 25 °C. The working principle of the nanogel particles is illustrated in Scheme 12.

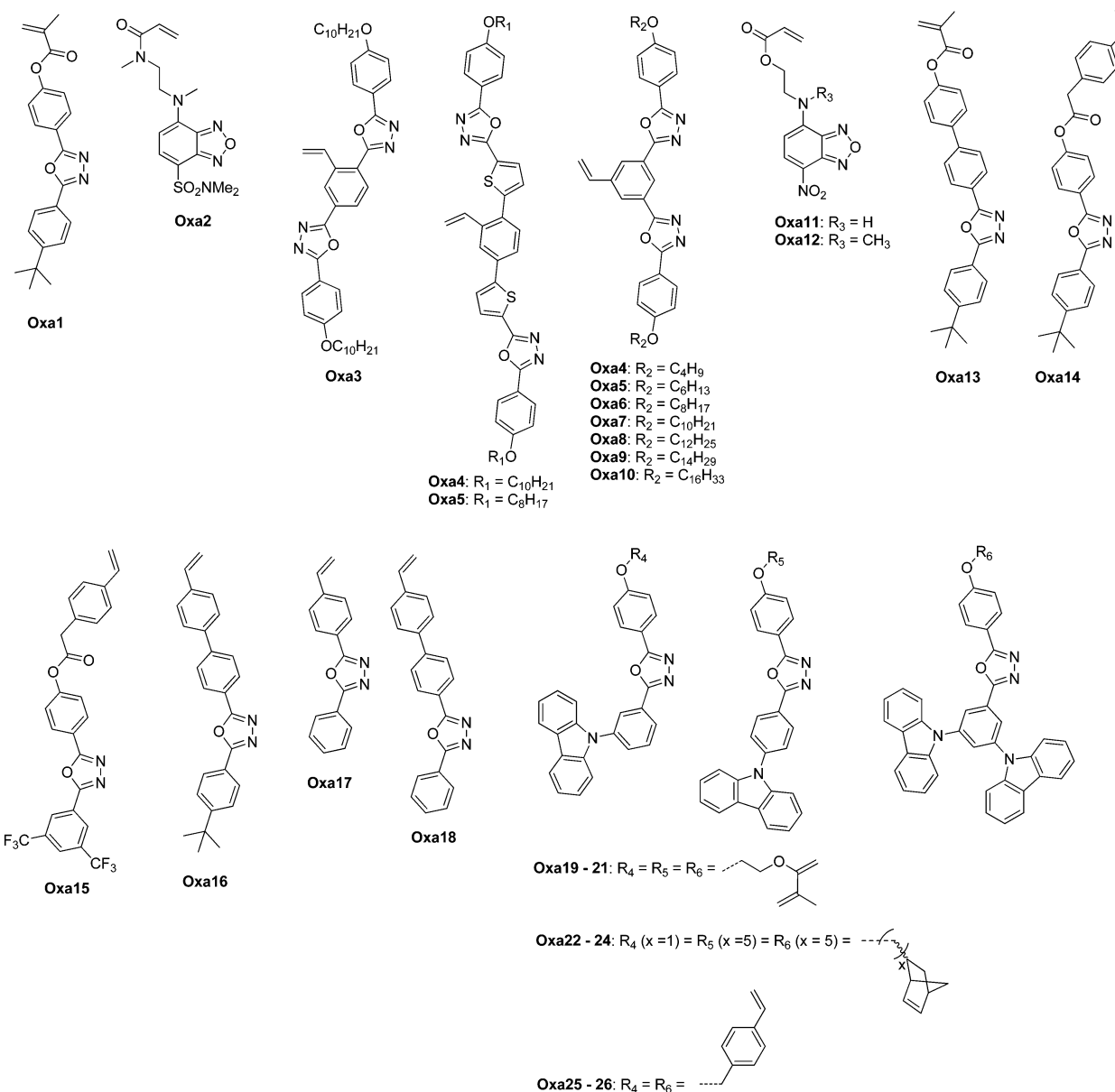
Oxadiazoles

It is generally known that 1,3,4-oxadiazoles can be obtained by the dehydration reaction of diacylhydrazines, whereas 1,2,5-oxadiazoles are synthetically available by dehydration of bis-oxime compounds of 1,2-dicarbonyls. Although two other isomers exist, only the two latter ones have been applied as functionalized monomer for the polymerization of side-chain pendant polymers.

Carroll *et al.* provided the synthesis of a methacrylate functionalized 1,3,4-oxadiazole **Oxa1** (see Scheme 13 for exact structures of the monomers), which was polymerized by the FRP procedure using AIBN in THF.²³⁵ The obtained homopolymers as well as **Oxa1** and carbazole moiety containing copolymers were investigated regarding their optical properties, in particular, UV-vis absorption, photoluminescence and electroluminescence in thin films.

The group of Uchiyama developed a polymeric thermometer which was fluorescently labeled with **Oxa2**.^{236,237} The copolymer particles were based on NIPAM as thermo-responsive comonomer and a cross-linker (BIS). A decreased water-uptake at elevated temperatures caused a change in the chemical surrounding of the fluorescent dye and, thus, an enhancement of the dye-fluorescence could be observed.

Zhou and coworkers tested the polymers containing oxadiazole functionalized styrene derivatives as repeating unit for electroluminescent devices. The authors started with a free radical polymerization of **Oxa3** (chlorobenzene, 90 °C, benzoyl



Scheme 13 Schematic representation of polymerizable oxadiazole derivatives.

peroxide initiator)²³⁸ and went over to more sophisticated polymer architectures, *i.e.* block copolymers with thiophene substituted styrene blocks by the ATRP technique.²³⁹ For their next approach, the authors combined the thiophene as well as the oxadiazole moieties in one monomer (**Oxa4/Oxa5**).²⁴⁰ As a polymerization technique, also ATRP was applied using CuBr, ethyl 2-bromo-2-methylpropionate (EBP) and Me₆TREN in *N*-methyl pyrrolidone (NMP). Additionally, the resulting polymers were investigated in terms of its liquid-crystalline behavior. Furthermore, the authors reported that a change in the substitution position on the styrene (**Oxa6** to **Oxa12**) affects the packing behavior of the polymer.²⁴¹

The incorporation of **Oxa11** into PNIPAM backbones was extensively studied by the group of Liu.²⁴² Firstly, the authors used Br-functionalized silica particles as ATRP initiator for the

growth of differently labeled PNIPAM blocks (as spirobifluorene monomer was utilized as second label).²⁴³ These coated particles revealed photoswitchable (due to spirobifluorene/merocyanine isomerization for the switching on/off the FRET) as well as thermoswitchable behavior (due to NIPAM repeating units). Furthermore, a PS-*b*-PNIPAM block copolymer was prepared by sequential RAFT polymerization.²²² The hydrophobic PS block was **Oxa11** and spirobifluorene labeled, whereas the hydrophilic block was rhodamine labeled (see also rhodamine section). Self-assembly of this polymer in aqueous media displayed micelle formation resulting in a FRET process that can be stimulated by multiple stimuli (*i.e.*, pH-, UV- as well as temperature-variation) to three different states. In the case of an **Oxa11** labeled PS block and a **Rh4** labeled PNIPAM block, a chemosensor for Hg(II) ions could be obtained.²²⁰

Another approach for tuning the FRET process by external stimuli was the copolymerization of **Oxa11** with NIPAM, **Rh5** (*R* = H, see Scheme 7 in the corresponding section for exact structure) and a polymerizable crown ether by emulsion polymerization in water.²⁴⁴ In this manner, a further sensitivity towards K(*i*) ions could be introduced.

Maynard applied a symmetric double-functional trithiocarbonate RAFT agent for the copolymerization of **Oxa12** with NIPAM.²⁴⁵ Subsequently, the endgroups were converted to protein-binding maleimide functionalities in order to connect two proteins by one polymer chain.

A wide range of publications focused on the application of oxadiazoles containing polymers in optoelectronic devices, in particular OLEDs, phosphorescent light emitting diodes and high performance memory devices. In this context, **Oxa13** was copolymerized with polymerizable carbazoles.²⁴⁶ **Oxa14** to **Oxa16** were copolymerized with polymerizable triphenylamines or carbazoles, respectively, using the NMP technique (also block copolymers were synthesized).^{247,248} **Oxa17** and **Oxa18** were used for the construction of random copolymer architectures with carbazole or triphenylamine moieties by NMP^{249,250} and **Oxa19** to **Oxa26** were polymerized by FRP and ROMP, respectively.²⁵¹

Others

A wide range of other dyes which are capable to be polymerized are listed in this section (see Scheme 14 for exact structures). So far, polymer films based on Nile blue **NB1** were applied as ethanol sensor due to their solvatochromic behavior.²⁵² In the case of Nile blue, the change of the maximum absorption wavelength in ethanol is significantly stronger in comparison to other solvents. Furthermore, **NB2** and **NB3** were copolymerized with BA for application as plasticizer-free fluorescent ion (*i.e.* H⁺ and Na⁺) optode microsphere sensors.²⁵³ However, the authors claimed that the approach of directly polymerizing the functionalized dye is not suitable due to the formation of side-products with undesired H⁺-binding properties and, therefore, undesired spectral properties. In contrast, the general problem of leaching of the plasticizer was overcome by grafting of the dye *via* amide or urea bondage onto the polymer with a low *T_g*.

So far, only some examples for stimuli-responsive polymers with some other non-classical chromophores exist. Spiropyranes in their closed form are not fluorescent. In contrast, the open merocyanine form is fluorescent. A switching between these two states can be obtained by UV- and visible light irradiation, respectively. For this purpose, **Sp1** was copolymerized with MMA and a donor triarylamine monomer in order to enable or disable the energy transfer between those two chromophores.²⁵⁴ Furthermore, the details about the copolymerization of **Sp2** with NIPAM^{222,243} or MMA²²⁴ can be found in the oxadiazole or naphthalimide section, respectively.

As second example for stimuli-responsive polymers based on polymerizable dyes that do not belong to the above listed ones, Men'shikova and coworkers reported the synthesis of **Lu** as well as its seed emulsion polymerization with styrene and DVB as

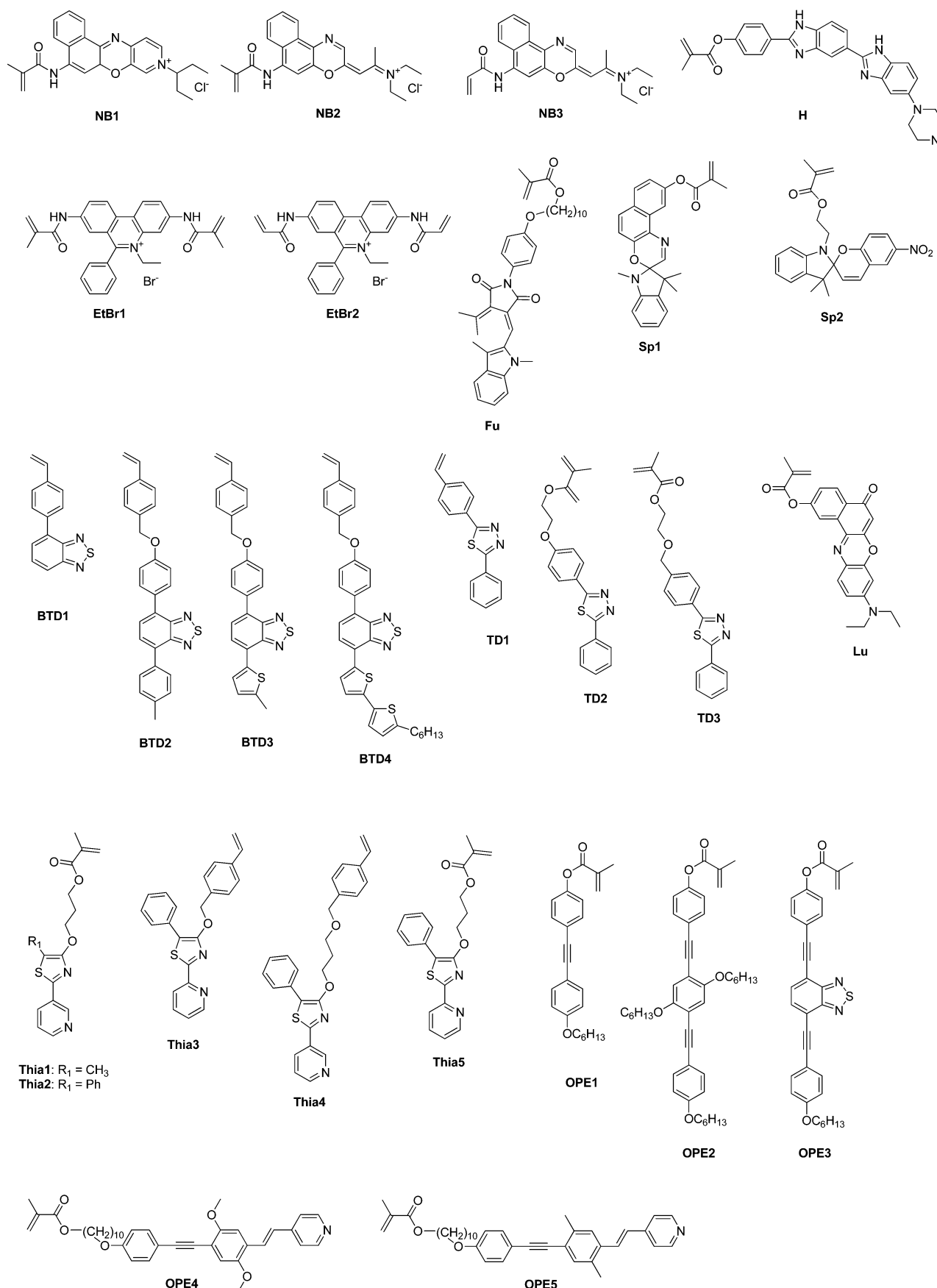
comonomers.²⁵⁵ As a result, monodisperse core-shell particles were obtained which sorb toluene vapor. This process was monitored by solid-state ¹H and ¹³C NMR spectroscopy. In the case of benzene vapor, the fluorescence also increased during the uptake.

The incorporation of luciferin analogous chromophores (*i.e.*, thiazoles **Thia1** to **Thia5**) was carried out by Schubert *et al.* According to their polymerizable functionalities, **Thia1** and **Thia2** were copolymerized with MMA;²⁵⁶ in contrast, **Thia3** and **Thia4** were copolymerized with styrene.²⁵⁷ The application of the RAFT polymerization technique using AIBN as initiator, CPDB as CTA and toluene as solvent enabled the formation of well-defined statistical copolymers. **Thia5** was copolymerized with MMA and a photoactive Ru(*ii*)-complex.²⁵⁸ The photophysical properties of all polymers were characterized by time-resolved lifetime measurements. Solvent-dependent donor lifetime measurements are depicted in Fig. 16. The non-exponential decay in the presence of the Ru(*ii*) acceptor in comparison to the single-exponential donor alone decay curve (**Thia5**-containing copolymer) proves a FRET process.

In addition, the group of Schubert published the synthesis and characterization of a series of polymerizable oligo(phenylene ethynylene)s.²⁵⁹ For the monomers **OPE1** to **OPE3**, the length of the conjugated system was altered (**OPE1**: dimer, **OPE2**: trimer) as well as the optoelectrical properties (**OPE2**: donor trimer, **OPE3**: acceptor trimer with benzothiadiazole moiety). The monomers were suitable for RAFT polymerization using AIBN as initiator, CPDB as CTA and toluene as solvent. Notable side-chain interactions in dilute solutions were induced within the homopolymers upon variation of the solvent/non-solvent ratio. Furthermore, the distance between the dyes was enlarged by copolymerization of the OPEs with MMA, which caused different types of resonant energy transfer in donor- and acceptor containing copolymers. Furthermore, worm-like conformations of the polymers in dilute solutions could be observed.²⁶⁰

In order to show that oligo(phenylene ethynylene)s are suitable for organic electronic devices, **OPE4** and **OPE5** were copolymerized with hole-transporting polymerizable carbazoles by Lin *et al.* using a FRP procedure.^{261–264} An oxadiazole containing dendron was attached to the terminal pyridine moiety by supramolecular self-assembly. This construction was tested as polymeric light-emitting diode.²⁶¹ The device displayed an electroluminescence emission of 519 nm under a turn-on voltage of 6.5 V, with a maximum luminance of 408 cd m⁻² at 18 V and a luminance efficiency of 0.39 cd A⁻¹ at 100 mA cm⁻², respectively. Additionally, the surface of gold NPs could be modified using these materials.^{262,263} As a result, the polymers crosslinked. As alternative to gold NP substrates, the crosslinking by organic substrates was also described.²⁶⁴

Furthermore, Haeussler *et al.* investigated the optoelectrical properties of benzothiadiazole-containing pendant polymers prepared using the RAFT polymerization technique.²⁶⁵ For this purpose, the authors synthesized block copolymers from **BTD1** to **BTD4** as well as a vinyl triarylamine as second block. The polymers were spin-casted and tested in organic photovoltaic devices. The characteristics (*i.e.* current-voltage



Scheme 14 Schematic representation of a series of polymerizable monomers bearing different types of chromophores.

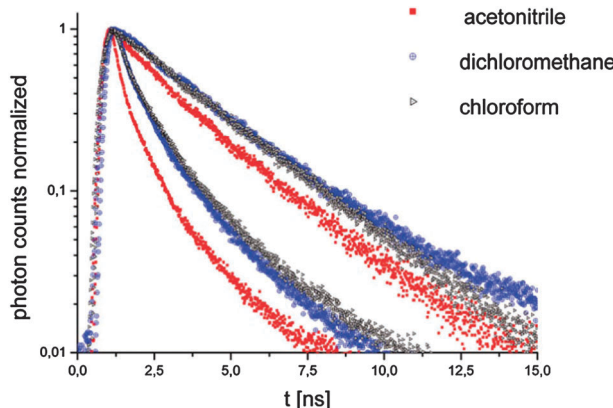


Fig. 16 Donor fluorescence curves of compound P(Thia5-co-MMA) (donor alone polymer, upper curves with longer fluorescence) and of P(Thia5-co-MMA-co-Ru(II)) (donor–acceptor polymer, lower curves with quenched fluorescence) in different solvents: acetonitrile (red squares), dichloromethane (blue circles), chloroform (black triangles). Excitation wavelength: 290 nm. Reprinted with permission from ref. 258. Copyright 2011 American Chemical Society.

curve as well as absorption spectrum and incident photon to current efficiency of this device are depicted in Fig. 17.

Lu and coworkers published the synthesis of a series of 1,3,4-thiadiazole containing monomers (TD1 to TD3).²⁶⁶ The monomers were polymerized by the FRP procedure using AIBN as initiator and cyclohexanone as solvent. HOMO and LUMO energy levels were determined by cyclovoltammetry as well as by fluorescence emission spectroscopy. The energy levels were found to be –6.35 to –6.14 eV and –3.02 to –2.84 eV, respectively. The polymers revealed either blue or green light emission.

With respect to future biological applications, the Hoechst dyes are generally suitable for the coloration of nuclei for fluorescence microscopy due to their binding to the DNA. Their polymerizable derivative **H** reveals a maximum absorption wavelength of 355 nm and emits in the blue to cyan region of

the visible light spectrum. So far, to the best of our knowledge, no publications exist, where **H** was polymerized or copolymerized although it is commercially available. This is also the case with the (meth)acrylamide functionalized ethidiumbromides **EtBr1** and **EtBr2** which bind to nucleic acids. The double functionalization of these monomers enables only the formation of cross-linked polymer architectures.

Optical properties of the dyes

In general, the optical properties of each dye can be fine-tuned by the introduction of functional groups. To the best of our knowledge, polymerizable aromatic dyes were so far not further modified on the aromatic system. Basically, these chromophores reveal only one reactive position which is used to introduce the polymerizable group. In contrast, a wide range of substituents can be introduced in azo-dye chromophores. Dependent on the substitution of the aryl moieties and the *cis-trans* isomerization, the absorption spectra of azo dyes cover all colors from yellow to violet. The synthetic strategy of the formation of azo-compounds enables a large variety of structures. The photochemical *trans-cis* back-isomerization of an azobenzene series showed that this process depends on the steric hindrance of the substituents.¹⁴⁶ In the particular case of **Azo7** to **Azo14** the switching rate was observed as follows: **H** > CH₃ > NO₃ > CN > OCH₃. For the halides, the order was Cl > F > Br > I. Noteworthy, also the thermal properties are influenced by the substituents. It was observed that electron withdrawing groups displayed enhanced stability and electron donating groups decreased the *T_g* values (up to 35 K variation). This finding is also supported by other azo-dye containing polymer studies.^{144,145} Among the halogen containing polymers, the thermal stability follows the inductive effects of halogens that are apparently overwhelmed by the polarizability and electron repulsion factors.

The optical properties of coumarin dyes can be influenced by the substitution on the 4-position. The absorption and emission

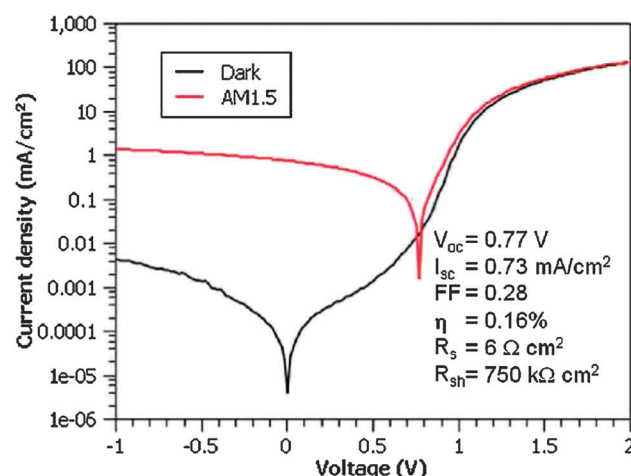
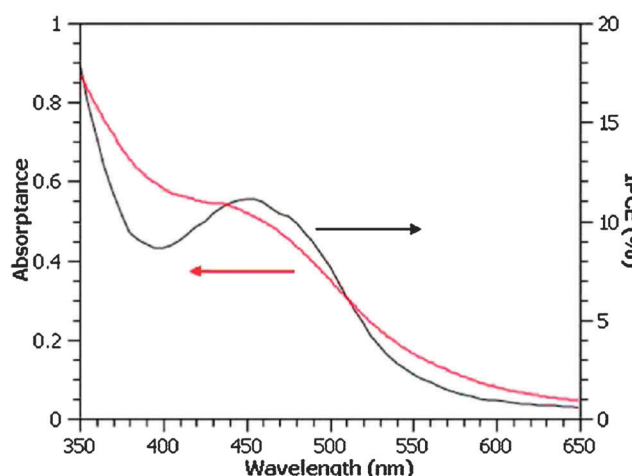


Fig. 17 Left: current–voltage curve of a 147 nm organic solar cell device consisting of a blend of a **BTD3** containing block copolymer as well as PCBM (blend ratio 1 : 4) as active layer. Right: incident photon to current efficiency (IPCE) and absorption spectra of active layer. Reprinted with permission from ref. 265. Copyright 2010 American Chemical Society.



wavelengths increase in the following order: H < CH₃ < CF₃. Furthermore, the linker plays a significant role. Ether linkers at the 7-position lower the maximum wavelengths of the absorption as well as the emission in comparison to amide linkers. Furthermore, an extension of the aromatic system in the case of benzocoumarins leads to an increase of the absorption of approximately 50 nm for the absorption and 40 nm for the emission.²⁶⁷

The exact position of the emission wavelength of a dye is also influenced by the microenvironment of the chromophore.²⁶⁸ Dependent on the polarity of the solvent, the HOMO/LUMO levels of the dyes can be stabilized at different energetic levels. Differences in the polarities of the ground and excited state of a chromophore increase this effect. In addition, additives like salts and pH-buffers, for instance, can also affect the emission wavelength. The attachment of a dye to a polymer chain leads to an embedding of this dye into a polymer coil in solution. As a consequence, also the polymer coil belongs to the microenvironment of the chromophore, and, thus, it can be adjusted by the choice of comonomer. Standard monomers (*e.g.*, styrene or MMA) usually do not have any influences on the optical properties. In contrast, stimuli-responsive monomers (*e.g.*, DEGMA, PEGMA, DMAEMA and NIPAM) strongly respond to

temperature changes. The reversible formation of hydrogen bonds in aqueous solutions causes the LCST behavior of these polymers. Above the LCST temperature, the water molecules are pulled out of the polymer coil and, consequently, the microenvironment of the dye is altered. Noteworthy, the majority of all dyes do not feature solvatochromic behavior. In particular, NB²⁵³ and merocyanines²⁶⁹ are reported for solvatochromism.

In general, the optical properties, in particular, maxima of the absorptions and emissions, are preserved after polymerization. However, negligible shifts (± 5 nm) of the absorption and emission spectra of the dyes after polymerization can be observed. Due to π - π stacking effects, bathochromic shifts in homopolymers as well as polymers with high dye content can be expected for all dyes. In electronic application a close packing of the chromophores is sometimes targeted to tune the optical properties by excimer formation. Furthermore, film-formation can also cause these effects. These shifts in the absorption maximum of up to 10 nm can be minimized by the introduction of bulky substituents on the dye itself. However, these effects cannot be fully prevented.

Table 1 lists the available optical property data – if reported – of all dyes reviewed in this contribution.

Table 1 Summary of the available data for absorption and emission maxima of the reviewed monomers in their according solvent

Monomer	Absorption λ_{\max} [nm]	Emission λ_{\max} [nm]	Solvent
Aromatic monomers	285–470	340–440	
Anthracene An1–An5	362	407	Cyclohexane
Diphenyl anthracene DPA1–DPA2	372	403, 425	Cyclohexane
Naphthalene monomers N1–N7	285	345	
F1, F2	320		THF
F3	445		Water (buffered)
F4	290, 354		Water (buffered)
Per1	434	435	Dichloromethane
Phenanthrene monomers P1–P2	254,	378	Cyclohexane
Pyrene	338	375	DMSO
Py1–Py5	377, 395, 467	377, 394, 416 (shoulder), 435 (shoulder)	THF
Azo-monomers	260–520		
Azo2	336		Dioxane
Azo3	341		Dioxane
Azo4	360		Dioxane
Azo5	349		Dioxane
Azo6	343		Dioxane
Azo9	350 (E) 438 (Z)		
Azo16	379 (E) 300, 473 (Z)		Chloroform
Azo17	366 (E) 260, 453 (Z)		Chloroform
Azo24	460 (NO ₂) 417 (Br) 405 (OCH ₃)		
Azo25	462 (NO ₂) 415 (Br) 403 (OCH ₃)		
Azo26	333		THF
Azo42	445		Chloroform
Azo43	365		Chloroform
Azo44	420, 520	430	DMF
Azo45	449		THF
Benzothiadiazoles	365–470	490–660	
BTD1	365	490	Homopolymer as thin film
BTD2	415	541	Homopolymer as thin film

Table 1 (continued)

Monomer	Absorption λ_{max} [nm]	Emission λ_{max} [nm]	Solvent
BTD3	440	610	Homopolymer as thin film
BTD4	467	658	Homopolymer as thin film
Coumarin monomers	320–400	450–510	
Coumarin 1 monomers (CH ₃ -substituent, amide linkage)	373	450	EtOH
Coumarin 152 Monomers (CF ₃ -substituent, amide linkage)	397	510	EtOH
Cou7–Cou10 (CH ₃ -substituent, ether linkage)	320		
Fluorescein monomers	485–555	510–585	
Fl1–Fl6	485	514	
Fl7	532–547 (Erythrosin) 537–547 (Eosin) 535–552 (Eosin)	556–581 557–564 554–571	THF, acetone or DMSO (Homopolymers revealed redshift in absorption- and emission spectra in more polar solvents, polymers tend to bleach, thermal stability of the polymers: erythrosin > Eosin Y > Eosin B)
Naphthalimide monomers	280–460	510–530	
Nap1	441	511	
Nap2	443	512	Dichloromethane
Nap3	424	450–620	Toluene
Nap4	404		Chloroform
	406		EtOH
	408		DMF
Nap5	404		Toluene
	410		Chloroform
	414		EtOH
	440		DMF
Nap6	442		Toluene
	430		Chloroform
	436		EtOH
	446		DMF
	458		
Nap7	428	517	Acetonitrile
Nap9	436	526	DMF
Nap10	340, 434	526	DMF
Nap11	434	524	DMF
Nap12	286, 338, 434	527	DMF
Nap13	290, 340, 436	527	DMF
Nap14	342 (354) 344 (356) 342 (354) 342 (356)		Toluene Chloroform EtOH DMF
Nap15	342 (354) 344 (356) 344 (356) 344 (356)		Toluene Chloroform EtOH DMF
Nap16	414 (pH = 11.2) 406 (pH = 7.6) 390 (pH = 3.4) 390 (pH = -0.6)	520	DMSO–water 1/1
Nap17	365	465	Dichloromethane–DMSO 9/1
Nap18	365	455	Acetonitrile
Nap19	440	550	Chloroform
OPE monomers	290–435	370–530	
OPE1	296	371	Chloroform
OPE2	318, 369	402	Chloroform
OPE3	312, 431	529	Chloroform
OPE4	320, 385	445	THF
OPE5	350	440	THF
Oxidiazoles	230–470	380–560	
Oxa1	315	380	Chlorobenzene
Oxa2	275, 456	560	Water
Oxa3	330	402	Chloroform

Table 1 (continued)

Monomer	Absorption λ_{max} [nm]	Emission λ_{max} [nm]	Solvent
Oxa4–Oxa5	371 (C8) 372 (C10)	437, 464 437, 461	Chloroform
Oxa11	470	518	Water
Oxa13	ca. 310	ca. 390	THF
Oxa17	293		As film
Oxa18	311		As film
Oxa19, Oxa22, Oxa25	241, 292, 339	424	Dichloromethane
Oxa20, Oxa23	237, 284, 341	414	Dichloromethane
Oxa21, Oxa24, Oxa26	234, 292, 337	434	Dichloromethane
Rhodamine monomers	530–550	560–570	
Rhodamine B Rh1–Rh3, Rh5–Rh9	548	570	
Rh4	530	566	Aqueous HCl, pH = 2
Thiadiazoles	310–325	390–400	
TD2	311	390	DMF
TD3	321	398	DMF
Thiazoles	250–370	410–450	
Thia1	342, 334	410, 411	Acetonitrile
Thia2	368, 361	446, 447	Acetonitrile
Thia3	253, 370	445	Acetonitrile
Thia4	250, 361	447	Acetonitrile
Thia5	375	447	Dichloromethane
Others			
EtBr	439	512	
Fu	396 (<i>E</i>) 528 (<i>C</i>)	–(<i>E</i>) 635–649 (<i>C</i>)	Chloroform
Lu		582	
NB2–NB3	493 499 504 628 635 457 522	574 596 598 667 674 556 668	EtOH–Water 20/80 Toluene Acetone DMF EtOH Water 1.0 N HCl (pH = 1) 0.1 N NaOH (pH = 11)
Sp2	470–650		As polymer NP suspension in water

Conclusions

The incorporation of dye-bearing monomers into polymeric architectures is an ongoing field of research. The widest range of applications of polymerizable dyes focuses on the simple addition of a labeling monomer to the polymerization feed for visualization purposes in macroscopic biological objects (*e.g.*, living cells) by fluorescence microscopy. In these cases, straight-forward free radical polymerization techniques or emulsion polymerizations are applied exclusively. In general, anthracene derivatives or fluorescein/rhodamine monomers are well-established depending on their micro-environment in the polymer (hydrophobic or hydrophilic character). In addition, more sophisticated polymerization techniques (*i.e.*, various kinds of controlled radical polymerization techniques) are required for the application of polymers as sensor materials or molecular switches due to the reproducible adjustment of the polymer chain-length in combination with narrow polydispersity index values. The fluorescence response as well as the absorption behavior of these systems can be tuned by the choice of the chromophore. For this purpose, an enlargement of the pool of dye-functionalized monomers (*e.g.*, dye classes

that have not yet been modified with polymerizable units, so far) can potentially lead to an extension of the playground of a wide range of external stimuli for sensing and/or switching of polymers. However, one has to keep in mind that important groups of dyes, for instance the phenothiazines, can act as radical scavenger and, thus, these molecules are not suitable for radical polymerization techniques. This problem can be circumvented by an appropriate functionalization (*e.g.*, the introduction of norbornene moieties for ROMP). Moreover, side-chain pendant polymer chains feature enhanced solubility and therefore enhanced processability for the fabrication of organic electronical devices, compared to their main-chain conjugated counterparts. Furthermore, they tend to phase-separate more easily in block copolymer architectures, which are accessible by well-known controlled radical polymerization techniques nowadays. Due to the short effective conjugation length, the brush-like polymers do not reach the best performances of conjugated polymers. In order to overcome this drawback, an enlargement of the conjugated system as well as the incorporation of band-gap lowering moieties (*e.g.*, thiophenes or benzothiadiazoles) might be performed to enhance the efficiencies. An alternative therefore could be the addition

Table 2 Summary of the applied polymerization techniques of the polymerizable dye-containing monomers as well as selected reaction conditions and the corresponding comonomers

Monomer	Polymerization technique	Solvent	Reaction temperature [°C]	Comonomers	Application
AcN An1	RAFT	Chlorobenzene	70 (16 h)	DPA1 , DPA2 ⁸⁸	Excitation energy transfer
	FRP	PGMEA ^a	60 (5 h)	PTBS, MAA ⁶⁵	Deep UV lithography
	FRP	THF	55 (24 h)	CyOPMI, (HBuVE), MMA ⁶⁶	Negative-tone photoimaging
	FRP	Toluene	60	Styrene ^{57,58}	Morphology characterization of immiscible polymer blends
	FRP	THF–toluene	60 (48 h)	Hexyl methacrylate, MMA ^{59,60}	Photodimerization
				6-((4'-cyano-[1,1'-biphenyl]-4-yloxy)hexyl methacrylate ⁷¹	LC polymer fibres
	ATRP	Anisole	70	MMA ⁶¹	Synthesis and characterization
	FRP	THF	55 (2 h) and 62 (12 h)	MMA ⁶⁹	Diels–Alder crosslinking
	ATRP	H ₂ O	60 (overnight)	MMA (diblock copolymer) ⁷⁰	Photodimerization
	ATRP	Toluene	60 (20 min)	DMAEMA ⁶³	Surface labeling
An2	FRP	THF	60 (24 h)	Azacrown ether methacrylate monomers ⁶⁴	Synthesis and characterization
	RAFT ^b	THF ^b	62 (20 h)	AEMA ⁸³	Amine and metal sensor
				Homopolymer and MMA ^{105,106}	Separation of SWCNTs
	<i>d</i>	<i>d</i>	<i>d</i>	Homopolymer ^{119,120}	Antireflective coating
	<i>d</i>	<i>d</i>	<i>d</i>	MMA ¹²¹	LC display element
	<i>d</i>	<i>d</i>	<i>d</i>	tBMA ¹²²	Photoresist
	FRP	Toluene	60	Neopentyl methacrylamide ¹³⁸	Structured polymer Langmuir–Blodgett films
	FRP	Benzene	60 (48 h)	MAA ¹²⁴	Studies on PMAA conformation
	Iniferter polymerization	Toluene	RT (10–80 min)	MAA, EGDMA ⁹⁹	Cross-linked coatings
An3	FRP	Bulk	70 (48 h)	VP ⁶⁷	Superabsorbent nanogel
	FRP	<i>n</i> -Hexane	60 (24 h)	Vinyl terminated poly(siloxanes) ⁶⁸	Polysiloxane labeling
An4	Living anionic polymerization	Cyclohexane or toluene	25 (10 min)	Homopolymer and block copolymer with 4-diphenylaminostyrene	Synthesis and characterization
	UV-induced selective surface grafting polymerization	Acetone	25	PS (block copolymer) ¹¹²	Janus particles
An5	Radical emulsion polymerization	H ₂ O	85	MMA, BA ¹²⁹	Polymer diffusion studies
Azo1	FRP	THF	60 (48 h)	6-((4'-Cyano-[1,1'-biphenyl]-4-yloxy)hexyl methacrylate ⁷¹	LC polymer fibres
Azo2–Azo6	<i>d</i>	<i>d</i>	<i>d</i>	BA, MMA, EtA ¹⁴³	Synthesis and characterization
Azo7–Azo15	<i>d</i>	<i>d</i>	<i>d</i>	Styrene, DVB ¹⁴⁸	Electrophoresis particles for electronic inks
Azo16/Azo17	FRP	Dioxane	80 (1.5 h)	MMA ^{144,145}	Synthesis and characterization
Azo18–Azo23	FRP	THF	60 (24 h)	Homopolymers ¹⁴⁶	Synthesis and characterization
Azo24	RAFT	THF	60 (48 h)	Homopolymer and Fu copolymer ¹⁴⁷	Dual-mode optical switchable polymers
(R ₁₀ = NO ₂)				Styrene, DVB ¹⁴⁸	Electrophoresis particles for electronic inks
Azo24/Azo25	ATRP	Toluene	70 (12 h)	DEGMA, Py2 ^{85,86,156}	Sensor for temperature and pH value
Azo26	FRP	Cyclohexanone	80 (4–8 d)	MMA ¹⁴⁹	Third-order nonlinear optics
Azo24–Azo25		Cyclohexanone	70 (8 h)	Styrene, carbazole monomers ¹⁵⁰	Memory devices
Azo27–Azo36	FRP	Toluene	230 (30 min)	Homopolymers ¹⁵¹	Color filters
Azo37/Azo38	ROMP	Propylene glycol mono-methylether acetate	Rt (90 min)	Homopolymers and copolymers with Azo37 or Azo38 ¹⁵²	Reusable acid sensors
Azo39/Azo40	FRP	Dichloro-methane	50	Homopolymers ¹⁵⁴	Reversibly bending polymer films
Azo41	FRP	Benzene	60 (48 h)	Homopolymers ¹⁵⁵	Three-dimensional photomobility
Azo42/Azo43	RAFT	Toluene	80	Homopolymers and PS block copolymers ¹⁵⁷	Photoinduced birefringence
Azo44	RAFT	Anisole	80 (24 h)	Homopolymers and PS block copolymers ¹⁵⁸	Metal ion detector
Azo45/Azo46	FRP	DMF	60 (2 d)	Py2 ¹⁰³	Functionalization of SWCNTs
		THF			

Table 2 (continued)

Monomer	Polymerization technique	Solvent	Reaction temperature [°C]	Comonomers	Application
BTD1–BTD4	FRP and RAFT	Chlorobenzene	70 (16 h)	Homopolymers and block copolymers with polymerizable triphenylamines ²⁶⁵ MMA ^{159–161}	Organic solar cell
Cou1	^d	^d	^d		OLED
Cou2	ATRP	<i>p</i> -Xylene	100 (48 h)	PMMA block copolymer ¹⁶²	Core cross-linked star polymers
	Radical miniemulsion polymerization	H ₂ O–CH ₂ Cl ₂	Rt (20 min)	1,4-Phenylene bismethacrylate ⁴⁰ Homopolymer ¹⁶³	<i>In vivo</i> large-animal-lymph migration of NPs
Cou3–Cou6	^h	^h	^h	Homopolymer and naphthopyran copolymer ¹⁶⁴	Intraocular lenses
Cou7	ATRP	THF	60 (20 h)	Homopolymer and methoxyethoxyethyl vinyl ether ¹⁶⁵	Photo-crosslinking
Cou8	Living cationic polymerization	CH ₂ Cl ₂	0	Maleic anhydride, styrene ¹⁶⁶	Reversible photoinduced crosslinking
Cou9	FRP	^g	^g		Self-assembly of photosensitive particles
Cou10– Cou12	FRP	DMF	60 (16 h)	Homopolymers, MAA copolymers ¹⁶⁷	Photoalignment of liquid crystals
Cou13– Cou41	FRP	Xylene	Reflux (18 h)	Homopolymers ¹⁵³	Synthesis and characterization
Cou42/Cou43	FRP	Dioxane	75 (24 h)	VP ^{168,169} Acrylamide ¹⁷⁰	Sensors
Cou44	RAFT	DMF	60	MMA and labelled PMMA- <i>b</i> -PS ¹⁷¹	Eu(III) complexation
Cou45	FRP	DMF	70	Homopolymer and VAc ¹⁷²	Antimicrobial coatings
DPA1/DPA2	RAFT	Chlorobenzene	70 (16 h)	AcN ⁸⁸ ^e	Excitation energy transfer
EtBr1/EtBr2	^e	^e	^e		
F1	Living anionic polymerization	Toluene	−78	Homopolymer ⁹⁶	Conformational study
F2	Living anionic polymerization	Toluene	−78 (12 h)	Homopolymer ^{95,96}	Conformational study
F3/F4	FRP	DMF	65 (5 h)	2-Ethoxyethyl methacrylate, 2-Ethoxyethyl methacrylate, EGDMA ¹⁰⁹	Cyanide sensor membrane
F5	Living anionic polymerization	THF	−78	VP (block copolymer) ⁹⁷	Self-assembly
	Living anionic polymerization	THF	−78 (1.3 h)	Star-polymers ⁹⁸	Ordered microporous films
	FRP	Benzene	70 (16 h)	DMAEMA and stearyl acrylate ¹¹⁰	Thermoresponsive luminescent electrospun fibers
	Living anionic polymerization	THF or <i>t</i> -butylbenzene	−78 or 20	Homopolymers ^{113–116}	Non-volatile memory devices
Fl1	RAFT	Dioxane	60 ^f	NIPAM, NAOS ¹⁷³ HEMA, ethylene dimethacrylate ¹⁷⁴ Styrene ¹⁷⁶	Multifunctional nanomedicines Optimization of femtosecond laser micromachining Polymer particles
	Radical dispersion polymerization	EtOH	70		Fe ₃ O ₄ core–shell composite particles
	Radical emulsion polymerization	H ₂ O	70 (8 h)	Styrene, NIPAM ¹⁷⁷	Fiber coatings
	FRP	Bulk	70 (5 h)	DVB ¹⁸²	Cellular delivery of anionic NPs, gold nanorod coating, functionalized plasmonic-fluorescent NPs
	FRP	Igepal-cyclohexane	Rt (1 h)	<i>N</i> -(3-Aminopropyl) methacrylamide, BIS, PEGMA ^{178–180}	Coating of magnetic nanodiamonds Cell uptake of polymer NPs
	Radical dispersion polymerization	H ₂ O	μW, 600 W (10 s)	AA ¹⁸³	Polyurea microcapsules
	Radical emulsion polymerization	H ₂ O	75 (3 h)	Styrene, MMA, styrene/HEMA ^{184,185}	Studies on the swelling behavior of crosslinked polymers
	FRP	EtOH	60 (21 h)	MAA ^{186,187}	Imprinted polymer nanoparticles
	FRP	H ₂ O	70 (44 h)	<i>N</i> -Vinylimidazole, BIS ¹⁸⁸	Formation of three-dimensional hydrogel multilayers
Fl2	FRP	EtOH–H ₂ O	25	NIPAM, TBAM, AA, BIS ¹⁷⁵	NP formation by PRINT method
	Radical photopolymerization	H ₂ O	Rt (10 min)	HEA and PEG ₅₇₅ diacrylate ¹⁸¹	Multiphase amphiphilic rods
	FRP	DMSO	RT	Trimethylolpropane ethoxylate triacrylate, 2-aminoethyl methacrylate hydrochloride ^{189–191}	
	Radical photopolymerization	DMF	70 (1 min)	HP ₄ MA, PEG ₇₀₀ DA, TETA, Rh1 (diblock and triblock particles) ¹⁹²	

Table 2 (continued)

Monomer	Polymerization technique	Solvent	Reaction temperature [°C]	Comonomers	Application
	RAFT	H ₂ O–acetone	60 (1 to 9 h)	NIPAM, <i>N</i> -acryloyl glucosamine ¹⁹³	Thermo-dependent switcher
	RAFT	DMA	70	Styrene, 2-(methacrylamido)-glucopyranose, disulfide diacrylate ¹⁹⁴	Degradable cross-linked glyco-particles
	ATRP	Acetone	70 (1 h)	NIPAM ¹⁹⁵	Coating of fluorescent microtubuli
	ATRP	Anisole	80 (25 h)	PBPEM- <i>g</i> -BA copolymer ¹⁹⁶	pH-Responsive fluorescent molecular bottlebrushes
	ATRP	Acetone	70	NIPAM and <i>t</i> BA ¹⁹⁷	Janus particle sensor
	FRP	THF	70 (8 h)	Acylamide ¹⁹⁹	pH and temperature responsive material
F16	<i>f</i>	<i>f</i>	<i>f</i>	MMA ²⁰⁰	SWCNT composite material
				MMA ¹⁰⁶	Separation of SWCNTs
F17	FRP	THF	70 (10 h)	Acylamide ¹⁹⁸	pH and temperature responsive material
Fu	FRP	THF	60 (24 h)	Homopolymers ²⁰¹	Holographic grating studies
	FRP	THF	60 (48 h)	Homopolymer and Azo16/Azo17 copolymers ¹⁴⁷	Dual-mode optical switchable polymers
H	<i>e</i>	<i>e</i>	<i>e</i>	<i>e</i>	
Lu	Radical seed emulsion polymerization	H ₂ O	40–60	MAA, styrene, DVB ²⁵⁵	Stimuli-responsive polymers
N1	FRP	Toluene	60	<i>N</i> -Dodecylmethacrylamide ^{47,48}	Photolithography and photoreaction
N2	<i>f</i>	<i>f</i>	<i>f</i>	Homopolymer ¹³⁶	<i>T</i> _g prediction by calculation
				DMAEMA ⁸⁰	Stimuli-responsive multi-functional membranes
	ATRP	CHCl ₃	25 (48 h)		Fe ₃ O ₄ composite particles
	Radical emulsifier-free emulsion polymerization	H ₂ O	70 (15 min)	Styrene and MAA copolymer ¹⁰⁰	
	Radical soap-free emulsion polymerization	H ₂ O	70 (8 h)	DVB and MMA or styrene ¹⁰¹	Colloid immobilization on Au surface
	<i>b</i>	<i>b</i>	<i>b</i>	Homopolymer ^{105,106}	Separation of SWCNTs
	<i>f</i>	<i>f</i>	<i>f</i>	Homopolymer ¹³⁵	Calculation of polymer properties
	FRP	Bulk	50 (24 h)	MMA ¹²³	Nonradiative energy transfer
	FRP	Cyclohexanol–ethylene glycol–H ₂ O	60 (12 h)	ODA, TRIM ¹⁴¹	Column material
	Radical emulsifier-free emulsion copolymerization	H ₂ O	60 (6 h)	Styrene ⁴⁹	Particle labeling
	FRP	Benzene	80	Maleic anhydride ⁵⁰	Conformational studies
	Ziegler-Natta olefin polymerization	Toluene	40	Ethylene ⁵¹	Ziegler-Natta olefin polymerization
	FRP	DMSO	60 (21 h)	Sodium styrenesulfonate ^{53,54}	Nanostructured micellar films, hybrid photosensitizers
	<i>b</i>	<i>b</i>	<i>b</i>	AA (as block copolymer) ⁵⁵	Terpolymer for enhanced oil recovery
	Free radical micellar copolymerization	H ₂ O	50 (16 h)	Sodium 2-acrylamido-2-methylpropane sulphonate and acrylamide ⁵²	Investigations on polymer/fullerene miscibility
	<i>b</i>	<i>b</i>	<i>b</i>	Homopolymer ¹⁰⁸	Calculation of the dielectric constant
	<i>f</i>	<i>f</i>	<i>f</i>	Homopolymer ¹³⁷	Non-volatile organic field-effect transistor memory
	<i>b</i>	<i>b</i>	<i>b</i>	Homopolymer ¹¹⁷	Studies on π–π stacking interactions
	FRP	Bulk	70	Homopolymer and PFS ¹⁴⁰	Studies on π–π stacking interactions
	<i>f</i>	<i>f</i>	<i>f</i>	Homopolymer ¹³⁷	Calculation of the dielectric constant
N4	FRP	Bulk	70	Homopolymer and PFS ¹⁴⁰	Studies on π–π stacking interactions
				Homopolymer ¹³⁷	Self-assembly and reversible switching
N5	ATRP	Toluene	RT	Rh8 ¹¹¹	Load bearing hydrogel implants
N6/N7	<i>d</i>	<i>d</i>	<i>d</i>	Homopolymers ¹⁴²	Synthesis and characterization
Nap1/Nap2	FRP	Bulk	70 (12 h)	MMA ²²³	Photo-switchable nanoparticles
Nap3	Radical miniemulsion polymerization	H ₂ O	60 (210 min)	MMA, Sp2 ²²⁴	

Table 2 (continued)

Monomer	Polymerization technique	Solvent	Reaction temperature [°C]	Comonomers	Application
Nap4–Nap6	FRP	Bulk	70 (8 h)	MMA ²²⁵	Coloring agents
Nap7	FRP	Bulk	80 (8 h)	Styrene ²²⁶	Metal ion sensor
Nap8	FRP	H ₂ O	50 (6 h)	3-(Trimethoxysilyl)-1-propano methacrylate, HEMA ²²⁷	Intra-arterial blood pH monitoring
Nap9–Nap13	FRP	Bulk	70 (12 h)	AN ^{228,229}	UV absorber, hindered amine light stabilizer
Nap14/Nap15	FRP	Bulk	70 (8 h)	MMA ²²⁵	Whitening materials
Nap16	RAFT	NMP	70 (36 h)	Homopolymer ²³⁰	Switchable polymer
Nap17	RAFT	NMP	70	Homopolymer ²³¹	Fluoride ion sensor
Nap18	Alkene polymerization	THF (Et ₃ N)	RT (24 h)	Homopolymer ²³²	Fluoride ion sensor
Nap19	FRP	Bulk	80 (24 h)	MMA ²³³	LUCO LED
Nap20	Radical emulsion polymerization	H ₂ O	70 (8 h)	NIPAM, BIS ²³⁴	Dual-fluorescent sensors for temperature and Hg ²⁺
NB1	Radical photopolymerization	EtOH–H ₂ O	RT (20 min)	PEGDMA ²⁵²	EtOH sensor
NB2/NB3	^a	^d	^d	BA ²⁵³	Plasticizer-free fluorescent, H ⁺ and Na ⁺ optode microsphere sensors
OPE1	RAFT	Toluene	70	Homopolymer ²⁶⁰	Conformational study
OPE1–OPE3	RAFT	Toluene–THF	70	Homopolymers, statistical copolymers, MMA ²⁵⁹	Energy transfer studies
OPE4/OPE5	FRP	THF	60 (24 h)	Homopolymer and polymerizable carbazole methacrylate ²⁶¹	Polymer light-emitting diode
				Homopolymer and N-vinyl carbazole ²⁶⁴	Supramolecular cross-linking
				Homopolymer and benzoic acid acrylates ²⁶³	Surface-modified gold NPs
				Homopolymer and N-vinyl carbazole ²⁶²	
Oxa1	FRP	THF	50–60 (48 h)	Homopolymer and carbazole methacrylate copolymer ²³⁵	Electroluminescent films
Oxa2	Radical emulsion polymerization	H ₂ O	70 (4 h)	NIPAM, BIS ^{236,237}	Hydrophilic fluorescent nanogel thermometer
Oxa3	FRP ATRP	Chlorobenzene Toluene	90 110 (2 d)	N-Vinylcarbazole ²³⁸ BECThS (block copolymer) ²³⁹	OLED OLED
Oxa4/Oxa5	ATRP	NMP	110 (4 d)	Homopolymers ²⁴⁰	LC electroluminescent polymer
Oxa6–Oxa12	FRP	Chlorobenzene	90 (36 h)	Homopolymers ²⁴¹	LC polymers
Oxa11	RAFT	Dioxane	80 (12 h)	P(St- <i>co</i> -Oxa11)- <i>b</i> -P(NIPAM- <i>co</i> -Rh7) ²²⁰	Sensor material
	RAFT	Dioxane	80 (12 h)	P(St- <i>co</i> -Oxa11- <i>co</i> -Sp2)- <i>b</i> -P(NIPAM- <i>co</i> -Rh7) ²²²	Sensor material
	ATRP	Isopropanol	25 (1.5 h)	P(NIPAM- <i>co</i> -Oxa11)- <i>b</i> -P(NIPAM- <i>co</i> -Sp2) ²⁴³	Photoswitchable and thermo-tunable multicolor fluorescent hybrid silica NPs
	Radical emulsion polymerization	H ₂ O	70 (7 h)	NIPAM, BIS, Rh9 ²⁴⁴	K ⁺ sensor
Oxa12	RAFT	DMF	80	NIPAM ²⁴⁵	Homodimeric protein–polymer conjugates
Oxa13	FRP	THF	50–60 (24 h)	Carbazole methacrylate ²⁴⁶	Polymer light-emitting diodes
Oxa14/Oxa15	NMP	Diglyme	130	Homopolymers, polymerizable triphenylamines (random copolymers and block copolymers) ²⁴⁷	OLED
Oxa16	NMP	<i>o</i> -Dichlorobenzene	130	Homopolymer, polymerizable carbazole (as block copolymer) ²⁴⁸	OLED
Oxa17	NMP	DMF	135	Polymerizable carbazoles ²⁴⁹	Memory device
Oxa18	NMP	DMF	135	Polymerizable triphenylamine ²⁵⁰	Memory device
Oxa19–Oxa21	FRP	THF	60 (3 d)	Homopolymer ²⁵¹	OLED
Oxa22–Oxa24	ROMP	CH ₂ Cl ₂	RT (overnight)	Homopolymer ²⁵¹	OLED
Oxa25/Oxa26	FRP ^b	THF ^b	60 (7 d) ^b	Homopolymer ²⁵¹	OLED
P1				Homopolymer ¹⁰⁸	Investigations on polymer/fullerene miscibility
P2	Radical emulsion polymerization	H ₂ O	70 (20 h)	BA, MMA, AA ^{125,126}	Study of the drying behavior of wet latex films

Table 2 (continued)

Monomer	Polymerization technique	Solvent	Reaction temperature [°C]	Comonomers	Application
Per1	Radical emulsion polymerization	H ₂ O	80 (20 min)	BMA, bisphenol A dimethacrylate ¹²⁷	Study of branching effects
	Radical emulsion polymerization	H ₂ O	85 (30 min)	MMA, BA ^{128,129} MMA, BA, AA ^{131,132} MMA, BA, MAA ¹³³ <i>t</i> BMA, EHA, MAA ¹³³	Polymer diffusion studies
Py1	NMP	<i>o</i> -Dichlorobenzene	125 (10 to 24 h)	Block copolymer with P3HT or PS ^{42,91,92}	Organic solar cells
Py2	<i>d</i>	<i>d</i>	<i>d</i>	Homopolymer	LC displays
Py2	Radical dispersion polymerization	Ionic liquid	70 (24 h)	AA ⁷⁸	Particle labeling
	Emulsifier-free radical polymerization	H ₂ O	70 (18 h)	Styrene ^{72–75}	Film labeling
	FRP	Bulk	<i>h</i>	Styrene, ^{76,77} MMA ⁷⁶	Labeling for <i>T</i> _g determination
	Radical dispersion polymerization	MeOH–H ₂ O	80 (12 h)	MMA ⁴⁹	NP labeling
	ATRP	Anisole	70 (1 h), 90 (24 h)	MMA (block and random copolymer) ⁷⁹	Self-assembly characterization
	ATRP	Anisole	90 (24 h)	MMA (block copolymer) ⁸¹	Photo- and pH-responsive composite NPs
	ATRP	THF	60 (18 h)	PS- <i>b</i> -PEO (triblock terpolymer) ⁸²	Photoresponsive self-assembly
	RAFT	Benzene	60 (12 h)	VP (block copolymer) ⁸⁴	Ratiometric pH sensor
	RAFT	Toluene	70 (12 h)	DEGMA, Azo24 ^{85,86}	Sensor for temperature and pH value
	NMP	Bulk	125 (4 h)	Styrene, DVB ⁸⁹	Fluorescence labeled macroinitiator
	Radical miniemulsion polymerization	H ₂ O	60–70 (6 h)	Styrene ¹⁰²	Fluorescent particle preparation
	FRP	THF	60 (2 d)	Azo44 and Azo45 ¹⁰³	Functionalization of SWCNTs
	ATRP	THF	60 (12 h)	PEG- <i>b</i> -TEPMA ^c (triblock terpolymer) ¹⁰⁴	Functionalization of SWCNTs
	FRP	Benzene	50 (48 h)	PS, PEGMA ¹⁰⁷	Dispersion of MWCNTs
Py3	Radical emulsion polymerization	H ₂ O	<i>h</i>	Styrene, AA ¹¹⁸	Contrast enhancement in fluorescence microscopy measurements
	FRP	EtOH–H ₂ O–HCl	RT	Dodecylmethacrylate, Hexanedioldimethacrylate ¹³⁴	Sol-gel silica thin films
Py4	FRP	Bulk	<i>h</i>	Styrene and BMA ¹³⁹	Studies of effects on the <i>T</i> _g
	Living anionic polymerization	Toluene	50 (5 h)	Styrene (block copolymer) ^{45,46}	Dispersion of SWCNTs
Py5	ROMP	<i>d</i>	<i>d</i>	Homopolymer ⁹⁰	Synthesis and characterization
Rh1	FRP	Bulk	<i>h</i>	Styrene ¹³⁹	Studies of effects on the <i>T</i> _g
	Radical photopolymerization	DMF	70 (1 min)	HP ₄ MA, PEG ₇₀₀ DA, TETA, Fl2 (diblock- and triblock particles) ¹⁹²	Multiphase amphiphilic rods
	FRP	MeOH	Reflux (72 h)	MMA, cholesterol monomer ²⁰³	Delivery of xenobiotics
	FRP	H ₂ O	40 (40 min)	IBCA, IHCA ²⁰⁴	NPs for the intravenous delivery of siRNA
	FRP	EtOH	60 (12 h)	BMA, MPC ²⁰⁵	Cell-penetrating macromolecules
	Radical photopolymerization	H ₂ O	rt	PEG ₇₀₀ DA ^{206,207}	Production of opaque microparticles by stop-flow lithography
	Radical photopolymerization	Ethylene glycol	RT	AA, acrylamide (copolymer) ²⁰⁹	Three-dimensionally patterned hydrogel pads
	FRP	Paraffin oil	Rt (3 h)	BIS, NIPAM ²¹⁰	Thermoresponsive microgel particles
	Radical photopolymerization	Acetone	RT (2 to 5 min)	NIPAM ²¹¹	Surface-confined hydrogels
	FRP	H ₂ O	70	BIS, allyl amine, NIPAM ^{212,213}	Responsive hydrogels
	FRP	H ₂ O	75 (2 h)	BIS, NIPAM ^{214,215}	Transfer of colloidal patterns by the reversible buckling process, Core-sheath nanofibers
	Radical dispersion polymerization	H ₂ O	70 (6 h)	BIS, NIPAM, AA ²¹⁶	Thermoresponsive nanogels
	Radical emulsion polymerization	H ₂ O	70 (12 h)	BIS, NIPAM ²¹⁷	Cell uptake of polymer NPs

Table 2 (continued)

Monomer	Polymerization technique	Solvent	Reaction temperature [°C]	Comonomers	Application
Rh2	Radical photopolymerization	H ₂ O	Rt (10 min)	HEA and PEG ₅₇₅ diacrylate ¹⁸¹	Formation of three-dimensional hydrogel multilayers
Rh3	FRP	THF	80 (72 h)	VP ¹⁹⁷	Janus particle sensor
	FRP	DMF	70 (24 h)	Homopolymer ²⁰²	Synthesis and characterization
Rh4	ATRP	MeOH	Rt (63 h)	MPC and DPA (block copolymer) ²⁰⁸	Fluorescently labeled biocompatible polymers
Rh5	FRP	MeOH	75 (2 h)	Polymerizable ionic liquids ²¹⁸	FRET in polymeric ionic liquids
	Radical emulsion polymerization	H ₂ O	70 (7 h)	NIPAM, BIS, Oxa11 ²⁴⁴	K ⁺ sensor
Rh6	RAFT	Dioxane	70 (1.5 h)	PEO- <i>b</i> -PNIPAM block copolymer ²¹⁹	Sensor material
Rh7	RAFT	Dioxane-THF	70 (2 h)	P(St- <i>co</i> -Oxa11)- <i>b</i> -P(NIPAM- <i>co</i> -Rh7) block copolymer ²²⁰	Sensor material
	RAFT	Dioxane-H ₂ O	70 (12 h)	P(NIPAM- <i>co</i> -FITC)- <i>b</i> -P(PEGMA- <i>co</i> -Rh7) ²²¹	Sensor material
	RAFT	Dioxane	70 (5 h)	P(St- <i>co</i> -Oxa11- <i>co</i> -Sp2)- <i>b</i> -P(NIPAM- <i>co</i> -Rh7) ²²²	Sensor material
Rh8	ATRP	Toluene		N5 ¹¹¹	Self-assembly and reversible switching
Rh9	FRP	THF	80 (72 h)	VP ¹⁹⁷	Janus particles
Sp1	FRP	THF	70 (3 d)	MMA, polymerizable triphenylamine ²⁵⁴	Polymeric switch
Sp2	RAFT	Dioxane	80 (12 h)	P(St- <i>co</i> -Oxa11- <i>co</i> -Sp2)- <i>b</i> -P(NIPAM- <i>co</i> -Rh7) ²²²	Sensor material
	Radical miniemulsion polymerization	H ₂ O	60 (210 min)	MMA, Nap ³ ²²⁴	Photo-switchable nanoparticles
	ATRP	Isopropanol	25 (7 h)	P(NIPAM- <i>co</i> -Oxa11)- <i>b</i> -P(NIPAM- <i>co</i> -Sp2) ²⁴³	Photoswitchable and thermo-tunable multicolor fluorescent hybrid silica NPs
TD1-TD3	FRP	Cyclohexanone	65 (6 h)	Homopolymers ²⁶⁶	
Thia1/Thia2	RAFT	Toluene	70	MMA ²⁵⁶	Synthesis and characterization
Thia3/Thia4	RAFT	Toluene	70	Styrene ²⁵⁷	Synthesis and characterization
Thia5	RAFT	DMA	85	MMA, polymerizable Ru(II) complex ²⁵⁸	Energy transfer study

^a Propylene glycol methyl ether acetate. ^b Commercially available. ^c 3-(Triethoxysilyl)propyl methacrylate. ^d Protected by patent. ^e Commercially available but no experimental data available. ^f Commercially available homopolymers or reference values from Polymer Handbook used.

^g Language: Chinese. ^h No information published.

of fluorescing dyes, which separately cover a certain part of the UV- and the visible light spectrum. Related to this approach, artificial organic antenna systems are thinkable for mimicking the light-harvesting part of the photosynthesis, for instance. Due to the asymmetry of the monomers, their synthesis will always be the limiting factor in this approach. Besides the “downwards” energy transfer, energy upconversion is also a future field for polymerizable fluorescent dyes.²⁷⁰ So far, the photon upconversion was achieved by triplet-triplet annihilation within polymeric matrices. Future developments will also be extended to polymer bound systems.

With respect to future biological applications, the variation of the particle size and the visualization could lead to new information about a number of biological processes. Thereby, the extension of the fluorescence colors of the dyes over the entire visible light spectrum might enable the monitoring of parallel processes that influence each other. So far, only the green and red fluorescent particles of fluorescein and rhodamine, respectively, have been well-established. However, one has to keep the specific characteristics of each class of dyes in

mind (e.g., toxicity of azo-compounds or hydrophobicity of aromatic dyes) that influence the biological behavior.

In terms of suspending SWNCTs or MWNCTs, the optical properties of the dye moieties play a minor role. Usually aromatic units are applied (e.g., pyrenes) due to their excellent interaction with the material. Chain-end functionalized polymers with one dye per polymer chain already feature the desired capability. Hence, the optimum is already achieved. Nevertheless, the functionalization of the solubilising polymer chains with dye moieties offers a wide range of possibilities. For example, electronic sensor materials on the molecular scale are imaginable.

Moreover, the application of diverse sensor systems is elucidated. The list of potential analytes in different environments or media is endless. As a consequence, tailor-made systems need to be developed for every system. So far, 1,8-naphthalimides have been overrepresented in the class of chemosensors due to their easy functionalization and good response to several anions and cations.

In contrast, the development of molecular switches or electronic memory devices goes in the direction of azo-compounds.

The required synthetic effort for a functionalization is rather limited. One might speculate that also other compounds (*e.g.*, fulgides or merocyanines) that undergo a large shift in a binding angle and/or binding distance by external stimuli will be incorporated into polymer architectures in the future.²⁷¹

With respect to electronic devices, robust monomers which do not tend to bleach over a long time period must be investigated. In some cases, this issue is only a task of device engineering (*e.g.*, the exclusion of oxygen). The benchmark for liquid crystalline displays or OLED application should be at least five years and for organic solar cell devices even longer. For this purpose, small heterocycles (*e.g.*, thiazoles or oxadiazoles) might be a good alternative due to their good stability and low cost production potential.

In general, the studies reviewed in this article support the conclusion that the incorporation of dye molecules leads to modified thermal properties of the polymers. The majority of all investigations showed that an increased content of dye affects an enhanced T_g value. The changes are fluent from low dye content polymers with predominant properties of the comonomer to homopolymers consisting of a polymerizable dye. At least all polymers are stable up to at least 250 °C. Nevertheless, the introduction of dye monomers leads to a decrease of the thermal stability. Furthermore, solubility mediating flexible alkyl side-chains influence the T_g value for conjugated oligomers.²⁴¹ This thermal property correlates with the length of the chain. However, the direction (*i.e.*, either increase or decrease) cannot be predicted. In addition, the chemical stability of the dyes in the polymer must be considered for each application. For long-term application of pH-sensors, for instance, an ester linkage is not useful.

Finally, all polymerizable dyes that have been reviewed in this contribution, are alphabetically listed in Table 2 including their polymerization technique, selected polymerization conditions (*i.e.*, solvent and temperature) as well as their comonomers and their corresponding applications.

Acknowledgements

The authors thank the Thuringian Ministry for Education, Science and Culture [grant #B514-09049, Photonische Mizellen (PhotoMIC), grant #B514-09051, NanoConSens] for financial support. Additionally, the Dutch Polymer Institute (technology area HTE) is acknowledged for financial support.

Notes and references

- B. Happ, A. Winter, M. D. Hager and U. S. Schubert, *Chem. Soc. Rev.*, 2012, **41**, 2222–2255.
- M. Beija, M. T. Charreyre and J. M. G. Martinho, *Prog. Polym. Sci.*, 2011, **36**, 568–602.
- H. Zollinger, *Color chemistry: syntheses, properties, and applications of organic dyes and pigments*, Wiley VCH, Weinheim, 3rd edn., 2003.
- M. Graetzel, *J. Photochem. Photobiol. C*, 2003, **4**, 145–153.
- M. Graetzel, *Nature*, 2003, **421**, 586–587.
- M. K. Nazeeruddin, E. Baranoff and M. Graetzel, *Sol. Energy*, 2011, **85**, 1172–1178.
- G. Moad, M. Chen, M. Haeussler, A. Postma, E. Rizzardo and S. H. Thang, *Polym. Chem.*, 2011, **2**, 492–519.
- X. Z. Liu, R. Zhu, Y. Zhang, B. Liu and S. Ramakrishna, *Chem. Commun.*, 2008, 3789–3791.
- W. Zhang, Z. Fang, M. J. Su, M. Saefs and B. Liu, *Macromol. Rapid Commun.*, 2009, **30**, 1533–1537.
- G. D. Sharma, P. Suresh and J. A. Mikroyannidis, *Synth. Met.*, 2010, **160**, 1427–1432.
- A. Keppler, S. Gendreizig, T. Gronemeyer, H. Pick, H. Vogel and K. Johnsson, *Nat. Biotechnol.*, 2003, **21**, 86–89.
- R. Y. Tsien, *Annu. Rev. Biochem.*, 1998, **67**, 509–544.
- B. A. Griffin, S. R. Adams and R. Y. Tsien, *Science*, 1998, **281**, 269–272.
- U. Resch-Genger, M. Grabolle, S. Cavaliere-Jaricot, R. Nitschke and T. Nann, *Nat. Methods*, 2008, **5**, 763–775.
- G. M. Hasselman, D. F. Watson, J. R. Stromberg, D. F. Bocian, D. Holten, J. S. Lindsey and G. J. Meyer, *J. Phys. Chem. B*, 2006, **110**, 25430–25440.
- C. A. Martinez-Huitle and E. Brillas, *Appl. Catal., B*, 2009, **87**, 105–145.
- E. Guivarch, S. Trevis, C. Lahitte and M. A. Oturan, *Environ. Chem. Lett.*, 2003, **1**, 38–44.
- A. C. Grimsdale, K. L. Chan, R. E. Martin, P. G. Jokisz and A. B. Holmes, *Chem. Rev.*, 2009, **109**, 897–1091.
- O. Nuyken, S. Jungermann, V. Wiederhirn, E. Bacher and K. Meerholz, *Monatsh. Chem.*, 2006, **137**, 811–824.
- P. I. Shih, C. F. Shu, Y. L. Tung and Y. Chi, *Appl. Phys. Lett.*, 2006, **88**, 251110.
- J. J. Lu, H. Li, B. Yao, B. Zhao, C. Weng, G. T. Lei, P. Shen, Z. Y. Xie and S. T. Tan, *J. Phys. Chem. B*, 2009, **113**, 4203–4208.
- Z. H. Lin, Y. D. Lin, C. Y. Wu, P. T. Chow, C. H. Sun and T. J. Chow, *Macromolecules*, 2010, **43**, 5925–5931.
- K. Lee, L. K. Povlich and J. Kim, *Analyst*, 2010, **135**, 2179–2189.
- D. T. McQuade, A. E. Pullen and T. M. Swager, *Chem. Rev.*, 2000, **100**, 2537–2574.
- C. C. Yang, Y. Tian, C. Y. Chen, A. K. Y. Jen and W. C. Chen, *Macromol. Rapid Commun.*, 2007, **28**, 894–899.
- D. A. Friesen, T. Kajita, E. Danielson and T. J. Meyer, *Inorg. Chem.*, 1998, **37**, 2756–2762.
- B. Happ, J. Schaefer, R. Menzel, M. D. Hager, A. Winter, J. Popp, R. Beckert, B. Dietzek and U. S. Schubert, *Macromolecules*, 2011, **44**, 6277–6287.
- G. Moad, E. Rizzardo and S. H. Thang, *Aust. J. Chem.*, 2009, **62**, 1402–1472.
- K. Matyjaszewski, *J. Macromol. Sci., Pure Appl. Chem.*, 1997, **A34**, 1785–1801.
- K. Matyjaszewski and J. H. Xia, *Chem. Rev.*, 2001, **101**, 2921–2990.
- C. J. Hawker, A. W. Bosman and E. Harth, *Chem. Rev.*, 2001, **101**, 3661–3688.
- N. Hadjichristidis, M. Pitsikalis, S. Pispas and H. Iatrou, *Chem. Rev.*, 2001, **101**, 3747–3792.

- 33 K. Kempe, A. Krieg, C. R. Becer and U. S. Schubert, *Chem. Soc. Rev.*, 2012, **41**, 176–191.
- 34 F. Thielbeer, S. V. Chankeshwara and M. Bradley, *Biomacromolecules*, 2011, **12**, 4386–4391.
- 35 A. Vollrath, D. Pretzel, C. Pietsch, I. Perevyazko, S. Schubert, G. M. Pavlov and U. S. Schubert, *Macromol. Rapid Commun.*, 2012, **33**, 1791–1797.
- 36 V. Mailaender and K. Landfester, *Biomacromolecules*, 2009, **10**, 2379–2400.
- 37 K. Letchford and H. Burt, *Eur. J. Pharm. Biopharm.*, 2007, **65**, 259–269.
- 38 A. Vollrath, A. Schallan, C. Pietsch, S. Schubert, T. Nomoto, Y. Matsumoto, K. Kataoka and U. S. Schubert, *Soft Matter*, 2013, **9**, 99–108.
- 39 J. P. Rao and K. E. Geckeler, *Prog. Polym. Sci.*, 2011, **36**, 887–913.
- 40 K. A. V. Zubris, O. V. Khullar, A. P. Griset, S. Gibbs-Strauss, J. V. Frangioni, Y. L. Colson and M. W. Grinstaff, *Chem-MedChem*, 2010, **5**, 1435–1438.
- 41 L. Yuan, W. Y. Lin, K. B. Zheng, L. W. He and W. M. Huang, *Chem. Soc. Rev.*, 2013, **42**, 622–661.
- 42 M. Sommer, S. Huttner, S. Wunder and M. Thelakkat, *Adv. Mater.*, 2008, **20**, 2523–2527.
- 43 C. J. Brabec, N. S. Sariciftci and J. C. Hummelen, *Adv. Funct. Mater.*, 2001, **11**, 15–26.
- 44 R. F. Service, *Science*, 2011, **332**, 293–293.
- 45 Y. H. Yan, S. B. Yang, J. Cui, L. Jakisch, P. Potschke and B. Voit, *Polym. Int.*, 2011, **60**, 1425–1433.
- 46 Y. H. Yan, J. A. Cui, P. Potschke and B. Voit, *Carbon*, 2010, **48**, 2603–2612.
- 47 W. J. Xu, T. S. Li, G. L. Zeng, S. Zhang, W. Shang, Y. J. Wu and T. Miyashita, *J. Photochem. Photobiol., A*, 2008, **194**, 97–104.
- 48 W. J. Xu, T. S. Li, G. J. Li, Y. J. Wu and T. Miyashita, *J. Photochem. Photobiol., A*, 2011, **219**, 50–57.
- 49 T. Taniguchi, T. Ogawa, Y. Kamata, S. Kobayashi, N. Takeuchi, M. Kohri, T. Nakahira and T. Wakiya, *Colloids Surf., A*, 2010, **356**, 169–175.
- 50 I. Popescu, A. Airinei, D. M. Suflet and M. I. Popa, *J. Polym. Res.*, 2011, **18**, 2195–2203.
- 51 N. Naga, Y. Wakita and S. Murase, *J. Appl. Polym. Sci.*, 2008, **110**, 3770–3777.
- 52 C. R. Zhong, P. Y. Luo, Z. B. Ye and H. Chen, *Polym. Bull.*, 2009, **62**, 79–89.
- 53 S. Zapotoczny, M. Golonka and M. Nowakowska, *Langmuir*, 2008, **24**, 5868–5876.
- 54 D. Drozd, K. Szczubialka and M. Nowakowska, *J. Photochem. Photobiol., A*, 2010, **215**, 223–228.
- 55 X. Zhang, C. J. Metting, R. M. Briber, F. Weilnboeck, S. H. Shin, B. G. Jones and G. S. Oehrlein, *Macromol. Chem. Phys.*, 2011, **212**, 1735–1741.
- 56 R. H. Liu, M. A. Winnik, F. Di Stefano and J. Vanketessan, *J. Polym. Sci., Part A: Polym. Chem.*, 2001, **39**, 1495–1504.
- 57 C. R. Lopez-Barron and C. W. Macosko, *Langmuir*, 2009, **25**, 9392–9404.
- 58 C. R. Lopez-Barron and C. W. Macosko, *Soft Matter*, 2010, **6**, 2637–2647.
- 59 M. Kondo, M. Takemoto, T. Matsuda, R. Fukae and N. Kawatsuki, *Bull. Chem. Soc. Jpn.*, 2010, **83**, 1333–1337.
- 60 M. Kondo, T. Matsuda, R. Fukae and N. Kawatsuki, *Chem. Lett.*, 2010, **39**, 234–235.
- 61 D. Neugebauer, D. Charasim, A. Swinarew, A. Stolarzewicz, M. Krompiec, H. Janeczek, J. Simokaitiene and J. V. Grazulevicius, *Polym. J.*, 2011, **43**, 448–454.
- 62 Z. Shi, L. Luo, S. Huang, B. M. Polishak, X.-H. Zhou, S. Liff, T. R. Younkin, B. A. Block and A. K.-Y. Jen, *J. Mater. Chem.*, 2012, **22**, 951–959.
- 63 S. El Habnouni, V. Darcos, X. Garric, J. P. Lavigne, B. Nottelet and J. Coudane, *Adv. Funct. Mater.*, 2011, **21**, 3321–3330.
- 64 H. Sakamoto, T. Anase, H. Osuga and K. Kimura, *React. Funct. Polym.*, 2011, **71**, 569–573.
- 65 G. Huh, K. O. Kwon, S. H. Cha, S. W. Yoon, M. Y. Lee and J. C. Lee, *J. Appl. Polym. Sci.*, 2009, **114**, 2093–2100.
- 66 C. W. Lee, J. W. Kim, J. H. Lee and K. D. Ahn, *React. Funct. Polym.*, 2009, **69**, 737–742.
- 67 V. B. Bueno, I. M. Cuccovia, H. Chaimovich and L. H. Catalani, *Colloid Polym. Sci.*, 2009, **287**, 705–713.
- 68 R. A. Domingues, I. V. P. Yoshida and T. D. Z. Atvars, *J. Polym. Sci., Part B: Polym. Phys.*, 2010, **48**, 74–81.
- 69 T. D. Kim, J. D. Luo, Y. J. Cheng, Z. W. Shi, S. Hau, S. H. Jang, X. H. Zhou, Y. Tian, B. Polishak, S. Huang, H. Ma, L. R. Dalton and A. K. Y. Jen, *J. Phys. Chem. C*, 2008, **112**, 8091–8098.
- 70 H. Morikawa, Y. Kotaki, R. Mihara, Y. Kiraku, S. Ichimura and S. Motokuchō, *Chem. Lett.*, 2010, **39**, 682–683.
- 71 M. Kondo, M. Takemoto, T. Matsuda, R. Fukae and N. Kawatsuki, *Mol. Cryst. Liq. Cryst.*, 2011, **550**, 98–104.
- 72 S. Ugur, O. Yargi, E. Gunister and O. Pekcan, *Appl. Clay Sci.*, 2008, **42**, 39–49.
- 73 S. Ugur, O. Yargi and O. Pekcan, *Appl. Clay Sci.*, 2009, **43**, 447–452.
- 74 S. Ugur, O. Yargi and O. Pekcan, *Polym. Compos.*, 2010, **31**, 77–82.
- 75 S. Ugur, S. Sunay and O. Pekcan, *Polym. Compos.*, 2010, **31**, 1611–1619.
- 76 C. M. Evans, R. W. Sandoval and J. M. Torkelson, *Macromolecules*, 2011, **44**, 6645–6648.
- 77 S. Kim and J. M. Torkelson, *Macromolecules*, 2011, **44**, 4546–4553.
- 78 H. Minami, A. Kimura, K. Kinoshita and M. Okubo, *Langmuir*, 2010, **26**, 6303–6307.
- 79 J. You, J. A. Yoon, J. Kim, C. F. Huang, K. Matyjaszewski and E. Kim, *Chem. Mater.*, 2010, **22**, 4426–4434.
- 80 J. Xue, L. Chen, H. L. Wang, Z. B. Zhang, X. L. Zhu, E. T. Kang and K. G. Neoh, *Langmuir*, 2008, **24**, 14151–14158.
- 81 H. K. Feng, Y. Zhao, M. Pelletier, Y. Dan and Y. Zhao, *Polymer*, 2009, **50**, 3470–3477.
- 82 S. Menon and S. Das, *J. Polym. Sci., Part A: Polym. Chem.*, 2011, **49**, 4448–4457.
- 83 M. Demetriou and T. Krasia-Christoforou, *J. Polym. Sci., Part A: Polym. Chem.*, 2012, **50**, 52–60.

- 84 K. Paek, S. Chung, C. H. Cho and B. J. Kim, *Chem. Commun.*, 2011, **47**, 10272–10274.
- 85 C. Pietsch, A. Vollrath, R. Hoogenboom and U. S. Schubert, *Sensors*, 2010, **10**, 7979–7990.
- 86 C. Pietsch, R. Hoogenboom and U. S. Schubert, *Polym. Chem.*, 2010, **1**, 1005–1008.
- 87 I. Perevyazko, A. Vollrath, S. Hornig, G. M. Pavlov and U. S. Schubert, *J. Polym. Sci., Part A: Polym. Chem.*, 2010, **48**, 3924–3931.
- 88 M. Chen, K. P. Ghiggino, E. Rizzardo, S. H. Thang and G. J. Wilson, *Chem. Commun.*, 2008, 1112–1114.
- 89 P. B. Zetterlund, N. Alam and M. Okubo, *Polym. J.*, 2008, **40**, 298–299.
- 90 D.-J. Liaw, *US Pat.*, 20 110 092 666, 2012.
- 91 M. Sommer, S. Huttner, U. Steiner and M. Thelakkat, *Appl. Phys. Lett.*, 2009, **95**, 183308.
- 92 M. Sommer, A. S. Lang and M. Thelakkat, *Angew. Chem., Int. Ed.*, 2008, **47**, 7901–7904.
- 93 I. Natori, S. Natori, H. Sekikawa, T. Takahashi and H. Sato, *J. Appl. Polym. Sci.*, 2010, **118**, 69–73.
- 94 I. Natori and S. Natori, *Polym. Adv. Technol.*, 2010, **21**, 784–788.
- 95 T. Sakamoto, Y. Fukuda, S. I. Sato and T. Nakano, *Angew. Chem., Int. Ed.*, 2009, **48**, 9308–9311.
- 96 K. Wanatabe, T. Sakamoto and T. Nakano, *Chirality*, 2011, **23**, E28–E34.
- 97 C. X. Li, J. C. Hsu, K. Sugiyama, A. Hirao, W. C. Chen and R. Mezzenga, *Macromolecules*, 2009, **42**, 5793–5801.
- 98 J. C. Hsu, K. Sugiyama, Y. C. Chiu, A. Hirao and W. C. Chen, *Macromolecules*, 2010, **43**, 7151–7158.
- 99 A. Bossi, M. J. Whitcombe, Y. Uludag, S. Fowler, I. Chianella, S. Subrahmanyam, I. Sanchez and S. A. Piletsky, *Biosens. Bioelectron.*, 2010, **25**, 2149–2155.
- 100 P. Govindaiah, Y. J. Jung, J. M. Lee, T. J. Park, D. Y. Ryu, J. H. Kim and I. W. Cheong, *J. Colloid Interface Sci.*, 2010, **343**, 484–490.
- 101 F. Tian, N. Cheng, N. Nouvel, J. Geng and O. A. Scherman, *Langmuir*, 2010, **26**, 5323–5328.
- 102 T. Taniguchi, N. Takeuchi, S. Kobaru and T. Nakahira, *J. Colloid Interface Sci.*, 2008, **327**, 58–62.
- 103 C. Vijayakumar, B. Balan, M. J. Kim and M. Takeuchi, *J. Phys. Chem. C*, 2011, **115**, 4533–4539.
- 104 C. Zhang, W. Zhu, L. Gao and Y. M. Chen, *Chin. J. Polym. Sci.*, 2011, **29**, 762–771.
- 105 X. Y. Pan and M. B. Chan-Park, *J. Polym. Sci., Part B: Polym. Phys.*, 2011, **49**, 949–960.
- 106 X. Y. Pan, L. L. Li and M. B. Chan-Park, *Small*, 2010, **6**, 1311–1320.
- 107 M. Matsuoka, M. Yamamoto, K. Adachi, Y. Tsukahara and T. Konno, *Des. Monomers Polym.*, 2010, **13**, 387–397.
- 108 K. Campbell, B. Gurun, B. G. Sumpter, Y. S. Thio and D. G. Bucknall, *J. Phys. Chem. B*, 2011, **115**, 8989–8995.
- 109 S. Vallejos, H. El Kaoutit, P. Estévez, F. C. García, J. L. de la Peña, F. Serna and J. M. García, *Polym. Chem.*, 2011, **2**, 1129–1138.
- 110 Y. C. Chiu, C. C. Kuo, J. C. Hsu and W. C. Chen, *ACS Appl. Mater. Interfaces*, 2010, **2**, 3340–3347.
- 111 J. Geng, F. Biedermann, J. M. Zayed, F. Tian and O. A. Scherman, *Macromolecules*, 2011, **44**, 4276–4281.
- 112 L. Y. Liu, M. W. Ren and W. T. Yang, *Langmuir*, 2009, **25**, 11048–11053.
- 113 C. L. Liu, J. C. Hsu, W. C. Chen, K. Sugiyama and A. Hirao, *ACS Appl. Mater. Interfaces*, 2009, **1**, 1974–1979.
- 114 K. Sugiyama, A. Hirao, J. C. Hsu, Y. C. Tung and W. C. Chen, *Macromolecules*, 2009, **42**, 4053–4062.
- 115 J. C. Hsu, C. L. Liu, W. C. Chen, K. Sugiyama and A. Hirao, *Macromol. Rapid Commun.*, 2011, **32**, 528–533.
- 116 J. C. Hsu, C. X. Li, K. Sugiyama, R. Mezzenga, A. Hirao and W. C. Chen, *Soft Matter*, 2011, **7**, 8440–8449.
- 117 K. J. Baeg, Y. Y. Noh, J. Ghim, B. Lim and D. Y. Kim, *Adv. Funct. Mater.*, 2008, **18**, 3678–3685.
- 118 R. F. Cossiello, A. Cirpan, F. E. Karasz, L. Akcelrud and T. D. Z. Atvars, *Synth. Met.*, 2008, **158**, 219–225.
- 119 D. McKenzie, D. Abdallah, A. G. Timko and M. D. Rahman, *WO Pat.*, 2 009 136 242, 2009.
- 120 M. Padmanaban, S. Chakrapani, F. M. Houlihan, S. Miyazaki, E. W. Ng and M. O. Neisser, *WO Pat.*, 2 011 039 560, 2011.
- 121 R. Ashizawa, H. Kita, M. Kondo and K. Hiraga, *WO Pat.*, 2 011 125 876, 2011.
- 122 J. F. Cameron, J. W. Sung, J. P. Amara, G. P. Prokopowicz, D. A. Valeri, L. Vyklicky, W.-S. S. Huang, W. Li, P. R. Varanasi and I. Y. Popova, *Eur. Pat.*, 2 216 684, 2010.
- 123 A. A. Aldongarov, N. N. Barashkov, I. S. Irgibaeva, O. A. Khakhel and Y. E. Sakhno, *Adv. Funct. Mater.*, 2008, **15**, 398–401.
- 124 L. Ruiz-Perez, A. Pryke, M. Sommer, G. Battaglia, I. Soutar, L. Swanson and M. Geoghegan, *Macromolecules*, 2008, **41**, 2203–2211.
- 125 J. C. Haley, Y. Q. Liu, M. A. Winnik and W. Lau, *J. Coat. Technol. Res.*, 2008, **5**, 157–168.
- 126 A. Turshatov, J. Adams and D. Johannsmann, *Macromolecules*, 2008, **41**, 5365–5372.
- 127 Y. Q. Liu, W. F. Schroeder, J. C. Haley, W. Lau and M. A. Winnik, *Macromolecules*, 2008, **41**, 9104–9111.
- 128 J. P. Tomba, X. D. Ye, F. G. Li, M. A. Winnik and W. Lau, *Polymer*, 2008, **49**, 2055–2064.
- 129 J. P. Tomba, D. Portinha, W. F. Schroeder, M. A. Winnik and W. Lau, *Colloid Polym. Sci.*, 2009, **287**, 367–378.
- 130 Y. Q. Liu, W. Schroeder, M. Soleimani, W. Lau and M. A. Winnik, *Macromolecules*, 2010, **43**, 6438–6449.
- 131 W. F. Schroeder, Y. Q. Liu, J. P. Tomba, M. Soleimani, W. Lau and M. A. Winnik, *J. Phys. Chem. B*, 2010, **114**, 3085–3094.
- 132 W. F. Schroeder, Y. Q. Liu, J. P. Tomba, M. Soleimani, W. Lau and M. A. Winnik, *Polymer*, 2011, **52**, 3984–3993.
- 133 M. Soleimani, J. C. Haley, W. Lau and M. A. Winnik, *Macromolecules*, 2010, **43**, 975–985.
- 134 M. H. Huang, H. M. Soyez, B. S. Dunn, J. I. Zink, A. Sellinger and C. J. Brinker, *J. Sol-Gel Sci. Technol.*, 2008, **47**, 300–310.
- 135 X. L. Yu, B. Yi and X. Y. Wang, *Eur. Polym. J.*, 2008, **44**, 3997–4001.

- 136 W. Q. Liu and C. Z. Cao, *Colloid Polym. Sci.*, 2009, **287**, 811–818.
- 137 J. Xu, L. Wang, G. J. Liang, L. X. Wang and X. L. Shen, *Polym. Eng. Sci.*, 2011, **51**, 2408–2416.
- 138 T. S. Li, M. Mitsuishi and T. Miyashita, *Thin Solid Films*, 2008, **516**, 2115–2119.
- 139 S. Kim, C. B. Roth and J. M. Torkelson, *J. Polym. Sci., Part B: Polym. Phys.*, 2008, **46**, 2754–2764.
- 140 C. Pugh, M. Paz-Pazos and C. N. Tang, *J. Polym. Sci., Part A: Polym. Chem.*, 2009, **47**, 331–345.
- 141 S. Karena and Z. El Rassi, *Electrophoresis*, 2011, **32**, 1044–1053.
- 142 W. Chen and L. Weng, *US Pat.*, 20 100 029 789, 2010.
- 143 F. Qiu, C. Ge, X. Gu and D. Yang, *Chin. Pat.*, 101 805 421, 2011.
- 144 F. A. Nicolescu, V. V. Jerca, D. M. Vuluga and D. S. Vasilescu, *Polym. Bull.*, 2010, **65**, 905–916.
- 145 F. A. Nicolescu, V. V. Jerca, C. Draghici, D. M. Vuluga and D. S. Vasilescu, *Des. Monomers Polym.*, 2009, **12**, 553–563.
- 146 P. D. S. Rosalyn, P. Kannan, A. Y. Nooraldeen, P. Mangayarkarasi and P. K. Palanisamy, *J. Optoelectron. Adv. Mater.*, 2008, **10**, 3368–3376.
- 147 C. Saravanan and P. Kannan, *Polym. Degrad. Stab.*, 2009, **94**, 1001–1012.
- 148 Y. Feng, J. Duan, X. Li, Z. Wen and W. Xu, *Chin. Pat.*, 101 544 850, 2009.
- 149 N. J. Li, J. M. Lu, X. W. Xia, Q. F. Xu and L. H. Wang, *Dyes Pigm.*, 2009, **80**, 73–79.
- 150 Q. F. Xu, Y. H. Liu, N. J. Li, X. W. Xia, J. F. Ge and J. M. Lu, *Eur. Polym. J.*, 2011, **47**, 1160–1167.
- 151 S. H. Kim, C. K. Jang, S. H. Jeong and J. Y. Jaung, *J. Soc. Inf. Disp.*, 2010, **18**, 994–1009.
- 152 A. S. Abd-El-Aziz, P. O. Shipman, P. R. Shipley, B. N. Boden, S. Aly and P. D. Harvey, *Macromol. Chem. Phys.*, 2009, **210**, 2099–2106.
- 153 A. S. Abd-El-Aziz, P. O. Shipman, E. G. Neeland, T. C. Corkery, S. Mohammed, P. D. Harvey, H. M. Mohamed, A. H. Bedair, A. M. El-Agropy, P. M. Aguiar and S. Kroeker, *Macromol. Chem. Phys.*, 2008, **209**, 84–103.
- 154 N. Hosono, T. Kajitani, T. Fukushima, K. Ito, S. Sasaki, M. Takata and T. Aida, *Science*, 2010, **330**, 808–811.
- 155 T. Yoshino, M. Kondo, J. Mamiya, M. Kinoshita, Y. L. Yu and T. Ikeda, *Adv. Mater.*, 2010, **22**, 1361–1363.
- 156 C. Pietsch, R. Hoogenboom and U. S. Schubert, *Angew. Chem., Int. Ed.*, 2009, **48**, 5653–5656.
- 157 H. Z. Cao, W. Zhang, J. Zhu, X. R. Chen, Z. P. Cheng, J. H. Wu and X. L. Zhu, *eXPRESS Polym. Lett.*, 2008, **2**, 589–601.
- 158 D. Zhou, X. L. Zhu, J. Zhu and Z. P. Cheng, *Polymer*, 2008, **49**, 3048–3053.
- 159 N. Otani and M. Haishi, *Jap. Pat.*, 2 010 027 956, 2010.
- 160 N. Ohtani and M. Haishi, *Ultraviolet polymer light-emitting diodes*, Doshisha University, Science and Engineering Research Institute, Kyoto, JAPON, 2008.
- 161 M. Haishi, T. Yamamoto, M. Murata and N. Ohtani, *J. Phys.: Conf. Ser.*, 2008, **109**, 012011.
- 162 M. Spiniello, A. Blencowe and G. G. Qiao, *J. Polym. Sci., Part A: Polym. Chem.*, 2008, **46**, 2422–2432.
- 163 M. Schraub and N. Hampp, *Proc. SPIE-Int. Soc. Opt. Eng.*, 2011, **7885**, 78851Z.
- 164 B. J. Xie, G. Wang and X. C. Zhao, *J. Appl. Polym. Sci.*, 2011, **122**, 3377–3382.
- 165 J. Motoyanagi, I. Nishimura and M. Minoda, *J. Polym. Sci., Part A: Polym. Chem.*, 2011, **49**, 4701–4707.
- 166 Y. Q. Zhao, F. Fei, C. L. Yi, J. Q. Jiang, J. Luo and X. Y. Liu, *Acta Phys.-Chim. Sin.*, 2010, **26**, 3230–3236.
- 167 C. Kim, J. U. Wallace, S. H. Chen and P. B. Merkel, *Macromolecules*, 2008, **41**, 3075–3080.
- 168 B. Y. Wang, X. Y. Liu, S. L. Ding and Z. X. Su, *J. Polym. Res.*, 2011, **18**, 1315–1322.
- 169 B. Y. Wang, X. Y. Liu, Y. L. Hu and Z. X. Su, *Polym. Int.*, 2009, **58**, 703–709.
- 170 B. Y. Wang, Y. L. Hu and Z. X. Su, *React. Funct. Polym.*, 2008, **68**, 1137–1143.
- 171 D. G. Li, J. Zhu, Z. P. Cheng, W. Zhang and X. L. Zhu, *React. Funct. Polym.*, 2009, **69**, 240–245.
- 172 H. J. Patel, M. G. Patel, A. K. Patel, K. H. Patel and R. M. Patel, *eXPRESS Polym. Lett.*, 2008, **2**, 727–734.
- 173 M. D. Rowe, D. H. Thamm, S. L. Kraft and S. G. Boyes, *Biomacromolecules*, 2009, **10**, 983–993.
- 174 L. Ding, D. Jani, J. Linhardt, J. F. Kunzler, S. Pawar, G. Labenski, T. Smith and W. H. Knox, *J. Opt. Soc. Am. B*, 2009, **26**, 1679–1687.
- 175 Y. Hoshino, H. Koide, T. Urakami, H. Kanazawa, T. Kodama, N. Oku and K. J. Shea, *J. Am. Chem. Soc.*, 2010, **132**, 6644–6645.
- 176 A. Srisopa, A. M. I. Ali and A. G. Mayes, *J. Polym. Sci., Part A: Polym. Chem.*, 2011, **49**, 2070–2080.
- 177 P. Govindaiah, S. J. Lee, J. H. Kim and I. W. Cheong, *Polymer*, 2011, **52**, 5058–5064.
- 178 A. Saha, S. K. Basiruddin, R. Sarkar, N. Pradhan and N. R. Jana, *J. Phys. Chem. C*, 2009, **113**, 18492–18498.
- 179 S. K. Basiruddin, A. Saha, N. Pradhan and N. R. Jana, *Langmuir*, 2010, **26**, 7475–7481.
- 180 A. R. Maity and N. R. Jana, *J. Phys. Chem. C*, 2011, **115**, 137–144.
- 181 L. M. Johnson, C. A. DeForest, A. Pendurti, K. S. Anseth and C. N. Bowman, *ACS Appl. Mater. Interfaces*, 2010, **2**, 1963–1972.
- 182 L. Moreau, A. Balland-Longeau, P. Mazabraud, A. Duchene and J. Thibonnet, *Chem. Commun.*, 2010, **46**, 1464–1466.
- 183 I. P. Chang, K. C. Hwang and C. S. Chiang, *J. Am. Chem. Soc.*, 2008, **130**, 15476–15481.
- 184 X. Wu, G. J. Price and R. H. Guy, *Mol. Pharmaceutics*, 2009, **6**, 1441–1448.
- 185 X. Wu, P. Griffin, G. J. Price and R. H. Guy, *Mol. Pharmaceutics*, 2009, **6**, 1449–1456.
- 186 M. A. J. Mazumder, N. A. D. Burke, F. Shen, M. A. Potter and H. D. H. Stover, *Biomacromolecules*, 2009, **10**, 1365–1373.
- 187 J. Li, M. A. J. Mazumder, H. D. H. Stover, A. P. Hitchcock and I. M. Shirley, *J. Polym. Sci., Part A: Polym. Chem.*, 2011, **49**, 3038–3047.

- 188 I. E. Pacios and I. F. Piérola, *J. Appl. Polym. Sci.*, 2009, **112**, 1579–1586.
- 189 J. Wang, S. M. Tian, R. A. Petros, M. E. Napier and J. M. DeSimone, *J. Am. Chem. Soc.*, 2010, **132**, 11306–11313.
- 190 S. E. A. Gratton, M. E. Napier, P. A. Ropp, S. M. Tian and J. M. DeSimone, *Pharm. Res.*, 2008, **25**, 2845–2852.
- 191 K. P. Herlihy, J. Nunes and J. M. DeSimone, *Langmuir*, 2008, **24**, 8421–8426.
- 192 J.-Y. Wang, Y. Wang, S. S. Sheiko, D. E. Betts and J. M. DeSimone, *J. Am. Chem. Soc.*, 2011, 5801–5806.
- 193 E. H. Min, S. R. S. Ting, L. Billon and M. H. Stenzel, *J. Polym. Sci., Part A: Polym. Chem.*, 2010, **48**, 3440–3455.
- 194 S. R. S. Ting, E. H. Min, P. B. Zetterlund and M. H. Stenzel, *Macromolecules*, 2010, **43**, 5211–5221.
- 195 L. Ionov, V. Bocharova and S. Diez, *Soft Matter*, 2009, **5**, 67–71.
- 196 A. Nese, N. V. Lebedeva, G. Sherwood, S. Averick, Y. C. Li, H. F. Gao, L. Peteanu, S. S. Sheiko and K. Matyjaszewski, *Macromolecules*, 2011, **44**, 5905–5910.
- 197 S. Berger, A. Synytska, L. Ionov, K. J. Eichhorn and M. Stamm, *Macromolecules*, 2008, **41**, 9669–9676.
- 198 X. L. Guan, S. J. Lai and Z. X. Su, *J. Appl. Polym. Sci.*, 2011, **122**, 1968–1975.
- 199 S. J. Lai, X. L. Guan and Z. X. Su, *J. Optoelectron. Adv. Mater.*, 2011, **5**, 600–605.
- 200 X. Q. Liu and M. B. Chan-Park, *J. Appl. Polym. Sci.*, 2009, **114**, 3414–3419.
- 201 S. Manickasundaram, P. Kannan, R. Kumaran, R. Velu, P. Ramamurthy, Q. M. A. Hassan, P. K. Palanisamy, S. Senthil and S. S. Narayanan, *J. Mater. Sci.: Mater. Electron.*, 2011, **22**, 25–34.
- 202 H. Yang, S. Vasudevan, C. O. Oriakhi, J. Shields and R. G. Carter, *Synthesis-Stuttgart*, 2008, 957–961.
- 203 L. De Jong, X. Moreau, A. Thiéry, G. Godeau, M. W. Grinstaff and P. Barthélémy, *Bioconjugate Chem.*, 2008, **19**, 891–898.
- 204 H. de Martimprey, J. R. Bertrand, C. Malvy, P. Couvreur and C. Vauthier, *Pharm. Res.*, 2010, **27**, 498–509.
- 205 T. Goda, Y. Goto and K. Ishihara, *Biomaterials*, 2010, **31**, 2380–2387.
- 206 S. K. Suh, K. W. Bong, T. A. Hatton and P. S. Doyle, *Langmuir*, 2011, **27**, 13813–13819.
- 207 H. B. Zhang, A. J. DeConinck, S. C. Slimmer, P. S. Doyle, J. A. Lewis and R. G. Nuzzo, *Chem.-Eur. J.*, 2011, **17**, 2867–2873.
- 208 J. Madsen, N. J. Warren, S. P. Armes and A. L. Lewis, *Biomacromolecules*, 2011, **12**, 2225–2234.
- 209 L. D. Zarzar, P. Kim, M. Kolle, J. Brinker, J. Aizenberg and B. Kaepr, *Angew. Chem., Int. Ed.*, 2011, **50**, 9356–9360.
- 210 J. Musch, S. Schneider, P. Lindner and W. Richtering, *J. Phys. Chem. B*, 2008, **112**, 6309–6314.
- 211 S. J. DuPont, R. S. Cates, P. G. Stroot and R. Toomey, *Soft Matter*, 2010, **6**, 3876–3882.
- 212 E. C. Cho, J. W. Kim, D. C. Hyun, U. Jeong and D. A. Weitz, *Langmuir*, 2010, **26**, 3854–3859.
- 213 E. C. Cho, J. W. Kim, A. Fernandez-Nieves and D. A. Weitz, *Nano Lett.*, 2008, **8**, 168–172.
- 214 D. C. Hyun, G. D. Moon, E. C. Cho and U. Y. Jeong, *Adv. Funct. Mater.*, 2009, **19**, 2155–2162.
- 215 E. Jo, S. W. Lee, K. T. Kim, Y. S. Won, H. S. Kim, E. C. Cho and U. Jeong, *Adv. Mater.*, 2009, **21**, 968–972.
- 216 J. E. Wong, C. B. Mueller, A. M. Diez-Pascual and W. Richtering, *J. Phys. Chem. B*, 2009, **113**, 15907–15913.
- 217 T. Tenuta, M. P. Monopoli, J. Kim, A. Salvati, K. A. Dawson, P. Sandin and I. Lynch, *PLoS One*, 2011, **6**, e25556.
- 218 S. Wakizono, K. Yamamoto and J. Kadokawa, *J. Photochem. Photobiol., A*, 2011, **222**, 283–287.
- 219 J. M. Hu, C. H. Li and S. Y. Liu, *Langmuir*, 2010, **26**, 724–729.
- 220 J. M. Hu, L. Dai and S. Y. Liu, *Macromolecules*, 2011, **44**, 4699–4710.
- 221 J. M. Hu, X. Z. Zhang, D. Wang, X. L. Hu, T. Liu, G. Y. Zhang and S. Y. Liu, *J. Mater. Chem.*, 2011, **21**, 19030–19038.
- 222 C. H. Li, Y. X. Zhang, J. M. Hu, J. J. Cheng and S. Y. Liu, *Angew. Chem., Int. Ed.*, 2010, **49**, 5120–5124.
- 223 A. Khosravi, H. S. Panah, K. Gharanjig, M. Khorassani, M. K. Zadeh and F. A. Taromi, *Iran. Polym. J.*, 2010, **19**, 491–499.
- 224 J. A. Chen, P. S. Zhang, G. Fang, P. G. Yi, X. Y. Yu, X. F. Li, F. Zeng and S. Z. Wu, *J. Phys. Chem. B*, 2011, **115**, 3354–3362.
- 225 T. N. Konstantinova and P. M. Miladinova, *J. Appl. Polym. Sci.*, 2009, **111**, 1991–1998.
- 226 I. Grabchev, S. Dumas and J. M. Chovelon, *Polym. Adv. Technol.*, 2008, **19**, 316–321.
- 227 C. X. Bai, W. Z. Jin, L. X. Wu, Y. L. Song, J. J. Jiang, X. D. Zhu and D. W. Yang, *IEEE Trans. Biomed. Eng.*, 2011, **58**, 1232–1238.
- 228 V. B. Bojinov, I. P. Panova and D. B. Simeonov, *Dyes Pigm.*, 2008, **78**, 101–110.
- 229 V. B. Bojinov and I. P. Panova, *Polym. Degrad. Stab.*, 2008, **93**, 1142–1150.
- 230 H. Tian, J. B. Jiang, B. Leng, X. Xiao and P. Zhao, *Polymer*, 2009, **50**, 5681–5684.
- 231 H. Tian, P. Zhao, J. B. Jiang and B. Leng, *Macromol. Rapid Commun.*, 2009, **30**, 1715–1718.
- 232 J. L. Hua, Y. Qu, Y. H. Jiang and H. Tian, *J. Polym. Sci., Part A: Polym. Chem.*, 2009, **47**, 1544–1552.
- 233 Y. S. Lee, J. Y. Jin, Y. M. Kim and S. H. Lee, *Synth. Met.*, 2009, **159**, 1804–1808.
- 234 S. Y. Liu and C. H. Li, *J. Mater. Chem.*, 2010, **20**, 10716–10723.
- 235 D. D. Evanoff, J. B. Carroll, R. D. Roeder, Z. J. Hunt, J. R. Lawrence and S. H. Foulger, *J. Polym. Sci., Part A: Polym. Chem.*, 2008, **46**, 7882–7897.
- 236 S. Uchiyama, C. Gota, K. Okabe, T. Funatsu and Y. Harada, *J. Am. Chem. Soc.*, 2009, **131**, 2766–2767.
- 237 S. Uchiyama, C. Gota, T. Yoshihara, S. Tobita and T. Ohwada, *J. Phys. Chem. B*, 2008, **112**, 2829–2836.
- 238 P. Wang, C. P. Chai, Q. Yang, F. Z. Wang, Z. H. Shen, H. Q. Guo, X. F. Chen, X. H. Fan, D. C. Zou and Q. F. Zhou, *J. Polym. Sci., Part A: Polym. Chem.*, 2008, **46**, 5452–5460.

- 239 Q. A. Yang, H. Jin, Y. D. Xu, Z. H. Shen, X. H. Fan, D. C. Zou and Q. F. Zhou, *J. Polym. Sci., Part A: Polym. Chem.*, 2010, **48**, 5670–5678.
- 240 Q. Yang, Y. D. Xu, H. Jin, Z. H. Shen, X. F. Chen, D. C. Zou, X. H. Fan and Q. F. Zhou, *J. Polym. Sci., Part A: Polym. Chem.*, 2010, **48**, 1502–1515.
- 241 Y. D. Xu, Q. Yang, Z. H. Shen, X. F. Chen, X. H. Fan and Q. F. Zhou, *Macromolecules*, 2009, **42**, 2542–2550.
- 242 S. Y. Liu and J. M. Hu, *Macromolecules*, 2010, **43**, 8315–8330.
- 243 S. Y. Liu, T. Wu, G. Zou and J. M. Hu, *Chem. Mater.*, 2009, **21**, 3788–3798.
- 244 S. Y. Liu, J. Yin, C. H. Li and D. Wang, *J. Phys. Chem. B*, 2010, **114**, 12213–12220.
- 245 L. Tao, C. S. Kaddis, R. R. O. Loo, G. N. Grover, J. A. Loo and H. D. Maynard, *Chem. Commun.*, 2009, 2148–2150.
- 246 P. Rungta, V. Tsyalkovsky, C. F. Huebner, Y. P. Bandera and S. H. Foulger, *Synth. Met.*, 2010, **160**, 2486–2493.
- 247 K. Tsuchiya, H. Kasuga, A. Kawakami, H. Taka, H. Kita and K. Ogino, *J. Polym. Sci., Part A: Polym. Chem.*, 2010, **48**, 1461–1468.
- 248 K. Tsuchiya, K. Sakaguchi, A. Kawakami, H. Taka, H. Kita, T. Shimomura and K. Ogino, *Synth. Met.*, 2010, **160**, 1679–1682.
- 249 Y. K. Fang, C. L. Liu and W. C. Chen, *J. Mater. Chem.*, 2011, **21**, 4778–4786.
- 250 W. C. Chen, Y. K. Fang, C. L. Liu, G. Y. Yang and P. C. Chen, *Macromolecules*, 2011, **44**, 2604–2612.
- 251 Y. D. Zhang, C. Zuniga, S. J. Kim, D. K. Cai, S. Barlow, S. Salman, V. Coropceanu, J. L. Bredas, B. Kippelen and S. Marder, *Chem. Mater.*, 2011, **23**, 4002–4015.
- 252 N. Chandrasekharan, S. Ibrahim, Y. Kostov and G. Rao, *Bioautomation*, 2008, **9**, 31–39.
- 253 E. Bakker and W. Ngeontae, *WO Pat.*, 2 009 023 287, 2009.
- 254 E. M. Lee, S. Y. Gwon, Y. A. Son and S. H. Kim, *Spectrochim. Acta, Part A*, 2012, **86**, 600–604.
- 255 A. Y. Men'shikova, Y. E. Moskalenko, A. V. Gribanov, N. N. Shevchenko, V. B. Faraonova, A. V. Yakimanskii, M. Y. Goikhman, N. L. Loretsyan, A. V. Koshkin and M. V. Alfimov, *Russ. J. Appl. Chem.*, 2010, **83**, 1997–2005.
- 256 R. Menzel, A. M. Breul, C. Pietsch, J. Schaefer, C. Fribe, E. Taeuscher, D. Weiss, B. Dietzek, J. Popp, R. Beckert and U. S. Schubert, *Macromol. Chem. Phys.*, 2011, **212**, 840–848.
- 257 A. M. Breul, C. Pietsch, R. Menzel, J. Schaefer, A. Teichler, M. D. Hager, M. Gottschaldt, J. Popp, B. Dietzek, R. Beckert and U. S. Schubert, *Eur. Polym. J.*, 2012, **48**, 1339–1347.
- 258 B. Happ, J. Schaefer, R. Menzel, M. D. Hager, A. Winter, J. Popp, R. Beckert, B. Dietzek and U. S. Schubert, *Macromolecules*, 2011, **44**, 6277–6287.
- 259 A. M. Breul, J. Schaefer, G. M. Pavlov, A. Teichler, S. Hoeppener, C. Weber, J. Nowotny, L. Blankenburg, J. Popp, M. D. Hager, B. Dietzek and U. S. Schubert, *J. Polym. Sci., Part A: Polym. Chem.*, 2012, **50**, 3192–3205.
- 260 G. M. Pavlov, A. M. Breul, M. D. Hager and U. S. Schubert, *Macromol. Chem. Phys.*, 2012, **213**, 904–916.
- 261 P. J. Yang, C. W. Wu, D. Sahu and H. C. Lin, *Macromolecules*, 2008, **41**, 9692–9703.
- 262 H. C. Chu, T. C. Liang, H. Padhy, S. J. Hsu and H. C. Lin, *Eur. Polym. J.*, 2011, **47**, 2266–2276.
- 263 T. C. Liang and H. C. Lin, *J. Mater. Chem.*, 2009, **19**, 4753–4763.
- 264 T. C. Liang and H. C. Lin, *J. Polym. Sci., Part A: Polym. Chem.*, 2009, **47**, 2734–2753.
- 265 M. Haeussler, Y. P. Lok, M. Chen, J. Jasieniak, R. Adhikari, S. P. King, S. A. Haque, C. M. Forsyth, K. Winzenberg, S. E. Watkins, E. Rizzardo and G. J. Wilson, *Macromolecules*, 2010, **43**, 7101–7110.
- 266 Y. X. Tao, Q. F. Xu, J. M. Lu and X. B. Yang, *Dyes Pigm.*, 2010, **84**, 153–158.
- 267 T. Z. Yu, Y. L. Zhao, X. S. Ding, D. W. Fan, L. Qian and W. K. Dong, *J. Photochem. Photobiol. A*, 2007, **188**, 245–251.
- 268 K. Nagy, S. Gokturk and L. Biczok, *J. Phys. Chem. A*, 2003, **107**, 8784–8790.
- 269 S. Cha, M. G. Choi, H. R. Jeon and S. K. Chang, *Sens. Actuators, B*, 2011, **157**, 14–18.
- 270 Y. C. Simon and C. Weder, *J. Mater. Chem.*, 2012, **22**, 20817–20830.
- 271 B. L. Feringa and W. R. Browne, *Molecular Switches*, John Wiley & Sons, Weinheim, 2011.